The National Academy of Sciences, India

(Registered under Act XXI of 1860)
Founded 1930

COUNCIL FOR 2005

Regd. No. R.N. 35621/78

CONTENTS

PROCEEDINGS

OF THE

NATIONAL ACADEMY OF SCIENCES, INDIA

2005

VOL LXXV SECTION–A PART I

Template synthesis of transition metal complexes derived from dehydroacetic acid and DL-histidine

P. VENKATESWAR RAO,* K. ASHWINI and KANEEZ FATIMA

Department of Chemistry, Nizam College, Hyderabad-500 001, India.

Received November 8, 2002; Revised March 12, 2003; Accepted March 26, 2004

Abstract

Transition metal complexes of the general formula [ML.x H_2O] wherein x = 1; when M = Oxovanadium(IV), Mn(II),Co(II), Ni(II) and Cu(II) and x = 2; when M = Fe(II); have been synthesized by template condensation of 3-acetyl-6-methyl-2H-pyran-(2,4)-3H-dione (dehydroacetic acid) and DL-histidine. Structures of the complexes have been proposed on the basis of elemental analyses, electrical conductance, magnetic moment and IR, UV-Vis and ESR spectral data. All the complexes have been proposed to possess octahedral geometry around the metal ions.

(**Keywords** :template synthesis/transition metal complexes/IR/ UV-Vis/ ESR/ dehydroacetic acid/ DL-Histidine)

Introduction

Although formation constant studies of aminoacid complexes are quite common[1-5], synthesis and characterization studies of transition metal complexes derived from aminoacids as ligands are of recent interest[6-12]. Macrocycles using aminoacids as ligands have been reported[13]. Some aminoacid complexes exhibit superoxide dismutase activity[14] and some other possess antibacterial and antiviral activities and certain others have antigastrointestinal infectious activities[15-17].

Besides their physiological activities, 3-acetyl-6-methyl-2H-Pyran-(2,4)-3H-dione and DL-histidine are potent chelating agents[18,19]. In view of their promising physiological activities, we hereby report the synthesis and characterization of transition metal complexes derived from the Schiff base obtained from 3-acetyl-6-methyl-2H-pyran-(2,4)-3H-dione and DL-Histidine (DHAHIS) [Fig. 1].

NH
N
O
H_3C
O
N
OH
H
O
O
CH_3
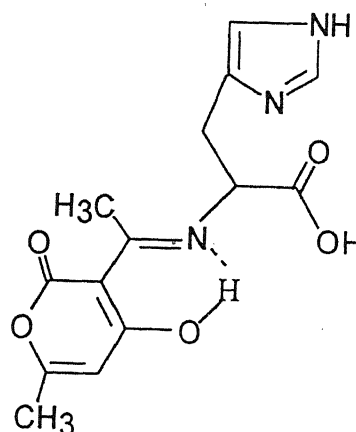
Fig. 1– Structure of ligand

Table 1–Analytical and conductivity data of the complexes.

Mol. formulae of the complexes	Found (calculated) %				Λ_M (mhos. cm^2 mole^{-1})
	Metal	Carbon	Hydrogen	Nitrogen	
VO(II)DHAHIS.H_2O	13.18	43.78	3.90	10.85	14.0
[VC_{14}-$H_{15}N_3O_7$]	(13.13)	(43..30)	(3.87)	(10.82)	
Mn(II)DHAHIS.H_2O	14.69	44.74	4.10	11 .20	2.9
[$MnC_{14}H_{15}N_3O_6$]	(14.61)	(44.68)	(3.99)	(1 1.17)	
Fe(II)DHAHIS.$2H_2O$	14.19	42.60	4.33	10.66	12.8
[$FeC_{14}H_{17}N3O_7$]	(14.14)	(42.55)	(4.30)	(10.63)	
Co(II)DHAHIS.H_2O	15.60	44.10	3.91	11.10	6.2
[$CoC_{14}H_{15}N_3O_6$]	(15.51)	(44.21)	(3.95)	(11.06)	
Ni(II)DHAHIS.H_2O	15.42	44.20	3.90	11.01	2.8
[$NiC_{14}H_{15}N_3O_6$]	(15.46)	(44.24)	(3.95)	(11.06)	
Cu(II)DHAHIS.H_2O	16.58	43.69	3.95	10.98	5.7
[$CuC_{14}H_{15}N_3O_6$]	(16.52)	(43.64)	(3.90)	(10.92)	

Materials and Method

3- acetyl-6-methyl- 2H -pyran (2,4) -3H -dione (Fluka) and DL-histidine (Sigma) were used as such. All the solvents were purified before use. All the metal salts used were of AR grade.

IR spectra were recorded as KBr pellets on a Perkin Elmer-1430 IR spectrophotometer in the range 4000-400 cm^{-1}. Micro analytical data for C,H and N were obtained from CDRI, Lucknow.Metal estimations were done on a Perkin-Elmer 1280 atomic absorption spectrophotometer. Conductivity measurements were carried out using a Systronics digital conductivity meter model No. 304. The electronic spectra of metal chelates were recorded on a DMR-21 UV-Vis spectrophtometer in the range 1300-300 nm in nujol at room temperature. The ESR spectra of Cu(II) and oxovanadium(IV) complexes were recorded on a Varian EPR-E_4 spectrometer as powder at room temperature. TG and DT analyses were carried out in 25-650 °C range using Leed and Northrup (USA) unit with a heating rate of 10 °C /min. and sensitivity 100 μV/finch. Magnetic susceptibilities of the complexes were measured at room temperature on a Faraday balance using [Hg (Co(SCN)$_4$)] as calibrant.

Preparation of Metal Complexes :

The metal chelates were synthesised by refluxing the methanolic solutions of metal chlorides (0.01 mol), 3-acetyl-6-methyl-2H-pyran (2,4)-3H-dione (0.02 mol, 0.336 g) in 15 ml of methanol and DL-histidine (0.02 mol, 0.382 g) in 10ml of distilled water [In case of Fe(II) and VO(IV) complexes, aqueous solutions of ferrous ammonium sulphate and vanadyl sulphate were used]. Potassium hydroxide (0.02 mole in 10 ml of methanol) was added to the reaction mixture and the pH of the solution was adjusted to ~8. A yellow solution indicated the formation of the Schiff base. The reaction mixture was refluxed for four hrs. It was evaporated to half of its volume and kept over night. The metal chelates were isolated in the crystalline form. The metal chelates thus separated out were filtered, washed repeatedly with methanol, distilled water and finally with

Petroleum ether (60-80°) and dried *in vacuum*. The purity of the complexes is checked by TLC.

Results and Discussion

All the metal complexes are coloured. They are stable towards air and moisture. They are insoluble in benzene, petroleum ether and are partially soluble in ethanol. They are soluble in DMF,DMSO and dioxane. They decompose at high temperatures. The molar conductance values of the metal chelates in 1x 10^{-3}M DMF solutions at 27°C suggest their non electrolytic nature. The analytical data (Table 1) of the metal complexes show that all the metal chelates have a 1 : 1 metal to ligand stoichiometry. All the complexes have a general configuration [ML.xH_2O]n where L = DHAHIS; x = 1or 2 and n = 1 or 2,3,4 .... etc., x = 1 and n = 2,3,4.. when M (II) = VO, Mn, Co, Ni and Cu and x = 2 and n = 1, when M(II) = Fe.

The IR spectrum of 3-acetyl-6-methyl-2H - pyran (2,4) -3H - dione shows bands at 3030,1710,1640 and 1470 cm^{-1} assignable to ν OH (hydrogen bonded), νC=O (lactone carbonyl), νC=O(acetyl carbonyl) and νC-O (phenolic) respectively[20] (Table 2). The IR spectrum of DL-histidine shows infrared frequencies at 3300,1610 and 1590 cm^{-1} which are attributable to νNH (imidazole), $\nu COO^{-}_{(asym)}$ and νC=N (imidazole) respectively[21]. In the IR spectra of all the metal chelates, no band is observed in the region 3030 cm^{-1} which is due to νOH of dehydroacetic acid, suggesting the cleavage of intra molecularly hydrogen bonded OH and participation of oxygen of phenolic group in coordination[20]. This is supported by an upward shift in νC-O (phenolic) at 1470 cm^{-1} to the extent of 20 cm^{-1} (ref. 2). In the spectra of all the chelates a broad trough appeared around 3500 cm^{-1} which is due to νOH of coordinated water. This is supported by the presence of a non ligand band at 840 cm^{-1} (ref.23). The presence of coordinated water is also supported by TG and DT analyses. The presence of a new sharp band in the region 1650-1660 cm^{-1} which can be assignable to ν C=N (azomethine) suggests the formation the Schiff base and participation of azomethine nitrogen in complexation[24]. This is further supported by the presence of ν M-N in the region 400-500 cm^{-1} (ref. 22) A negative shift to the extent of 20-30 cm^{-1} in νC=N (imidazole), which is present at 1590cm^{-1} in histidine suggests the participation of νC=N (imidazole) in complexation[23]. The shift in $\nu COO_{(asym)}$ of histidine from 1610 cm^{-1} to 1580 cm^{-1} suggests the participation of oxygen of COO^{-} in coordination[25]. $\nu COO^{-}_{(sym)}$ is present at 1410 cm^{-1}. The difference in $\nu COO^{-}_{(asym)}$and $\nu COO^{-}_{(sym)}$ which is ($\Delta\nu$ = 150 cm^{-1}) is prescribed to monodentate carboxylates. In the spectra of Mn(II), Co(II), Ni(II) and Cu(II) a down ward shift of 20 cm^{-1} is observed in ν C=O (lactone carbonyl) which is attributed to the participation of lactone carbonyl in coordination[20]. The presence of new bands in the region 400-600 cm^{-1} can be assigned to ν M-N and νM-O vibrations[22] respectively. A strong band at 930 cm^{-1} in oxovanadium(IV) complex is due to νV=O[25]. From the IR spectral data it may be concluded that the ligand DHAHIS is coordinating through the oxygen of phenolic group, azomethine nitrogens (free as well as imidazole ring) and oxygen of COO^{-} group. In Mn(II), Co(II), Ni(II) and Cu(II) complexes the lactone carbonyl has been observed to be participating in complexation.

Thermogravimetric analysis shows a weight loss equivalent to one mole of water coordinated per mole of the complex in case of oxovanadium(IV), Mn(II), Co(II), Ni(II) and Cu(II) complexes. In case of Fe(II) complex the weight loss is equivalent to two moles of water per mole of the complex. Differential thermal analysis shows that the loss of water is a one step process in all the complexes except in Fe(II) complex, where in it is a two step process. In differential thermal analysis one endothermic peak is obtained in all the complexes, except in Fe(II) complex where in two endothermic peaks are obtained. The loss of water occurs at 148°C for Mn(II) complex, 152°C for Co(II) complex, 158°C for Ni(II) complex, 160°C for Cu(II) complex and 164°C for oxovanadium(IV) complex. The Fe(II) complex loses its coordinated water at 160°C and 166°C in a two step process

Table 2– Characteristic infrared frequencies of the ligand, DHAHIS and its complexes (in cm^{-1}).

Compound	νOH/νNh	νC=O(lactone)	νC-N (free)	νCOO^-	νC=N (ring)	νC=O (phenolic)	New bands
DHA [Dehydroacetic acid]	3030(b)	1710(5)	-	-	-	1470(5)	-
Histidine	3300(5)	-	-	1610(5)	1590(5)	-	
VO(II) Complex [VO(II)DHAHIS.H_2O]	3500-3250(b)	1710(5)	1650(5)	1580(5)	1570(5)	1480(5)	440(w), 550(m) 850(s), 930(s)
Mn (II) Complex [Mn(II). DHAHIS.H_2O]	3520-3250(b)	1680(s)	1660(s)	1585(s)	1560(s)	1490(s)	440(w), 530(m) 580(m), 840(m)
Fe (II) Complex [Fe (II) DHAHIS.H_2o]	3500-3250(b)	1710(s)	1650(s)	1580(s)	1565(s)	1485(s)	450(w), 530(m) 580(m), 840(m)
Co (II) Complex [Co (II) DHAHIS.H_2o]	3500-3250(b)	1680(s)	1660(s)	1585(s)	1560(s)	1490(s)	440(w), 520(m) 580(m), 840(m)
Ni (II) Complex [Ni (II) DHAHIS.H_2o]	3500-3300(b)	1680(s)	1660(s)	1580(s)	1560(s)	1490(s)	460(w), 530(s) 590(m), 840(s)

Table 3 : Magnetic and electronic spectral data of the complexes.

Complex	μ_{eff}	Electronic spectral bands (in cm^{-1})
Oxo vanadium (IV) complex	1.85	11764 $^2B_2 \rightarrow ^2E$, 16400 $^2B_2 \rightarrow ^2B_1$, 24800 $^2B_2 \rightarrow ^2A_1$, 27700 charge transfer
Mn(II) complex	5.89	8540, 17240, 26800
Fe(II) complex	5.10	10820 $^5T_{2g} \rightarrow ^5E_g$, 22200 charge transfer
Co(II) complex	4.10	9400 $^4T_{1g}(F) \rightarrow ^4T_{2g}(F)$, 21276 $^4T_{1g}(F) \rightarrow ^4T_{2g}(P)$, 26000 charge transfer
Ni(II) complex	2.90	8760 $^3A_{2g}(F) \rightarrow ^3T_{2g}(F)$, 15625 $^3A_{2g}(F) \rightarrow ^3T_{1g}(P)$, 26300 $^3A_{2g}(F) \rightarrow ^3T_{1g}(P)$
Cu(II) complex	1.87	12800 $^2B_1 \rightarrow ^2A_1$, 16800 $^2B_1 \rightarrow ^2E$, 26500 charge transfer

The magnetic and electronic spectral data is shown in Table 3. They are according to the proposed structures of the complexes (Fig. 2-4)

The ESR spectra of oxovanadium(IV) and Cu(II) complexes were recorded as powder at room temperature. The g_{av} value for oxovanadium(IV) complex is found to be 1.97. The $g_{\parallel}$, $g_{\perp}$ and g_{av} values for Cu(II) complex have been found to be 2.201,2.059 and 2.106 respectively. The g_{av} value for oxovanadium(IV) complex suggests an octahedral geometry. The g values for Cu(II) complex suggest a distorted octahedral geometry. These values are also in accordance with the single unpaired electron present in the d orbitals of the metal ions.
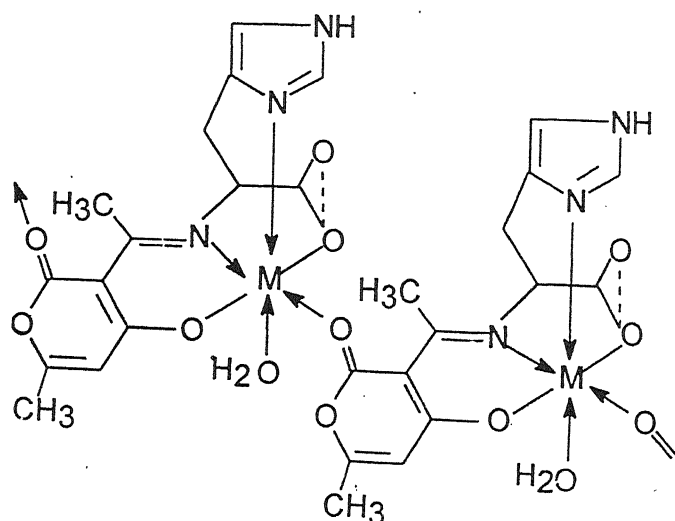
Fig 2– Where M(II) = Mn, Ni, Co and Cu
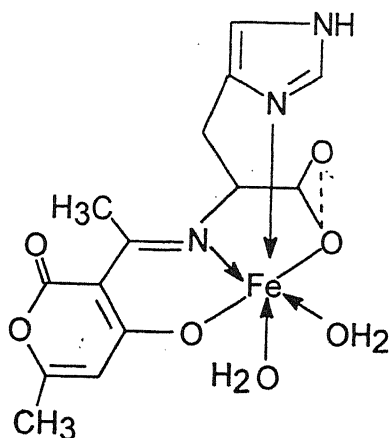
Fig 3– Fe(II) complex
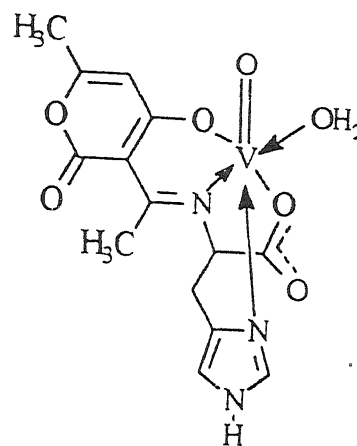
Fig 4– Oxovanadium(IV) complex

On the basis of elemental analyses, conductivity measurements, TG and DT analyses, magnetic data, IR, UV-Vis and ESR spectral data octahedral geometry has been proposed around the metal ions.

Acknowledgements

The authors thank the Head, Department of Chemistry, Osmania University and Principal, Nizam College for providing necessary facilities and for recording spectra.

References

1. Shoukry Mohamed, M. (1996) *Talanta* **43**(2) : 177.
2. Sharma, P. K. & Dubey, S.N. (1995) *J. Indian Chem. Soc.* **72**(9) : 577.
3. Shoukry Mohamed M., Shehata, Mohamed R, Abdel-Razik, Afaf & Abdel Kalim, AT.I. (1999) *Monatsh Chem.* **130**(3) : 409..
4. Lavanant, H. eleve, Hecquent, Emilie & Hoppilliard Yannik (1999) *Int. J. Mass. Spectrom.* **185** : 11.
5. Fernandes, Maria Celina M.M., Paniago, Euclear B. & Carvalho, Sandro (1997) *J. Braz. Chem. Soc.* **8**(5) : 537.
6. Ren, Reii & Yang, Pin (1999) *Chin. J. Chem.* **17**(6) : 625.
7. Russel, N. R., Van Hoof, N. & Mc Namara, M. (1998) *Proc. Int. Symp. Cyclodextrins* **9** : 427.
8. Nath, Mala &Arora Poonam (1993) *Synth. React. Inorg. Met. Org. Chem.* **23**(9) : 1523.
9. Fabbrizzi, Luigi, Piersandro P., Parodi L., Perotti A. & Taglietti, Angelo, (1995) *J. Chem. Soc. Chem. Commum.* **23** : 2439.

10. Hasan Aly, M.A. (1994) *Egypt. J. Pharma. Sci.* **35**(1-6) : 165.

11. Vergopoulos, Vassilios, Priebseh, Wolfgang; Fritzshe, Martina & Rehder, Dieter (1993) *Inorg. Chem.* **32**(9) : 1844.

12. El. Shahawi, Mohamed S. (1993) *Tr. Met. Chem.* **18**(4) : 385.

13. Kodama, Mutsuo. (1996) *Bull Chem. Soc. Jpn.* **69**(11) : 3179.

14. Beijing, Shifan, (1996) *Daxue Xuebao, Ziran Kexueban* **32**(3) : 362.

15. Khurshid S. Javaid (1996) *Pak. J. Pharmacol* **13**(1) : 41.

16. Johannes, Ludger, Kambadur, Ravi, Lee-Hellmich, Helen; Hodgkinson, Colin A., Arnheiter, Heinz & Meier Ellen. (1997) *J. Virol.* **71**(12) : 9792.

17. Thompson Richard Paul Hepworth, Powell, Jonathan Joseph, Phillips, Rosemary Helen, Chevalier, Sylvaine Francorsie & Aline, P.C.T. *Int. Appl. Wo* **9816** : 218.

18. Yang zu pei, Zang, Banglao, Yu, Yueying, Zhang, Hongyu & Shoanvi Shifan (1998) *Daxue. Xuebao. Ziran Kexueban* **26**(1) : 57.

19. Gautam M.P., Yadav, Ashok & Limaye, S. N. (1998) *Asian J. Chem.* **10**(3) : 415.

20. Mane P.S. Shirodkar, S.G . Arbad B.R. & Chondhekar, T.K. (2001) *Indian. J. Chem.* **40**(A) : 648.

21. Silverstein & Bassler (1997) *Spectrometric Identification of Organic compounds,* John Wiley & Sons Inc. New York.

22. Nakamoto, K. (1997) *Infrared and Raman Spectra of Inorganic and Coordination Compounds* 5th Ed, John Wiley & Sons Inc. New York : 57.

23. Kamruddin S.K. & Roy, A. (2001) *Indian J. Chem.* **40**A : 211.

24. Lata, N., Gupta, Manisha & Mathur, Pavan (2001) *Indian J. Chem.* **40**A : 247.

25. Warad, D.U., Satish C.O., Kulkarni V.H. & Chandra Shekar, S. Bajgur (2000) *Indian. J. Chem.* **39**A : 415.

PROC. NAT. ACAD. SCI. INDIA, 75 (A), I, 2005

Heterobinuclear complex formation in solution by nitrilotriacetic acid (NTA) with mercury(II) and some divalent metal ions

DIVYA BARTARIA and V. KRISHNA*.

Department of Chemistry, University of Allahabad, Allahabad - 211 002, India.

Received April 5, 2003; Revised February 16, 2004; Accepted April 15, 2004

Abstract

The heterobinuclear complexes formed by nitrilotriacetic acid (NTA) with Hg(II)-Be(II), Hg(II)-Pb(II), Hg(II)-Cd(II), Hg(II)-Mn(II), Hg(II)-Co(II), Hg(II)-Ni(II) and Hg(II)-Cu(II) have been investigated potentiometrically in the biologically relevant conditions and the stability constants have been evaluated using SCOGS computer program. Only HgLM type of hetero-binuclear complex has been detected. The observed order of the stability constants and the solution structures of mixed metal complexes have been discussed.

(**Keywords** : heterobinuclear complexes/ stability constant/ NTA)

Introduction

The present paper reports the heterobinuclear complex formation of nitrilotriacetic acid (NTA) with Hg(II)-Be(II), Hg(II)-Pb(II), Hg(II)-Cd(II), Hg(II)-Mn(II), Hg(II)-Co(II), Hg(II)-Ni(II) and Hg(II)-Cu(II) in aqueous solution. All the studies have been carried out by pH titrimetry at 37°C and I = 0.1 mol dm^{-3} ($NaNO_3$). The computations have been made with the aid of the SCOGS[1] computer program.

Materials and Method

Solutions of Hg(II), Be(II), Pb(II), Cd(II), Mn(II), Co(II), Ni(II) and Cu(II) metal ions were prepared and standardised by EDTA titrations[2]. A 0.1 M solution of nitrilotriacetic acid (NTA) was prepared by dissolving it into two equivalents of alkali (NaOH) which was prepared in double distilled water and had earlier been standardised against a standard oxalic acid solution. Solutions of carbonate free sodium hydroxide (E. Merck) and nitric acid (A.R.) were standardised potentiometrically.

A digital pH-meter (century-model-CP 90 1-S) with a glass electrode was used to determine the changes in hydrogen ion concentration. The pH-meter has a reproducibility of ± 0.01 pH.

Four reaction mixtures were prepared by keeping the total volume 50 ml in each case and the molar ratio of ligand, primary and secondary metals undertaken was kept 1: 1: 1.

Solution A : 10 ml $NaNO_3$ (0.5 mol dm^{-3}) + 10 ml HNO_3 (0.1 mol dm^{-3}) + 30 ml H_2O

Solution B : 10 ml $NaNO_3$ (0.5 mol dm^{-3}) + 10 ml HNO_3 (0.1 mol dm^{-3}) + 5 ml NTA (0.1 mol dm^{-3}) + 25 ml H_2O

Solution C : 10 ml $NaNO_3$ (0.5 mol dm^{-3}) + 10 ml HNO_3 (0.1 mol dm^{-3}) + 5 ml NTA (0.1 mol dm^{-3}) + 5 ml Hg(II) (0.1 mol dm^{-3}) + 20 ml H_20

Solution D : 10 ml $NaNO_3$ (0.5 mol dm^{-3}) + 10 ml HNO_3 (0.1 mol dm^{-3}) + 5 ml NTA (0.1 mol dm^{-3}) + 5 ml Hg (II) (0.1 mol dm^{-3}) + 5 ml M (II) (0.1 mol dm^{-3}) + 15 ml H_2O.

where M(II) is the secondary metal ion of the various systems mentioned above. The other experimental details have been described elsewhere[3]. For the evaluation of stability constant of mixed-metal complexes of the ligand NTA by the SCOGS program, the complex formation has been assumed to take place according to :

$$pM_1 + qM_2 + rL_1 + sL_2 + tOH \rightleftharpoons (M_1)p\,(M_2)q\,(L_1)r\,(L_2)S\,(OH)_t$$
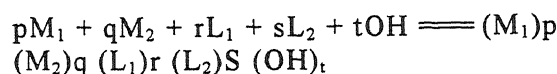
$$\beta pqrst = \frac{[(M_1)_p(M_2)_q(L_1)_r(L_2)_s(OH)_t]}{[M_1]^p[M_2]^q(L_1)^r[L_2]^s[OH]^t}$$

where L_1 stands for the ligand NTA and L_2 for the secondary ligand which is absent in the present study. p, q, r, s and t are stoichiometric numbers; p, q, r and s are usually positive number or zero. t is a negative number for a protonic species and a positive number for a hydroxy species. Preliminary estimates of binary and ternary constants obtained by least square method were further refined by the SCOGS program. Ionic product of water (K_w) and activity coefficient of hydrogen ion under the experimental conditions were obtained from literature[5].

Results and Discussion

NTA behaves[6] as a tri or quadridentate ligand coordination taking place from N atom and two or three COO^- groups, respectively. Thus, it titrates as a triprotic acid, the pK values being 10.95, 3.94 and 2.08 corresponding to the successvie deprotonation of three carboxyl groups. Summation of three pK values indicates the overall stability constant of the ligand. Table 1 represents the proton-ligand, M(II)-ligand binary and hydrolytic constants at 37°C and I = 0.1 mol dm^{-3} ($NaNO_3$). The charges of all the complex species reported in this Table are omitted for clarity.

Proton-ligand formation constants

The proton-ligand formation constants of NTA determined by Irving-Rossotti titration technique[4] given in Table 1(a) show three replaceable protons, and the values reported here agree with the literature values[7].

Metal-ligand formation constants

The metal-ligand formation constants of binary and ternary complexes were evaluated using computer techniques. The refined values of log β of binary and hydrolytic species and the estimated values of $\log\beta_{11100}$ for the ternary complex were supplied to the computer as the input data. The computer gives the values of the constants ($\log \beta_{pqrst}$) and also the concentration distributions of the complex species at different pH values as the output.

Table 1– Proton-ligand constant, M(II)-ligand binary and hydrolytic constants in aq. solution at 37 ± 1° and I = 0.1 mol dm^{-3} $NaNO_3$.

(a) *Proton-ligand formation contants*

	p	*q*	*r*	*s*	*t*	logβ
LH_3	0	0	1	0	-3	16.97
LH_2	0	0	1	0	-2	14.89
LH	0	0	1	0	-1	10.95

(b) *Hydrolytic constants of M(II) aq. ion and metal-ligand binary constants.*

	p	*q*	*r*	*s*	*t*	logβ
Hg (OH)	1	0	0	0	1	-3.84
$Hg(OH)_2$	1	0	0	0	2	-6.38
Cd(OH)	0	1	0	0	1	-9.60
HgL	1	0	1	0	0	14.60
PbL	0	1	1	0	0	11.34
CdL	0	1	1	0	0	9.78
MnL	0	1	1	0	0	7.46
CoL	0	1	1	0	0	10.38
NiL	0	1	1	0	0	11.50
CuL	0	1	1	0	0	12.94
CdL(OH)	0	1	1	0	1	11.25

Table 2– Stability constant values for the mixed-metal complexes of NTA at 37°C and I = 0.1 mol dm^{-3} ($NaNO_3$)

Reactions			$\log\beta_{11100}$
$Hg^{2}+NTA^{3-}+Be^{2+}$	$\rightleftharpoons$	$[Hg\text{-}NTA\text{-}Be]^+$	17.50
$Hg^{2}+NTA^{3-}+Pb^{2+}$	$\rightleftharpoons$	$[Hg\text{-}NTA\text{-}Pb]^+$	16.90
$Hg^{2}+NTA^{3-}+Cd^{2+}$	$\rightleftharpoons$	$[Hg\text{-}NTA\text{-}Cd]^+$	17.15
$Hg^{2}+NTA^{3-}+Mn^{2+}$	$\rightleftharpoons$	$[Hg\text{-}NTA\text{-}Mn]^+$	16.50
$Hg^{2}+NTA^{3-}+Co^{2+}$	$\rightleftharpoons$	$[Hg\text{-}NTA\text{-}Co]^+$	17.00
$Hg^{2}+NTA^{3-}+Ni^{2+}$	$\rightleftharpoons$	$[Hg\text{-}NTA\text{-}Ni]^+$	17.36
$Hg^{2}+NTA^{3-}+Cu^{2+}$	$\rightleftharpoons$	$[Hg\text{-}NTA\text{-}Cu]^+$	17.40

The results of the overall stability constant ($\log\beta$) of the heterobimetallic complexes of NT A have been presented in Table 2. The overall trend of $\log\beta_{11100}$ values of Hg(II)-NTA-M(II) systems is observed as : Hg(II)-Mn(II) < Hg(II)-Pb(II) < Hg(II)-Co(II) < Hg(II)-Cd(II) < Hg(II)-Ni(II) < Hg(II)-Cu(II) < Hg(II)-Be(II). The ternary complexes formed with the metals of the first transition series follow the Irving Williams order :

Hg(II)-Mn (II) < Hg(II)-Co(II)

< Hg(II)-Ni(II) < Hg(II)-Cu(II)
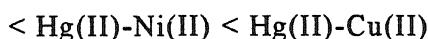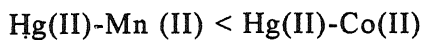
Be(II) being the smallest in size has the highest value of stability constant in the ternary systems. A number of computer models have been included during computation and the final results showed the presence of HgLM mixed metal species in fairly good concentrations.

As is revealed from the species distribution curves, H_3L, H_2L and HL types of protonated species of the ligand are found to exist in decreasing order of their concentration with the gradual rise in pH. Deprotonation equilibria of the carboxyl groups of NTA may be shown according to eqn. (1), (2) and (3).

$$H_3L + OH^- \rightleftharpoons H_2L^- + H_2O \quad (1)$$

$$H_2L^- + OH^- \rightleftharpoons HL^{2-} + H_2O \quad (2)$$

$$HL^{2-} + OH^- \rightleftharpoons L^{3-} + H_2O \quad (3)$$
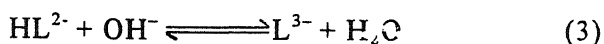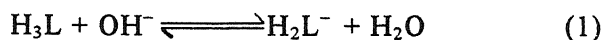
Hg(II) and the secondary metal ions M(II) taken understudy are existent in the free state and there is a gradual fall in their concentration with the rise in pH from ~1.0 to 3.0. The buffer region at pH > 1.5 may be due to metal-induced deprotomition of the ligand. Both the metal ions i.e. Hg(II) and M(II) are found to coordinate with the ligand forming binary complexes Hg(II)-L and M(II)-L, which are making their first appearance at pH~1.5 and passing through a wide maxima in the pH range ~ 1.6 to 3.0. The formation of binary complex species is governed according to the following general equilibria :

$$L^{3-} + Hg^{2+} \rightleftharpoons [HgL]^- \quad (4)$$

$$L^{3-} + M^{2+} \rightleftharpoons [ML]^- \quad (5)$$
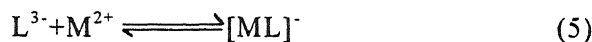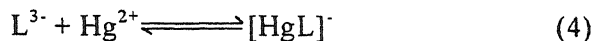
The larger and steep fall in the concentration of Hg(II) in comparison to M(II) indicates the involvement of the former in binary as well as ternary complexation. There is a gradual incline in the concentration of mixed metal complex in the pH range ~ 1.6 to 3.0 with the concomitant decline in the concentration of free metal ions as well as protonated ligand species. Fall in the concentration of mixed-metal complex beyond pH~3.0 may be due to the formation of hydroxo species. Formation of hydroxo species has been considered as the buffer regions corresponding to metal-ligand complex formation equilibria are found to be overlapping with the hydrolytic equilibria of Hg^{2+}(aq) ions in Hg(II)-L-Be(II), Hg(II)-L-Mn(II), and Hg(II)-L-Co(II) systems, although $Hg(OH)^+$ species is identifiable in traces in all the systems. Formation of hydroxo species is governed according to the equilibria:

$$Hg^{2+} + H_2O \rightleftharpoons Hg(OH)^+ + H^+ \quad (6)$$

$$Hg^{2+} + 2H_2O \rightleftharpoons Hg(OH)_2 + 2H^+ \quad (7)$$
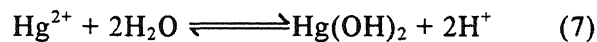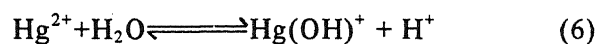
Moreover, a binary hydroxo species i.e. $[CdL(OH)]^{2-}$ is also identifiable in Hg(II)-L-Cd(II) system in small amount. This species is negligible at low pH region, while reaches its maximum abundance (≈18%) at pH ~ 2.7. It's formation may be explained by assuming the equilibrium :

$$[CdL]^- + H_2O \rightleftharpoons [CdL(OH)]^{2-} + H^+ \quad (8)$$
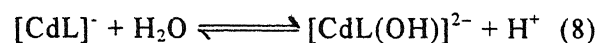
It has been reported that in certain of its complexes, NTA functions as a tridentate, one carboxyl group remaining uncoordinated[8]. In the present study, one metal is expected to bind with only two carboxyl groups forming tetrahedral complex and leaving one carboxyl group free. Thus, the remaining carboxyl group and imino-N

can be utilized to bind with another metal to form ternary complex.

In all the mixed-metal systems of the present study since the ligand possesses four potential binding sites, there are two possibilities for the binding of NTA with the metal ions. In the Hg(II)-NTA-M(II) species, the first possibility is that Hg(II) binds the ligand in a pyrocatechol like mode and M(II) in a glycine-like manner and *vice-versa*. The higher stability of Hg(II)-NTA species compared to the M(II)-NTA complexes suggests the first structure to be more probable. Similar conclusions have been drawn by Nair *et al.*[9] in case of the ligand dopa.

It is clear from the speciation curves that the deprotonation of carboxylato groups of NTA in the mixed-metal systems takes place generally at pH~1.5 to 3.5 and the maximum concentrations of complex species have been found in this pH-range. But it has been reported [10] that in the mixed-ligand systems, the deprotonation takes place beyond pH~3-4. This demonstrates that the mixed-metal complex formation is preferred as compared to mixed-ligand systems. However, as pointed out by Amico *et al.*[11] it is not possible to know in advance which way electronic and stereochemical properties of different metal ions will affect the stabilities of the mixed-metal complex-formation.

References

1. Sayce, LG. (1968) *Talanta* **15** : 1397.
2. Welcher, F.J. (1957) *"The Analytical uses of ethylenediaminetetraacetic acid"*, D. Van Nostarand Company, New York, p. 164.
3. Singh, K.P., Mishra, G.K. & Krishna, V. (2000) *Proc. Nat. Acad. Sci. India* **70(A), III** : 233.
4. Irving, H.M. & Rossotti, H.S. (1953) (1954) *J. Chem. Soc.* 3397, 2904.
5. Harned, H.S. Owen, B.B. (1958) *"The Physical Chemistry of Electrolytic Solution"*, Reinhold, New York, p. 639.
6. Mavani, I.P., Jejurkar, C.R. & Bhattacharya, P.K. (1972) *Indian J. Chem.* **10** : 742.
7. Perrin, D.D. (1979) *"Stability Constants of Metal Ion Complexes"*, Pergamon, New York.
8. Arnold, F.H. (1991) *Bio/Technology* 9 : 151.
9. Nair, M.S., Arasu, P.T., Mansoor, S., Sheik, Shenbagavalli, P. & Neelakantan, M.A. (1995) *Indian J. Chem.* **34A** : 365.
10. Das, Sunanda & Srivastava, M.N. (1990) *Indian J. Chem.* **29A** : 707.
11. Amico, P., Daniele, P.G., Arena, G., Ostacoli, G., Rizzareth, E. & Sammartano, S. (1980) *Inorg. chim. Acta* **44** : 219.

PROC. NAT. ACAD. SCI. INDIA, 75 (A), I, 2005

Synthesis and characterization of *o*-chlorophenoxides of zirconium(IV)

S. C. CHAUDHRY*, C. VERMA, S. S. BHATT and NEERAJ SHARMA

Department of Chemistry, Himachal Pradesh University, Summer Hill, Shimla-171 005, India

Received September 25, 2003; Revised March 4, 2004; Accepted April 15, 2004

Abstract

Zirconium(1V) phenoxides of type $ZrCl_{4-n}(OC_6H_4Cl\text{-}o)_n$ (where n = 1, 2) have been prepared by the interaction of the zirconium tetrachloride with *o*-chlorophenol. These phenoxides showed considerable reactivity towards bases, resulting in addition complexes of composition $ZrCl_{4-n}(OC_6H_4Cl\text{-}o)_n$ .2py and $ZrCl_{4-n}(OC_6H_4Cl\text{-}o)_n$.B (where py = pyridine, B = phen, bipy). These complexes have been characterized by elemental analysis, electrical conductance, molecular weight, IR, ^{1}H NMR and thermal studies.

(**Keywords** : zirconium complexes/*o*-chlorophenol/ aryloxides/ nitrogenous bases/addition compounds)

Introduction

The chemistry of zirconium(1V) is of topical interest and has been increasingly witnessing many advances elucidating its both medicinal[1-3] and biological role[4] as well as its catalytic applications[5-8]. A broad review of the literature on the complexes of zirconium(1V) shows that zirconium(1V) phenoxides[9-11] have drawn comparatively far less attention in comparison to the alkoxide complexes, which may be due to tedious procedures required for the preparation of the former. In view of the above, it was contemplated to synthesize and characterize some new zirconium(1V) aryloxides using *o*-chlorophenol and zirconium tetrachloride.

Materials and Method

Zirconium tetrachloride was purified by sublimation while *o*-chlorophenol was distilled before use. Solvents and various bases were made anhydrous before use. Trimethylsilyl derivative of *o*-chlorophenol ($Me_3SiOC_6H_4Cl\text{-}o$), was prepared by well established procedure involving the reaction of Me_3SiCl with *o*-chlorophenol in the presence of triethylamine.

The infrared spectra (KBr pellets and Nujol) were recorded on a Beckmann IR 4250 spectrophotometer (4000-200 cm^{-1}) and ^{1}H NMR spectra on a JEOL JNM PMX 60 SI spectrometer using $CDCl_3$ / TFA as solvent. Thermograms (TG and DTA curves) of the complexes (5-10 mg) were recorded on simultaneous DT-TG Shimadzu (DT-40) Thermal Analyzer, using Pt / Pt-Rh (10%) thermocouple at a heating rate of 10°C min^{-1}. Molecular weights were determined cryoscopically and molar conductance of complexes were measured on Elico-conductivity bridge CM-Type 82 T. Zirconium was estimated gravimetrically as ZrO_2 and chlorine by Volhard's method.

Preparation of $ZrCl_{4-n}(OC_6H_4Cl\text{-}o)_n$ (where n = 1 or 2) :

Compounds of composition $ZrCl_2(OC_6H_4Cl\text{-}o)_2$ and $ZrCl_3(OC_6H_4Cl\text{-}o)$ were prepared by the reaction of zirconium tetrachloride taken as suspension (2.38 g, .0102 mol) in dry benzene with equimolar (2.05 g, .0102 mol) and bimolar (4.09 g, 0.0204 mol) amounts of trimethylsilyl o-chlorophenoxides in the same solvent. The reaction mixture was refluxed for 3-4 hrs. The red

solid formed was filtered under anhydrous conditions and trimethylchlorosilane formed during course of reaction was distilled off. The solid mass was washed several times with benzene and petroleum ether and finally dried under *vacuo*. The compounds were recrystallised in MeOH + $CHCl_3$ mixture (yield 70 %).

Preparation of addition compounds of $ZrCl_{4-n}(OC_6H_4Cl\text{-}o)_n$ (where n = 1 or 2) with nitrogenous bases:

Known amounts of $ZrCl_2(OC_6H_4Cl\text{-}o)_2$ and $ZrCl_3(OC_6H_4Cl\text{-}o)$ were suspended in benzene and were reacted with equimolar amounts of 1,10-phenanthroline and 2,2′-bipyridyl and bimolar amount of pyridine dissolved separately in same solvent with continuous stirring. The reactions were slightly exothermic. The formation of addition compounds was indicated by dissolution of the parent phenoxide and change of colour of the resulting solution. After stirring the solution overnight, solid compounds separated out. These addition compounds were separated by filtration, washed with petroleum ether and finally dried under *vacuo*.

Results and Discussion

The reactions of zirconium tetrachloride with stoichiometric amounts of trimethylsilyl *o*-chlorophenoxide resulted in the formation of mono-and bis-derivatives:

$$ZrCl_4 + nMe_3SiOC_6H_4Cl\text{-}o \xrightarrow[\text{reflux}]{C_6H_6} ZrCl_{4-n}(OC_6H_4Cl\text{-}o)_n \downarrow + nMe_3SiCl \quad (n=1,2)$$
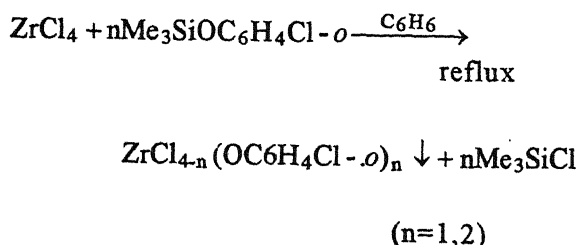
The reactions require 3-4 hrs. of refluxing in benzene. It is also pertinent to mention here that attempts to isolate tetrakis derivative by the reaction of $ZrCl_4$ with excess of $Me_3SiOC_6H_4Cl\text{-}o$ in benzene or high boiling solvents (toluene and xylene) even under prolonged refluxing were unsuccessful and this reaction, at no stage, appears to proceed beyond bis-substitution.

The *o*-chlorophenoxides of zirconium(1V) are red in colour and change their colour on exposure. They are insoluble in most of organic solvents, partially soluble in nitrobenzene and nitromethane and soluble in methanol. Molecular weight determination of these complexes in nitrobenzene suggest their dimeric nature in this solvent. Low molar conductance values of millimolar solutions of these compounds in nitrobenzene indicate them to be non-electrolytes. Stoichiometric composition of the solids isolated was established by elemental analysis given in (Table 1).

^1H NMR Spectra:

In the room temperature proton NMR spectra of the complexes $ZrCl_2(OC_6H_4Cl\text{-}o)_2$ and $ZrCl_3(OC_6H_4Cl\text{-}o)$, there is complete absence of resonance around δ 4.78 ppm and δ 0.28 ppm assigned to phenolic -OH proton and methyl protons of trimethylsilyl (Me_3Si-) group, respectively. Further, the appearance of signals due to aromatic ring protons as an ill resolved multiplet in δ 6.9-7.3 ppm range which is slightly downfield compared to those in pure *o*-chlorophenol (δ 6.67-7.10 ppm) or its trimethylsilyl derivative which is in the range δ 6.70-7.11 ppm, has confirmed the coordination of phenolic oxygen to zirconium atom. This is in accordance with earlier observations made by Clark and coworkers[12] in tantalum(V) phenoxides.

IR Spectra:

Further information about the structure of these complexes has been obtained from the IR spectra. The *o*-chlorophenoxides of zirconium (1V), $ZrCl_2(OC_6H_4Cl\text{-}o)_2$ and $ZrCl_3(OC_6H_4Cl\text{-}o)$, showed $\upsilon_{(Zr-Cl)}$ modes[13] around 360-340 cm^{-1} region and interestingly, there is no splitting of bands due to $\upsilon_{(Zr-Cl)}$ mode, thus indicating that chlorines tend to remain as far apart from each

other as possible and thus lie at *trans* position. The $\upsilon_{(C-O)}$ mode observed at 1260 cm^{-1} in free *o*-chlorophenol and at 1210 cm^{-1} in trimethylsilyl *o*-chlorophenoxide has been found to shift to lower wavenumbers by (~ 60-70 cm^{-1}) in the complexes under study. Coordination from the phenolic oxygen of *o*-chlorophenol has been confirmed by the appearance of entirely new bands (not present in pure phenol and its silyl derivative) in the 590-540 cm^{-1} region assigned to terminal $\upsilon_{(Zr-O)}$ mode while bands in the 500-480 cm^{-1} region have been attributed to bridging Zr–O→Zr modes.
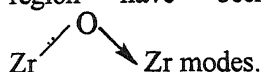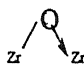
Based upon above results, a dimeric structure bridging through phenoxo group has tentatively been proposed for $ZrCl_2(OC_6H_4Cl\text{-}o)_2$ on next page.

Similar structure exhibiting bridging through *o*-chlorophenoxide groups may be proposed for $ZrCl_3(OC_6H_4Cl\text{-}o)$.

Thermal Studies:

The TG/DTA curves of $ZrCl_3(OC_6H_4Cl\text{-}o)$ and $ZrCl_2(OC_6H_4Cl\text{-}o)_2$ have revealed a two stage decomposition of these compounds. An initial

Table 1–Analytical and IR spectral data of *o*-chlorophenoxides of Zirconium(IV) and their addition compounds with nitrogenous bases

Compd. (Empirical formula)	Colour & physical state	Analysis % Found / (Calcd.) Zr	Cl	C	H	Molar cond. in $PhNO_2$ (Ω^{-1} $cm^2mol.^{-1}$)	Mol. Wt* Found / (Calcd.)	IR bands (cm^{-1}) $\nu_{(Zr-O)}$	Zr–O→Zr	$\nu_{(Zr-Cl)}$	$\nu_{(Zr-N)}$
$ZrCl_2(OC_6H_4Cl\text{-}o)_2$	Dark Red Solid	21.74 (21.26)	34.56 (34.03)	34.70 (34.51)	1.85 (1.91)	0.849	845 (417)	586	488	360	_
$ZrCl_3(OC_6H_4Cl\text{-}o)$	Dark Red Solid	28.12 (28.04)	43.11 (43.66)	22.01 (22.14)	1.40 (1.23)	0.466	563 (325)	578	485	358, 342	_
$ZrCl_3(OC_6H_4Cl\text{-}o)$. 2py	Reddish brown solid	20.60 (20.81)	32.70 (32.40)	43.71 (43.81)	3.35 (3.19)	1.008	_	580	_	355, 340	289
$ZrCl_2(OC_6H_4Cl\text{-}o)_2$. 2py	Reddish brown solid	15.76 (15.85)	24.56 (24.68)	45.08 (45.90)	3.79 (3.13)	0.649	_	576	_	352	278
$ZrCl_3(OC_6H_4Cl\text{-}o)$. bipy	Brick red solid	18.75 (18.95)	29.40 (29.50)	39.11 (39.90)	2.69 (2.49)	0.515	_	558	_	350, 342	285
$ZrCl_2(OC_6H_4Cl\text{-}o)_2$. bipy	Purple solid	15.32 (15.91)	24.03 (24.77)	46.70 (46.05)	2.28 (2.79)	1.104	612 (573)	565	_	358	278
$ZrCl_3(OC_6H_4Cl\text{-}o)$. phen	Reddish brown solid	18.21 (18.05)	28.02 (28.11)	42.28 (42.30)	2.55 (2.37)	0.924	490 (505)	548	_	360, 345	280
$ZrCl_2(OC_6H_4Cl\text{-}o)_2$. phen	Reddish brown solid	15.24 (15.26)	23.74 (23.76)	48.90 (48.20)	2.50 (2.68)	0.879	_	560	_	348	286

(where py = pyridine; bipy = 2, 2′–bipyridyl; phen = 1, 10- phenanthroline)

(*Mol. wt. determined in nitrobenzene)

Cl Cl

OC_6H_4Cl-*o*

o-ClH_4C_6O —— Zr Zr —— OC_6H_4Cl-*o*

OC_6H_4Cl-*o*

Cl Cl
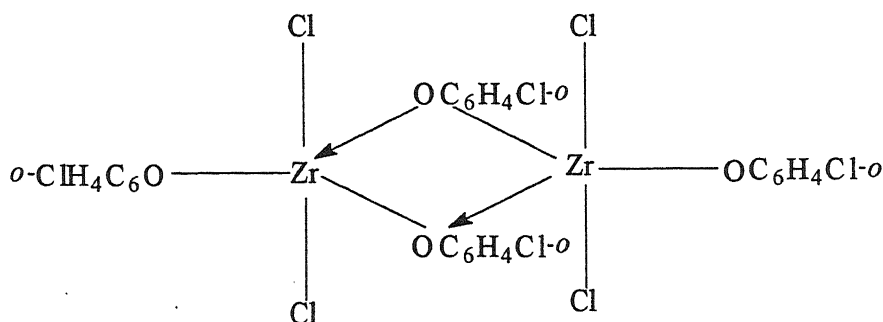
weight loss of 42.18 % in case of $ZrCl_3(OC_6H_4Cl$-*o*) has been attributed to the formation of $ZrOCl_2$ as an intermediate while a weight loss of 34.74 % in $ZrCl_2(OC_6H_4Cl$-*o*$)_2$ appears to correspond to the removal of one chlorophenoxo group. The subsequent weight losses of about 18 % in the former and about 32 % in the latter in the second stage have been rationalized in terms of the formation of ZrO_2 as the final residue in both the cases. These decompositions were accompanied by feeble exothermic peaks in DTA curves.

Reactions with nitrogenous bases:

Although, like alkoxides,[14,15] acceptor properties of metal phenoxides[16-18] in general are quite low in contrast to those of their corresponding halides, yet in the present studies, phenoxides of zirconium(1V) have shown considerable reactivity towards bases such as pyridine (py), 1,10-phenanthroline (phen) and 2,2′-bipyridyl (bipy). The formation of the resulting compounds has been rationalized in term of the following reactions:

$$ZrCl_{4-n}(OC_6H_4Cl\text{-}o)_n + 2py \xrightarrow[\text{8-10 hrs}]{C_6H_6,\ \text{Stir.}} ZrCl_{4-n}(OC_6H_4Cl\text{-}o)_n 2py$$

$$ZrCl_{4-n}(OC_6H_4Cl\text{-}o)_n + B \xrightarrow[\text{8-10 hrs}]{C_6H_6,\ \text{Stir.}} ZrCl_{4-n}(OC_6H_4Cl\text{-}o)_n B$$
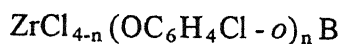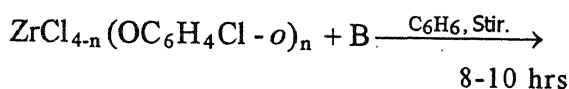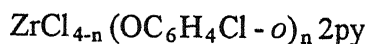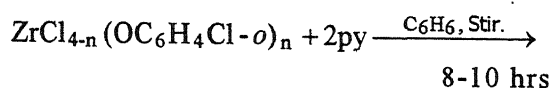
(where B = phen or bipy; and n = 1,2)

The reactions with these bases were quite fast and exothermic. Adducts are lighter in colour as compared to parent phenoxides. Analytical data of all the complexes are consistent with the proposed stoichiometric composition (Table 1). Molar conductance values of millimolar solutions of these adducts in nitrobenzene indicated that they are non-electrolytes while molecular weight determinations in nitrobenzene suggest that they exist as monomers in this solvent.

Infrared spectra of these compounds have shown all the bands, which are characteristic of the coordinated ligand. Entirely new bands around 290-270 cm^{-1} region have been assigned to $\upsilon_{(Zr\text{-}N)}$ modes. Interestingly, no band that could be assigned to bridging Zr–O→Zr modes in any of the adducts has been observed suggesting thereby that there is a breakdown of dimeric structure of the parent phenoxides on adduct formation. On the basis of limited analytical, conductance, molecular weight determination and IR spectral data, an octahedral structure may tentatively be assigned for these addition compounds.
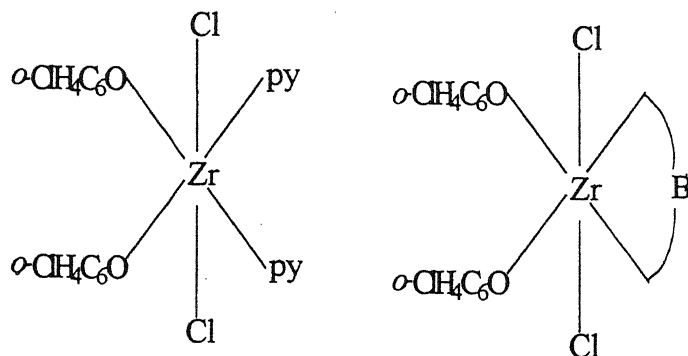
References

1. Tietze, L. F., Buhr, W., Looft, J. & Grote, T. (1998) *Chem. Eur. J.* **4**(8) : 1554.
2. Tietze, L.F. & Buhr, W. (1995) *Angew Chem. Int. Ed. Engl.* **34**(12) : 1366.
3. Natarajan, M., Nalini, P., Dawn, S.S., Marry, D. & Balu, K. (2001) *J. Sci. and Ind. Res.* **60** : 348.
4. Khallow, K. I., Sulayman, K. D. & Ezzat, S. S. (2001) *Bulletino Chimico Farmaceutico* **140**(4) : 224; C. A. (2002) **136** 256227.
5. Chan, M. C. W., Tam, K. H., Pui Y. L. & Zhu, N. Y. (2002) *J. Chem. Soc., Dalton Trans.* 3085.
6. Shiraki, Y., Nakamoto, Y. & Souma, Y. (2002) *Journal of Molecular Catalysis A-Chemical* **187** : 283.
7. Krohn, K. & Kupke, J. (1998) *Eur. J. Org. Chem.* 679.
8. Terao, J., Torii, K., Saito, K., Kambe, N., Baba, A. & Sonoda, N. (1998) *Angew Chem. Int. Ed.* **37**(19) : 2653.
9. Shah, A., Singh, A. & Mehrotra, R. C. (1993) *Indian J. Chem.* **32** A : 632.
10. Steffey, B. D., Diego, N. T., Chebi, E., Kreschner, J. L., Fanwick, P. E. & Rothwell, I. P. (1990) *Polyhedron* **9** : 839.
11. Malhotra, K. C., Mehrotra, G. & Chaudhry, S. C. (1980) *Nat. Acad. Sci. Lett.* **3** : 21.
12. Clark, R. G., Nielson, J. A. & Richard, E. F. C. (1987) *Polyhedron* **6** :1765.
13. Shah, A., Singh A. & Mehrotra, R. C. (1986) *Polyhedron* **5** :1285.
14. Bradley, D. C. (1960) *Prog. Inorg. Chem.* **2** :316.
15. Clark, R. J. H. (1968) *The Chemistry of Titanium and Vanadium,* Elsevier, New York, p. 298.
16. Watenpaugh, K. & Caughlan, C. N. (1966) *Inorg. Chem.* **5** :1782.
17. Malhotra, K. C., Sharma, N. & Chaudhry, S. C. (1981) *Trans. Metal Chem.* **6** : 238.
18. Chaudhry, S. C., Mehta, S. & Gupta, J. (1991) *Proc. Nat. Acad. Sci. India* **61**(A) : 341.

PROC. NAT. ACAD. SCI. INDIA, 75 (A), I, 2005

Kinetics of oxidation of alanine by chloramine – T in perchloric acid medium, catalysed by Os (VIII)

R. A. SINGH* and V. K. SRIVASTAVA

*Chemical Kinetics Research Laboratory, Department of Chemistry, T. D. P. G. College, Jaunpur - 222 002, India

Email- rasinghtdc@rediffmail.com

Received December 22, 2003; Revised March 4, 2004; Accepted April 15, 2004

Abstract

Kinetics of oxidation of alanine by chloramine – T have been studied in perchloric acid medium. The product of oxidation of alanine are ammonia, carbon dioxide and acetaldehyde. The reaction shows first order kinetics with [CAT], first order kinetics with alanine and also it is dependent on first power of concentration of catalyst. During the reaction it is observed that there is a negative effect of perchloric acid concentration. The rate of oxidation is independent of ionic strength of medium, indicating interaction in rate determining step is ion-dipole type, not ion-ion type. A suitable mechanism consistent with kinetic data has been proposed.

(**Keywords** : chloramine–T/alanine/osmiumtetroxide/perchloric Acid)

Introduction

Kinetics of oxidation of alanine by different oxidants like bromamine–B, hexacyanoferrate (III), N-bromosuccinimide, N-bromoacetamide, pyridinium bromochromate with catalyst and without catalyst have been investigated previously[1]. The oxidation of alanine with chloramine-T catalysed by OsO_4 have yet not been reported. The present investigation reports oxidation of alanine by CAT in presence of OsO_4 catalyst in acidic medium. Here the order of reaction with respect to each reactant is determined and also the effect of temperature is investigated to understand the nature of the reaction. With the help of temperature measurements the various thermodynamic parameters have been calculated.

Materials and Method

The requisite amount of standard solution of each of alanine, perchloric acid, osmium tetroxide, and water were taken in a reaction vessel and placed in an electrically operated thermostatic digital water bath to maintain the desired temperature (30°C). In another conical flask required volume of chloramine-T was taken which was also kept in same thermostat to attain the same temperature. When the solution of both reaction vessel and conical flask attained the temperature of thermostat, the solution of chloramine-T was poured in the solution of reaction vessel and immediately a stop watch was started to record the time at the beginning of reaction. After vigorously shaking the reaction mixture for a few seconds, 10 ml of reaction mixture was immediately taken out and acidified KI solution was added in it. The equivalent I_2 liberated was titrated with standard hypo solution using starch as indicator. The estimation of unconsumed chloramine-T was carried out iodometrically at different intervals of time. These titre values were used for calculation of rate constant.

The above kinetic procedure was followed at different initial concentrations of various reagents used in acidic media at different temperatures *viz.* 25, 30, 35 & 40°C. These kinetic run were used to ascertain the dependence of the reaction on various reagents used here. The rate of reaction – (*dc/ dt*) was calculated from the slopes of the curve plotted between unconsumed chloramine-T and time[6].

Result and Discussion

(1) Effect of oxidant : The plot of [CAT] (chloramine-T) against - (*dc / dt*), at fixed concen-

tration of alanine, medium and catalyst is a straight line with unit slope indicating first order kinetics with respect to [CAT]. The first order rate constants are independent of initial concentration of CAT.

Table 1– Variation of rate with oxidant concentration

$[HClO_4] \times 10^3 = 1.00$ mol dm^{-3}, [Alanine] x $10^3 = 2.50$ mol dm^{-3},
$[OsO_4] \times 10^6 = 5.00$ mol dm^{-3}, T - 30^0 C

[CAT] x 10^3 (mol dm^{-3})	0.50	1.00	1.50	2.00	2.50
$-(dc/dt) \times 10^8$ (mol dm^{-3} s^{-1})	1.11	2.22	2.94	3.77	4.90
$k_1 \times 10^4$ (s^{-1})	5.55	3.70	3.19	2.85	3.02

(2) Effect of medium : The rate of reaction decreases with increase in perchloric acid (medium) concentration. This suggests that H^+ ions produced by medium reacts with alanine to form a species which is non reactive[2]. The reaction is therefore hindered. The plot of $[HClO_4]$ *vs* rate is a straight line with negative slope.

Table 2 –Variation of rate with medium concentration

[Alanine]x10^3=2.50 mol dm^{-3}, [CAT]x10^4=2.00 mol dm^{-3},
$[OsO_4] \times 10^6$=5.00 mol dm^{-3}, T = 30^0 C

$[HClO_4]$ (mol dm^{-3})	1.50	2.00	2.50	3.00	3.50
$-(dc/dt) \times 10^8$ (mol dm^{-3} s^{-1})	12.70	10.00	7.00	4.11	1.60
$k_1 \times 10^4$ (s^{-1})	9.76	7.69	5.38	3.16	1.23

(3) Effect of Substrate : When the concentration of alanine is increased, by keeping the concentration of other reactants constant, it is observed that the rate of reaction increases. When the graph is plotted in [alanine] *vs* rate, it is observed that the slop of the graph is one. Therefore reactions shows first order kinetics with respect to alanine concentration.

Table 3- Variation of rate with substrate concentration

$[HClO_4] \times 10^3 = 1.00$ mol dm^{-3}, [CAT]x10^4=2.00 mol dm^{-3},
$[OsO_4] \times 10^6 = 5.00$ mol dm^{-3}, T = 30^0 C

[Alanine]x10^3 (mol dm^{-3})	0.50	1.00	1.50	2.00	2.50
$-(dc/dt) \times 10^8$ (mol dm^{-3} s^{-1})	1.92	3.22	4.69	6.66	8.33
$k_1 \times 10^4$ (s^{-1})	1.60	2.60	3.90	5.55	6.94

(4) Effect of Catalyst : It is observed that the rate of reaction is directly proportional to the first power of concentration of OsO_4 and the plot $[OsO_4]$ *vs* $-(dc/dt)$ gives a straight line showing first order dependence on $[OsO_4]$

Table 4 -Variation of rate with catalyst concentration

$[HClO_4]$x10^3=1.00 mol dm^{-3}, [Alanine]x10^3=2.50 mol dm^{-3},
[CAT] x 10^4 = 2.00 mol dm^{-3}, T=30°C

$[OsO_4] \times 10^6$ (mol dm^{-3})	1.00	2.00	3.00	4.00	5.00
$-(dc/dt) \times 10^8$ (mol dm^{-3} s^{-1})	1.59	3.09	4.61	5.97	7.38
$k_1 \times 10^4$ (s^{-1})	1.22	2.37	3.54	4.59	5.83

(5) Effect of Ionic strength : The rate of reaction does not changes on increasing the concentration of $NaClO_4$, responsible for change of ionic strength of medium[3]. The value of – *(dc/dt)* remains approximately constant on changing the concentration of $NaClO_4$, showing negligible effect of ionic strength.

Table 5 - Variation of ionic strength

$[HClO_4]\times10^3$=1.00mol dm^{-3}, $[CAT]\times10^4$=2.00 mol dm^{-3}, [Alanine] x 10^3 = 2.00 mol dm^{-3}, $[OsO_4]$ x 10^6 = 5.00 mol dm^{-3}. T = 30^0 C					
$[NaClO_4]\times10^3$ (mol dm^{-3})	0.00	1.00	2.00	3.00	4.00
$-(dc/dt)\times10^8$ (mol dm^{-3} s^{-1})	1.00	2.00	3.00	4.00	5.00
$k_1\times10^4$ (s^{-1})	5.13	4.97	4.90	5.16	4.94

(6) Effect of Temperature : Observations at 25, 30, 35 and 40°C shows that the rate of reaction increases gradually with temperature. In this temperature range the plot of log – (dc/dt) *vs* $(1/T)$ is a straight line according to Arrhenius equation[4]. With the help of this plot the value of activation energy Ea is obtained as 10.49 k J mol^{-1}

Table 6 – Variation of rate with temperature.

$[HClO_4]\times10^3$=1.00 mol dm^{-3}, $[Alanine]\times10^3$=3.00 mol dm^{-3} $[CAT]\times10^4$=2.00 mol dm^{-3}, $[OsO_4]\times10^6$= 5.00 mol dm^{-3}				
T °C	25	30	35	40
$-(dc/dt)\times10^8$ (mol dm^{-3} s^{-1})	2.17	2.77	3.95	5.13
$k_1\times10^4$ (s^{-1})	1.80	2.30	3.29	4.27

Table 7– Other thermodynamic parameters at T = 30^0C

log A	3.95
ΔS^*	- 41.27 $Jk^{-1}mol^{-1}$
ΔH^*	41.52 $kJmol^{-1}$
ΔG^*	54.02 $kJmol^{-1}$

The value of – (dc/dt) was determined at certain fixed concentration of chloramine–T at which hardly 20 – 25% reaction had occurred[7].

The value of k_1 i.e. first order rate constant was calculated from the formula

$$k_1 = \frac{-(dc/dt)}{[CAT]^*}$$

here $[CAT]^*$ is concentration of CAT at which rate is measured.

Mechanism

In accordance with experimental results the possible proposed mechanism is given below[8], where S proposed stands for alanine

$$S + H^+ \underset{k_{-1}}{\overset{k_1}{\rightleftharpoons}} SH^+ \text{(non reactive)} \quad \text{(a)}$$

$$S + H_2OsO_5 \underset{k_{-2}}{\overset{k_2}{\rightleftharpoons}} \underset{\text{Complex}}{C_1} + H^+ \quad \text{(b)}$$

$$C_1 + (CAT^-) \xrightarrow{k_d} [H_3OsO_5]^+ + \text{Product} \quad \text{(c)}$$

$$[H_3OsO_5]^+ + (CAT^-) \longrightarrow [H_2OsO_5] + (CAT)^{/} \quad \text{(d)}$$
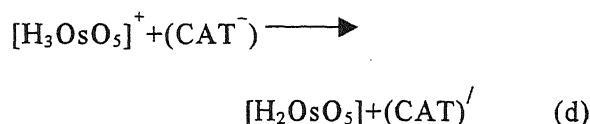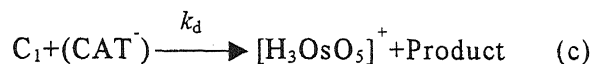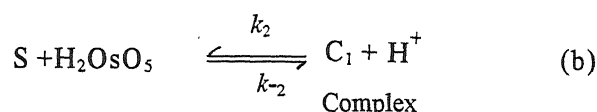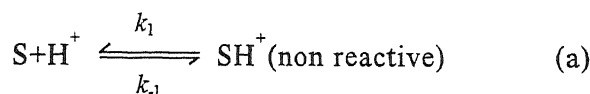
$(CAT)^{/}$ represents $CH_3C_6H_4SO_2NHCl$ and the product is corresponding aldehyde i.e. acetal-dehyde.

The rate of loss of CAT is given as

$$-\frac{d[CAT]}{dt} \quad k_d\,[C_1]\,[CAT^-] \quad (1)$$

On applying steady state approximation to $[C_1]$ we have from step (b) and (c)

$$[C_1] = \frac{k_2\,[S][H_2OsO_5]}{k_{-2}\,[H^+] + k_d[CAT^-]} \quad (2)$$

On comparing eqn. (1) & (2), we have

$$-\frac{d[CAT^-]}{dt} = \frac{k_d k_2 [S][H_2OsO_5][CAT^-]}{k_{-2}[H^+] + k_d[CAT^-]} \quad (3)$$

on assuming $k_2 [H^+] > k_d [CAT^-]$ we have

$$-\frac{d[CAT^-]}{dt} = \frac{k_d k_2 [S][H_2OsO_5][CAT^-]}{k_{-2}[H^+]} \quad (4)$$

Since $[CAT^-] = [CAT]$

$$-\frac{d[CAT]}{dt} = \frac{k_d K_2 [S][H_2OsO_5][CAT]}{[H^+]} \quad (5)$$

where $K_2 = \frac{k_2}{k_2}$

The rate law (5) fully explains all the observed kinetics with respect to chloramine-T alanine, $[H^+]$ and osmium tetroxide.

Acknowledgements

The authors thank the U.G.C. New Delhi, for financial assistance in the form of a major project; and to Dr. R.S. Singh, Principal T.D.P.G. College Jaunpur for his kind support.

References

1. Krishana, B. & Singh, H.S. (1996) *Z. Phys. Chem.*, **231** : 399
2. Mayell, J.S. & Engrg (1968) *Chem. (Proc. Res. Divel)*, 129
3. Singh, M.P. (1968) *Aust. J. Chem.* **21** : 193.
4. Swaranlakshmi, N., Uma. V., Sethuran B. & Rao, T.N. (1987), *Indian J. Chem. Sec. A*, **26** : 592.
5. Kothari, S. & Banerji, K.K. (1997) *Indian. J. Chem. Sec. B*, **36** :1156
6. Narayanan, N. & Balusubramanian, T.R. (1984) *Indian J. Chem. Sec. B*, **25**: 229.
7. Singh, B., Ratan, A. & Singh, D. (1990) *Oxidation Comm.* **13** : 230.
8. Singh, A.K. (1988) *J. Mol Cat.* **48** : 207
9. Nalwaya, N., Jain, A. & Hiran, B.L. (2002) *J. Indian Chem. Soc.* **79** : 587.

PROC. NAT. ACAD. SCI. INDIA, 75 (A), I, 2005

Photocatalytic bleaching of chromotrop-2R over zinc oxide particulate system

NILESH JAIN, SHARAD KOTHARI and RAMESHWAR AMETA*

*P.G. Department of Chemistry, Government College, Banswara-327001, India.

E-mail:kotharisharad2003@yahoo.com.in

Received April 29, 2003; Revised March 3, 2004; Accepted April 26, 2004

Abstract

The photocatalytic bleaching of Chromotrop-2R has been observed spectrophotometrically in presence of zinc oxide. The effects of various parameters like dye concentration, pH, amount of semiconductor, light intensity on the rate of the photocatalytic bleaching are observed. A tentative mechanism for the photocatalytic bleaching of Chromotrop-2R is proposed.

(Key words : photocatalytic bleaching / chromotrop- 2R / photocatalyst)

Introduction

Tomkiewicz[1] reported the scalling properties in photocatalysis. Volodin[2] reported the photoinduce phenomena on the surface of wide-band-gap oxide catalyst. Effect of Na_2CO_3 addition on photocatalytic decomposition of liquid water over various semiconductor catalyst was investigated by Sayama and Arakawa[3]. Matthews[4] reported the kinetic of photocatalytic bleaching of methylene blue on TiO_2 surface where as photobleaching of methyl orange has been reported by Mills *et al*[5,6]. Photobleaching of basic blue-24, over zinc oxide particulate system has been reported by Ameta *et al*[7]. Chen and Chau[8] reported the photobleaching of methyl orange in aqueous solution with suspended TiO_2 and Sharma *et al*[9] investigated photocatalytic bleaching of orange-G in aqueous ZnO solutions. No work has been reported on photocatalytic bleaching of chromotrop-2R. This was the motivation behind the present work.

Materials and Method

Chromotrop-2R and zinc oxide were respectively obtained from Reidel and Merck. The stock solution of chromotrop-2R was prepared in doubly distilled water. 0.6 g of zinc oxide was added to 50.0 mL [1.06×10^{-4}M] solution of chromotrop-2R. A Mysore 200W tungsten lamp was used as irradiation. A water filter was used to cut-off thermal radiations. The desired pH of the solution was adjusted by addition of previously standardized H_2SO_4/ NaOH solutions. The pH of the solution was measured by digital pH meter (Systronics model 335). The intensity of light was measured by a Surya Mapi (CEL-SM-201) solarimeter. The progress of the reaction was measured by spectrophotometer (Systronics model 166). For absorbance measurements the solution was made free from ZnO particles and other impurities by centrifuging.

Results and Discussion

The photocatalytic bleaching of chromotrop-2R was observed at λ_{max} = 500 nm. The optimum condition was obtained at [chromotrop-2R] = 1.06 x 10^{-4}M,light intensity = 28 mW cm^{-2},pH = 10.0, ZnO = 0.60 g and temperature = 308 K.

$$\text{Rate} = k\,[\text{chromotrop-2R}]$$

The plot of 2+log O.D. *vs.* exposure time is a straight line which indicates that the photocatalytic bleaching of chromotrop-2R follow psuedo first

order kinetics. The rate constant (k) for the reaction was determined using the expression.

$$k = 2.303 \times \text{slope}$$
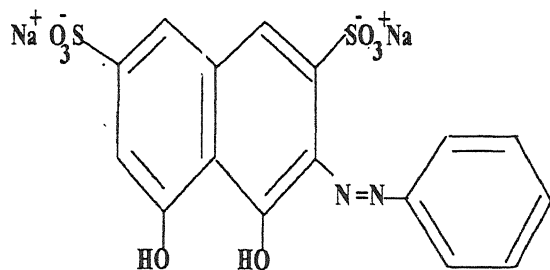
Chromotrop-2R

Effect of Variation of pH : The effect of variation of pH on the rate of photocatalytic bleaching of chromotrop-2R was investigated and is reported in Table 1. ZnO dissolves in the presence of highly acidic media, so photocatalytic bleaching could not be investigated in lower pH range. The rate of photocatalytic bleaching of chromotrop-2R increases with increase in pH up to a pH value of 10.0 and then decreases again with increase in pH value above 10.0. This behaviour may be explained on the basis that the increase in the rate of photocatalytic bleaching may be due to the increased availability of OH^- at higher pH values. By combining with holes, OH^- ions will generate more hydroxyl radicals ($OH^\bullet$) which are considered responsible for the photocatalytic bleaching.

Above a pH value of 10.0, the more OH^- ions will compete with the electron rich dye. The OH^- ions will make the surface of the semiconductor negatively charged and as a consequence of repulsive force between two negatively charged species (OH^- ions and the electron rich dye) the approach of chromotrop-2R molecules to the semiconductor surface will be retarded. This will result in a decrease in the rate of photocatalytic bleaching of chromotrop-2R dye.

Table 1– The dependence of the pseudo first order rate constant k for the photocatalytic bleaching of chromotrop-2R on various parameters at 308K.

pH[a]	$k \times 10^5$ (s-1)	[Dye][b] x 10^4 M	$k \times 10^5$ (s^{-1})	Mass of ZnO[c]/g	$k \times 10^5$ (s^{-1})	I^d (/mWcm^{-2})	$k \times 10^5$ (s^{-1})
6.0	1.82	0.50	2.54	0.3	3.64	10.0	2.82
6.5	1.87	0.62	3.02	0.4	3.94	17.5	3.40
7.0	2.00	0.71	3.32	0.5	4.35	22.5	3.98
7.5	2.09	0.75	3.46	0.6	4.80	28.0	4.78
8.0	2.24	0.81	3.76	0.7	4.79	32.5	5.48
8.5	2.44	1.06	4.79	0.8	4.80	35.0	5.80
9.0	2.66	1.12	4.70			40.0	6.52
9.5	2.92	1.36	4.58			45.0	7.00
10.0	4.79	1.67	4.42				
10.5	3.80	2.13	4.22				
11.0	3.56						

a. [CM] =1.06×10^{-4}M, ZnO= 0.6 g, light intensity = 28.0 mWcm^{-2}

b. ZnO = 0.6 g, pH = 10.0, light intensity = 28.0 mWcm^{-2}

c. [CM] = 1.06×10^{-4}M, pH= 10.0, light intensity = 28.0 mWcm^{-2}

d. [CM] = 1.06×10^{-4}M, pH=10.0, ZnO = 0.60 g.

Effect of variation of dye concentration : The effect of variation of dye concentration on the rate of the reaction was also studied by using different concentration of the chromotrop-2R solution. The results are given in Table 1. It was observed that as the concentration of chromotrop-2R is increased, the rate of photocatalytic bleaching also found to increase, reaching a maximum at 1.06×10^{-4} M. Further increase in concentration resulted in to a decrease in the rate of photocatalytic bleaching . It may be due to the fact that as the concentration of the dye was increased, more dye molecules were available for excitation and for energy transfer. But if the concentration of chromotrop - 2R was increased above 1.06×10^{-4} M, the dye will start acting as a filter for the incident light. It will prohibit the desired light intensity to reach the dye molecules near the semiconductor particles and thus a decrease in the rate of photocatalytic bleaching .

Effect of amount of ZnO : The effect of variation of amount of ZnO on the rate of the photocatalytic bleaching of the chromotrop-2R was also observed. The results are reported in Table 1. It was observed that the rate of reaction increases with increase in the amount of ZnO (0.60 g). Beyond 0.60 g, the rate of reaction becomes constant. This may be due to the fact that in the initial stage as the amount of semiconductor increased, the exposed surface area of the semiconductor also increases, but after this limiting value (0.60g), any further increase in the amount of semiconductor will not increase the exposed surface area but increase the thickness of the semiconductor layer.

Effect of variation of light intensity : The effect of variation of light intensity on the rate of photocatalytic bleaching of chromotrop-2R was observed. The results are reported in Table 1. It may be due to the fact that increase in light intensity increases the rate of photocatalytic bleaching. As the intensity of light increases, the number of photons striking per unit area of the semiconductor (ZnO) also increases. A linear behaviour between light intensity and the rate of reaction was observed. Since an increase in the light intensity increases the temperature of dye solution and a thermal reaction may occur, therefore, higher intensities were avoided.

Mechanism : On the basis of the observed data, the following tentative mechanism may be proposed for photocatalytic bleaching of chromotrop-2R.

$$^{1}CM_{0} \xrightarrow{h\nu} {}^{1}CM_{1}$$

$$^{1}CM_{1} \xrightarrow{ISC} {}^{3}CM_{1}$$

$$^{3}CM_{1} + ZnO \longrightarrow CM^{+} + ZnO(e^{-})$$

$$ZnO(e^{-}) + O_2 \longrightarrow ZnO + O_2^{-\bullet}$$

$$CM^{+} + OH^{-} \longrightarrow CM + OH^{\bullet}$$

$$CM + OH^{\bullet} \longrightarrow \text{Product}$$
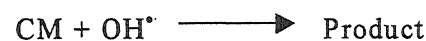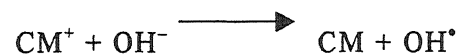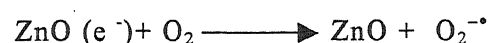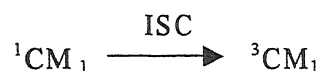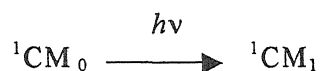
When the solution of the chromotrop-2R dye(CM) was exposed to light in presence of zinc oxide, initially the $^{1}CM_{0}$ molecules were excited to first excited singlet state($^{1}CM_{1}$). Then there excited molecules were transferred to the triplet state through inter system crossing(ISC). The triplet dye ($^{3}CM_{1}$) may donate its electron to the semi-conductor and the dye becomes positively charged. The dissolved oxygen of the solution will pull an electron from the conduction band of the semiconductor, thus, regenerating the semicon-ductor.

The positively charged molecules of the dye (CM^{+}) will immediately react with OH^{-} ions to form $OH^{\bullet}$ radicals which will convert the dye molecules into products, which are colorless. The participation of $OH^{\bullet}$ as an active oxidizing species was confirmed by carrying out same reaction in presence of some hydroxyl radical scavengers like 2-propanol, where the rate of bleaching was drastically reduced.

Acknowledgements

The authors thank the P.G. Department of Chemistry, Govt. College, Banaswara for providing the necessary laboratory facilities. Thanks are also due to Prof. S.C.Ameta and Dr. B.K.Sharma for their critical discussions.

References

1. Tomkiewicz, M.(2000) *Catal. Today* **58** : 115.
2. Volodin, A.M. (2000) *Catal. Today* **58** : 103.
3. Sayama, K. & Arakawa, H. (1994) *J. Photochem. Photobiol.* 77A : 243.
4. Matthews, R.W.(1991) *Water Poll. Res. J. Canada* **25** : 1169.
5. Mills, A. & Green (1999) *J. Photochem, Photobiol.* **59A** : 199.
6. Peral, J. & Mills, A. (1993) *J. Photochem. Photobiol.* **73A** : 47.
7. Ameta, R., Kumari, C., Bhatt, C.V. & Ameta, S.C. (1998) *Ind. Quim.* **333** : 36.
8. Chen, L.C. & Chau, T.C. (1993) *J. Mol. Catal.* **85** : 201.
9. Sharma, A., Ameta, R., Mathur, R.P. & Ameta, S.C. (1995) *Hung. J.Ind. Chem.* **23** : 31.

PROC. NAT. ACAD. SCI. INDIA, 75 (A), I, 2005

Influence of personal characteristics on trace / toxic metal levels in hair

RITA MEHRA* and MEENU JUNEJA

Department of Pure and Applied Chemistry, M.D.S. University, Ajmer-305 009, India.

Received April 30, 2002; Revised April 5, 2004; Accepted June 2, 2004

Abstract

The influence of various parameters *viz.* use of cosmetics, food and drinking habit of workers exposed to metal pollution, have been investigated by analyzing scalp hair of the subjects for Pb, Cd, Cu, Fe, Ni, Zn and Mn metals and grouped on the basis of age. It was observed that Pb and Cd hair levels were high in non-vegetarian subjects as compared to vegetarian subjects. Higher Cd and Cu levels were found in controls with respect to dye users and Ni and Zn levels with respect to henna users. It was also observed that there is no contribution of liquor towards hair metal concentration. Higher levels of hair metal concentration was observed in vegetarian subjects of 31-40 years age group than non-vegetarian subjects. In dye users Pb, Cd, Cu, Ni and Zn hair metal concentrations decreased in contrast to Fe and Mn, which increase with increasing age.

(**Keywords** : atomic absorption spectrophotometry/ human hair/ toxic/trace metal)

Introduction

In recent years there has been growing interest in the use of trace element concentrations in human hair for monitoring the body burden of trace elements[1-5]. Many human tissues like, human hair, bone, teeth and nails can be used as biomarkers of environmental burden of metal levels[6-7]. Jenkins describes the importance of using human hair and nail for biological monitoring in environmental and occupational exposures with geographical distribution and chronic trends[8]. Human hair is an attractive biological material because of the simplicity of sampling, transport and handling, as well as because it can provide information about concentrations of some trace elements that are considerably more concentrated in hair than in other biological materials[9-10]. Concentrations of many elements in scalp hair are relatively higher than those in fluids or other easily accessible tissues. Determining trace elements in human hair has importance in biological, medical and environmental studies, as human hair represents an interesting biological matrix for studies in both the organic and inorganic field[11].

Hair may reflect concentrations of minerals that were in the hair follicle at the time the hair was formed. Many workers reported that hair analysis for trace metal status provided a useful tool for monitoring human exposure to various factors for varying amount of metals[12-21] depending upon nutrition, environment, race, health, age, sex, diet, body location, hair color, as well as drugs taken by subjects.

The lack of available data about the concentration of the metals in relation to such parameters, considered contemporarily, led to the study of hair samples collected from different subjects. The present study was undertaken to estimate the trace metal concentration in humans using hair as a biopsy material. The hair metal burden with three parameters-food habit, drinking habit and use of hair cosmetics by different subjects has also been assessed.

Materials and Method

Sampling: Hair samples were collected from the nape of the scalp by cutting approximately 2 mm from the scalp using a pair of sterlised stainless steel scissors washed with ethanol. All hair samples were kept sealed in plastic bags prior to analysis. Samples taken weighed about one gram. A questionnaire was filled up for the personal and medical history of the subjects according to World Health Organization.

Washing: The hair samples were cut into pieces of about 2 cm. Samples prewashed with nonionic detergent, were soaked in deionized water for 10 min. This was followed by soaking in acetone to remove external contamination, followed by washing with deionized water, then the samples were dried at 110°C for one hour and stored in a desiccator [22].

Digestion and preparation of water clear solution: The dried hair samples were wet digested with 10 ml of 6:1 mixture of concentrated nitric acid and concentrated perchloric acid and kept overnight at room temperature and consequently heated at 160-180°C until complete evaporation and obtaining a crystalline white dry deposit or a water clear solution. The sediment was then diluted with 0.1 N nitric acid.

Analysis: The concentration of metals were determined by using Perkin Elmer AAS model – 250 with air acetylene flame. A series of standards were prepared in deionized water for instrumental calibration by diluting commercial standards containing 1000 ppm of the metals. A number of blanks were also prepared for minimization of errors due to contamination. The main instrumental parameters (like wave length, band width, lamp current) for the estimation of specific metals by Atomic Absorption Spectrophotometer were also set up for each metal separately.

Results and Discussion

The variation of metal concentrations in human hair with varying food habit, drinking habit and cosmetic use by different subjects has been discussed.

Fig. 1 shows the mean concentrations of Pb Cd, Cu, Fe, Ni, Zn and Mn in hair of vegetarian and non-vegetarian subjects. The mean values (in μg/g) ±S.D. for vegetarian subjects were Pb 32.97±70.25, Cd 0.63±0.75, Cu 11.53±7.47, Fe 184.27±134.03, Ni 28.87±22.03, Zn 203.17±57.28 and Mn 8.29±8.87. Comparison with non-vegetarian subjects reveal that the latter had some-what higher levels of Pb and Cd as exception in contrast to Cu, Fe, Zn and Mn content in hair of vegetarian subjects, although all were nonsignificant at $P < 0.05$. The mean Ni concentrations were approximately same in both kind of subjects. It has also been reported[23-27] that absorption rate of inhaled cadmium is much higher (40-60%) than that taken through gastrointestinal track (2-5%). The lead content in the food can be influenced by a number of factors including biological uptake from soils into plants, use of lead, arsenic pesticides and addition of lead by leaching from improperly glazed pottery used as food storage or dining utensils. For the remaining metals, the higher values in vegetarian subjects are supported by the analysis of different type of fruits as given by Mahaffey *et al*[28]. Iron is a nutritionally essential metal and the increased iron levels in hair of subjects were statistically analysed to observe the effect of food habit alongwith other elements. The statistically nonsignificant results with respect to food habit for other micronutrients confirm that the raised levels in scalp hair mainly reflects occupational exposure to the metals besides other factors.
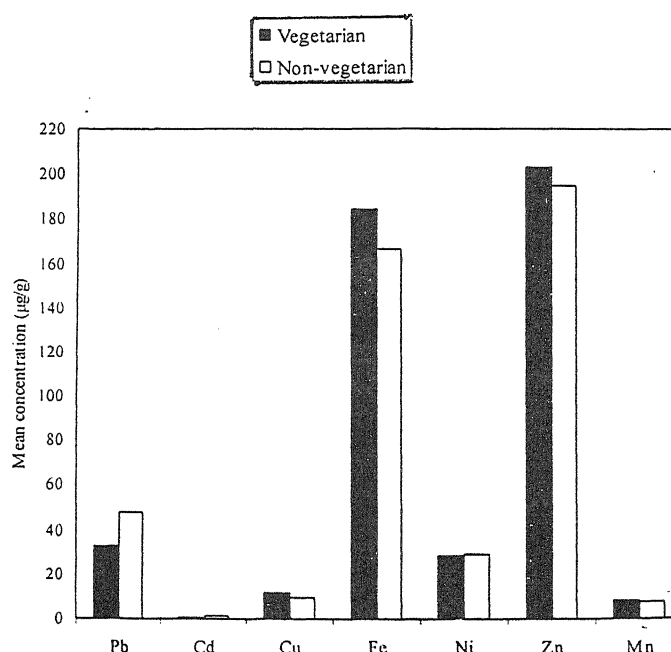
Fig. 1–Mean Pb, Cd, Cu, Fe, Ni, Zn and Mn concentration in hair of subjects with vegetarian and non-vegetarian food intake.

The variation in the mean hair metal levels due to the application of cosmetics like dye, henna (mehndi) on it, has been shown in Fig 2. It has been reported in literature that the hair cosmetics contain metal salts or the complexes which contribute to the concentration of the metals either through absorption of the salts followed by uptake by hair root or by the absorption on the shaft of the hair[29]. The metal ions in the dye formulation or hair cosmetics are present in the coloring agents and, therefore, many of the metals found in hair like Al, Be, Co, Cu, Fe, Hg and Zn also appear in the cosmetics or dyes.
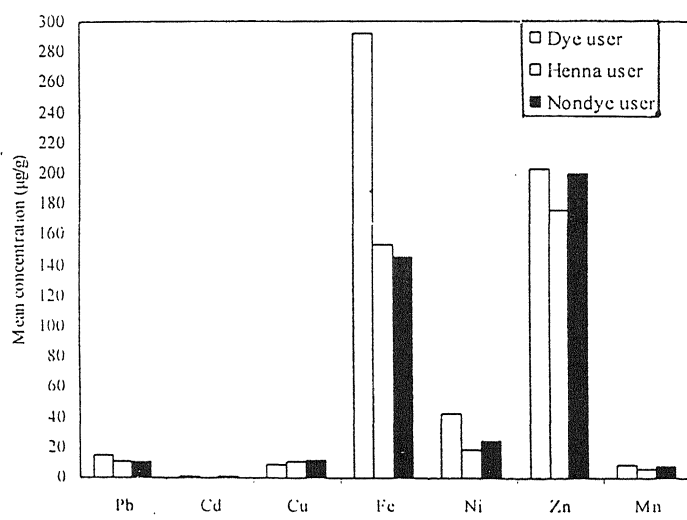
Fig. 2–Mean Pb, Cd, Cu, Fe, Ni, Zn and Mn concentration in hair of subjects with use of cosmetics.

In the present work higher concentrations of Cd and Cu were obtained in the controls with respect to the subjects using dyes but they were not significant. Conversely, elevated levels of Pb, Fe, Ni, Zn and Mn were found in hair applied with dye of which Pb, Fe and Ni levels were significant, and is also in agreement with the reported literature. The variation in individual metal levels is a function of concentration of particular metal present in specific brand of dye used. The significant concentration of lead observed in the hair not applied with dyes is attributed to other factors like place of residence of the subjects in vicinity of heavy traffic areas.

The analysis of samples applied with henna (Mehndi) reveals, that it has no contribution toward adding to the metal concentration in hair. The insignificant data at $P < 0.05$ also affirms this finding. Due to nonavailability of data on the relationship between the amount of henna in hair and trace metal concentration in hair we could not compare our results with those of other researchers. The significant data for Ni and Zn in controls with respect to that of hair applied with henna may be related to the occupational exposure to the metal in the workplace alongwith other factors like smoking and food habits.

No significant variation has been found in metal concentrations of the hair of those who consume alcohol (Fig 3).
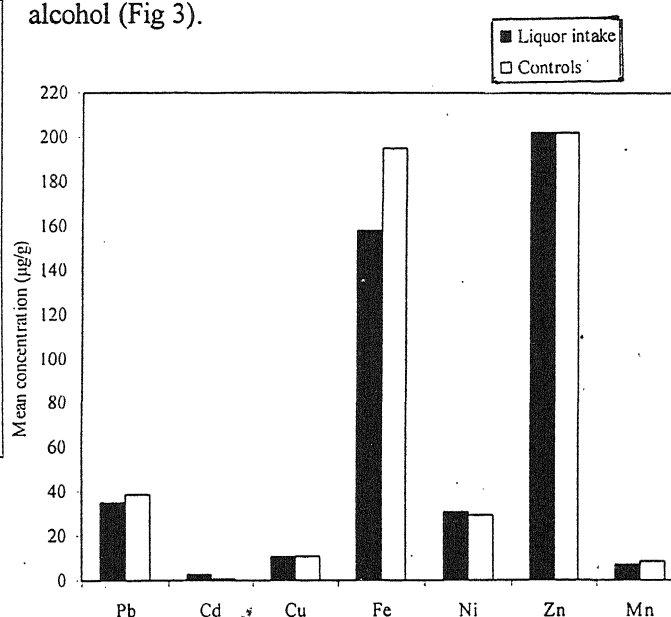
Fig. 3–Mean Pb, Cd, Cu, Fe, Ni, Zn and Mn concentration in hair of subjects with liquor intake and controls.

The agewise picture of the mean concentrations of Pb, Cd, Cu, Fe, Ni, Zn and Mn as a function of food habits is depicted in Table 1. The data in the table reveal that barring 31- 40 years age group in which high concentration of the metals taken for study has been observed in hair with respect to non-vegetarian food type no such generalization could be made for other age groups. Regarding the variation of metal concentrations in between vegetarian subjects of different age groups, from 21-30 to 51- 60 years, it is observed that the levels increase from 21-30 to 31- 40 years age group and thereafter decreases. Similar assessment in between

Table 1– Mean hair metal concentrations as a function of food habit

Subjects	Age in yrs.	Mean concentration of elements (μg/g)±S.D.						
		Pb	Cd	Cu	Fe	Ni	Zn	Mn
Vegetarian	21-30	40.80±89.48	0.65±1.20	10.18±2.66	176.99±66.47	19.56±10.60	200.74±49.93	10.95±18.08
Non-vegetarian	21-30	17.29±12.88	0.47±0.24	8.06±2.73	377.06±58.20	29.74±8.18	165.14±21.14	18.36±2.19
Vegetarian	31-40	27.18±65.16	0.91±0.74	18.06±18.13	215.03±164.58	32.16±25.71	235.91±58.13	8.76±4.76
Non-vegetarian	31-40	61.61±115.75	2.13±5.76	10.23±4.73	152.398±69.34	28.23±16.51	214.94±63.92	8.76±6.08
Vegetarian	41-50	29.38±63.43	0.50±0.47	9.34±3.39	186.11±100.80	28.29±16.94	196.90±47.02	6.29±3.28
Non-vegetarian	41-50	9.34±6.60	0.36±0.30	10.52±4.43	171.25±73.88	25.60±13.72	186.56±46.95	7.38±2.54
Vegetarian	51-60	11.49±5.81	0.40±0.22	13.32±7.49	157.90±107.75	33.39±20.95	171.92±26.06	7.99±3.27
Non-vegetarian	51-60	42.69±64.57	0.52±0.40	8.95±4.46	185.29±43.73	31.73±13.39	179.38±23.51	7.96±1.99

Table 2– Mean hair metal concentrations as a function of hair cosmetics

Subjects	Age in yrs.	Mean concentration of elements (µg/g)±S.D.						
		Pb	Cd	Cu	Fe	Ni	Zn	Mn
Dye User	21-30	—	—	—	—	—	—	—
Henna User	21-30	20.63±12.56	0.27±0.14	10.25±2.46	160.27±20.99	19.22±5.22	167.98±14.40	7.16±0.87
Non Dye User	21-30	18.58±3.29	0.71±1.19	9.94±3.00	215.14±102.52	19.46±10.57	205.26±46.16	12.06±18.11
Dye User	31-40	24.55±6.12	0.74±0.44	10.82±1.30	382.82±273.56	52.41±33.60	246.06±150.86	10.49±5.81
Henna User	31-40	10.72±1.18	0.43±0.11	7.68±0.90	116.32±20.71	18.52±1.78	180.31±13.06	4.99±1.98
Non Dye User	31-40	9.19±8.93	2.02±5.21	15.38±15.12	155.88±58.02	26.51±16.84	225.25±70.50	8.95±5.70
Dye User	41-50	6.29±2.02	0.27±0.20	8.64±2.34	153.79±84.37	23.14±11.84	164.46±46.25	7.11±3.01
Henna User	41-50	5.26±4.59	0.22±0.07	11.09±5.48	154.00±83.08	17.75±13.79	181.29±42.76	6.99±3.22
Non Dye User	41-50	4.91±3.58	0.44±0.42	10.23±4.01	152.32±68.11	25.16±11.84	198.55±48.96	6.31±2.16
Dye User	51-60	—	—	—	—	—	—	—
Henna User	51-60	—	—	—	—	—	—	—
Non Dye User	51-60	2.49±1.99	0.46±0.29	11.64±6.30	154.16±81.39	32.41±17.24	179.08±22.56	7.67±3.10

Table 3–Mean hair metal concentrations as a function of drinking habit

Subjects	Age in yrs	Mean concentration of elements (μg/g)± S.D.						
		Pb	Cd	Cu	Fe	Ni	Zn	Mn
Liquor intake	21-30	---	---	---	---	---	---	---
Controls	21-30	10.80±8.76	0.28±0.17	9.31±2.53	214.26±103.17	22.70±11.28	186.47±49.27	13.53±16.86
Liquor intake	31-40	43.39±73.30	3.28±7.08	12.30±6.62	149.80±70.63	28.04±9.74	202.49±41.17	9.13±5.57
Controls	31-40	47.90±107.87	0.56±0.52	14.53±15.28	205.21±145.18	30.93±24.50	225.41±66.58	8.59±5.58
Liquor intake	41-50	10.67±9.07	0.52±0.47	10.31±4.91	161.27±70.55	24.02±13.59	184.03±58.13	7.75±2.98
Controls	41-50	25.53±58.20	0.38±0.34	9.69±3.18	189.10±100.72	30.22±16.58	190.11±44.22	6.86±3.49
Liquor intake	51-60	16.59±13.37	0.56±0.44	7.77±3.72	183.87±43.68	34.23±16.46	182.11±16.80	8.01±2.01
Controls	51-60	30.29±53.54	0.40±0.19	13.35±6.60	134.63±90.00	31.60±18.49	177.70±25.25	7.51±3.59

the different age groups taking non-vegetarian diet shows that there is a decrease in Fe, Ni and Mn concentration up to 41-50 years followed by increase in 51-60 years age group, whereas Pb, Cd, Cu and Zn are found to increase initially followed by a decrease in concentrations in higher age groups. The average values for few metals have also been reported by Mahaffey *et al*[28] in particular food type but the variations of the metal concentrations in contrast to the above observation in other age groups can be accounted for by the fact that workers with non-vegetarian food intake also consume fruits and vegetables. The low levels of metals in higher age groups is due to absorption by the intestinal efficiency which reduces with the age. Other factors inhibiting the metal absorption also tend to reduce their intraluminal solubility or provoke competitive interactions during transportation through mucosa. Besides these, it cannot be ruled out that the chemical form of the metal present in the gut, also influence its absorption because some salt forms which are highly soluble are readily absorbed as compared to those which are relatively less soluble.

Table 2 presents the mean metal concentrations of young and old subjects applying hair cosmetics like hair dye and henna alongwith those not using hair cosmetics taken as controls. Use of dye was limited to only two age groups and it was found that Pb, Cd, Cu, Ni and Zn decreases with increasing age groups in contrast to Fe and Mn which increases with increasing age groups. The concentration of metals were found to decrease in subjects using henna on hair but since henna does not contain these metals, the observation cannot be linked to this parameter. No definite trend could be observed for metal concentration in hair of controls.

As regards the correlation of the elements under study with age groups in subjects using dyes is concerned, it was observed that the concentration decreased from 31-40 to 41-50 years age groups. This signifies lesser absorption of metals with growing age. The alteration of metal concentrations with age group in the group of subjects applying henna as hair cosmetics is erratic showing both the type of changes increase in Pb, Cu, Fe, Zn and Mn and decrease in Cd and Ni. No subjects of 51-60 years age group were found to use henna. This kind of variation shows that this factor is of secondary significance while correlating with hair metal concentrations.

The variation in toxic and trace metals viz Pb, Cd, Cu, Fe, Ni , Zn and Mn in hair of subjects taking liquor alongwith the respective controls are shown in Table 3. Although Cd and Mn levels are apparently high in subjects with drinking habit in all age groups in contrast to Pb, no specific correlation could be drawn since in other metals the variation does not follow a sequence in drinking subjects in different age groups. When the mean hair metal levels in different age groups of drinking subjects were compared, no definite trend was obtained. Similar observation was also noted for those in subjects of varying age not taking liquor. The findings can be supported by the fact that their apparently exist no source of metals in production of liquor and as such no correlation, whatsoever, is expected.

To conclude we can say that while determining the assay of hair for the metals discussed in this paper and to investigate and interpret its linking with food type, cosmetic use and drinking habit of the workers and controls it is suggested that the particular brand of the dye used be also analysed for the metal content so that the magnitude of increase can also be accounted for besides a qualitative correlation between the two. It is also inferred that where analysis of the food stuff is essential for developing a correlation between the food type and hair metal concentrations it is also important to take into account the chemical form of the particular element, competitive interaction of the metals which are chemically similar. The age of the subjects under consideration also plays a role as it affects the intestinal efficiency and hence the absorption and assimilation of the metals in the body tissues.

Acknowledgements

One of the authors greatfully acknowledges the University Grants Commission for financial assistance. We also thank Dr. P.K. Seth, Director ITRC, Lucknow, Dr. K. Lal, Director NPL, New Delhi and Dr. H.N. Saiyed, Director and Dr. D.J. Parikh, Deputy Director NIOH, Ahmedabad for their invaluable cooperation in metal analysis of the samples.

References

1. Mehra, R. & Juneja, M. (2004) *Indian J Biochem Biophys* **41** : 53
2. Ellis, K.J., Yasumura, S. & Cohn, S.H. (1981) *Am J Indust Med* **2** : 323.
3. Ferguson, J.F., Hibhard, K.A. & Tig, R.L.H. (1981) *Environ Pollut (Ser B)* **2** : 235.
4. Mehra, R. & Juneja, M. (2003) *Chem & Environ Res* **12** : 165.
5. Sukumar, A. & Subramanian, R. (1992) *Sci Total Environ* **114** : 161.
6. Nowak, B. & Kozlowski, H. (1998) *Biol Trace Elem Res* **62** : 213.
7. Mehra, R. & Bhalla, S. (1998) *CPCB Publications, DUERM*-**1** LATS/10/1997-98.
8. Jenkins, D.W. (1979) *Toxic trace metals in mammalian hair and nails* EPA-600|4-79-049.
9. Katz, S.A. & Katz, B.R. (1992) *J Appl Toxicol* **12** : 79.
10. Ciszweski, A., Wasiak, W. & Ciszweska, W. (1997) *Anal Chim Acta* **343** : 225.
11. Mehra, R. & Juneja, M. (2003) *Indian J Biochem Biophys* **40** : 141.
12. Shrestha, K. P. & Schrauzer, G.N. (1989) *Sci Total Environ* **79**: 171.
13. Mehra, R. & Juneja, M. (2004) *J Indian Chem Soc*, **81** : 349.
14. Valkovic, V. (1988) *Trace Element Levels*, Vol. 2, CRC Press, Boca Raton, Florida.
15. Sturaro, A., Parvoli, G., Doretti, L., Allegri, G. & Costa, C. (1994) *Biol Trace Elem Res.* **40**: 1.
16. Cosor, Arban, R. & Allegri, G. (1989) *Giorn Ital Chim Clin.* **14** : 73.
17. Klevay, L.M. (1972) *Am J Clin Nutr* **25** : 263.
18. Klevay, L.M. (1973) *Arch Environ Health* **26** : 169.
19. Mehra, R. & Bhalla, S. (1996) *J Indian Coun Chem* **12**: 8.
20. Combs, D.K., Goodrich, R.D. & Meiski, J.C. (1982) *J Am Soc* **54**: 39.
21. Manson, P. & Zlotkin, S. (1985) *Can Med Assoc J* **133** : 186.
22. Chatt, A. & Katz, S.A. (1988) *The Biological basis for Trace Elements in Hair, Hair Analysis, Applications in Biomedical and Environmental Sciences*, VCH Publishers, New York.
23. Arunachalam, J., Gangadharan, S. & Yegnasubramanian, S. (1978) *Nuclear Activation Techniques in the Life Sciences*, IAEA Symp. Vienna, IAEA/STI/Pub/**492** : 499.
24. Izumi, K. (1988) *Tokyo Ika Daizaku Zasshi*, 41 : 43.
25. Herber, R.F.M., Wibowo, A.A.E., Das, H.A., Egger, R.J., VanDeyck, W. & Ziehuis, R.L. (1983) *Internatl Arch Environ Health* **53** : 127.
26. Mahaffey, K.R., Corneliussen, P.E., Jelinek, C.F. & Fiorino, J.A. (1975) *Environ Health Perspect* **12** : 63.
27. Athar, M. & Vohora, S.B. (1995) *Heavy Metals and Environment,* Wiley Eastern Limited, New Delhi.
28. Mahaffey, K.R., Goyer, R.A. & Haseman, J.K. (1973) *J Lab Clin Med* **82** : 92.
29. Commerce Clearing House Inc. (1978) *Food Drug Cosmetic Law Report,* Chicago.

PROC. NAT. ACAD. SCI. INDIA, 75 (A), I, 2005

Applications of fractional calculus

JAIVEER SINGH and C.L.KOUL

Department of Mathematics, Malaviya National Institute of Technology, Jaipur-302 017, India.

Received September 25, 2003; Accepted March 13, 2004

Abstract

As applications of the generalized Lagrange's expansion of a function $f(z)$, provided by Osler in the theory of fractional calculus, six useful results are derived here.

(**Keywords** : Generalized Langrange's expansion/ Generalized class of polynomials/ *H*-functions of one and several variables/ *R-L* fractional derivatives)

Introduction

Osler[1] provided extensions to the familiar Lagrange's expansion of a function $f(z)$ in the theory of fractional calculus. As applications of their generalizations a number of useful results are derived in this paper.

Results Required

(i) The generalized Lagrange expansion given by Osler[1]

$$f(z) = a \sum_{k=-\infty}^{\infty} \left\{ D_z^{ak+\gamma} f(z)\,\theta'(z)[q(z)]^{-ak-\gamma-1} \right\}_{z=z_0}$$

$$\times [\theta(z)]^{ak+\gamma} / \Gamma(ak+\gamma+1)$$

$$0 < a \leq 1 \qquad (1)$$

and its integral analog, also due to Osler[1] is:

$$f(z) = \int_{-\infty}^{\infty} \left\{ D_z^{\eta+\gamma} f(z)\,\theta'(z)[q(z)]^{-\eta-\gamma-1} \right\}_{z=z_0}$$

$$\times [\theta(z)]^{\eta+\gamma} / \Gamma(\eta+\gamma+1)\, d\eta \qquad (2)$$

where

$\theta(z) = (z-z_0)q(z)$, γ being arbitrary and the integral is valid for all z on the simple closed curve C given by $|\theta(z)| = |\theta(0)|$ and $\theta'(z) = \frac{z}{z_0} e^{z/z_0}$.

(ii) Srivastava[2] introduced a general class of polynomials of one variable $S_n^m[x]$ defined and represented as

$$S_n^m[x] = \sum_{k=0}^{n/m} \frac{(-n)_{mk}}{k!} A_{n,k}\, x^k, \; n = 0,1,2,\ldots \qquad (3)$$

where m is an arbitrary positive integer and $A_{n,k}$ $(n, k \geq 0)$ are arbitrary constant coefficients, real or complex.

A general class of multivariable polynomials introduced also by Srivastava[3] is defined and represented in the following form

$$S_{V_1,\ldots,V_n}^{U_1,\ldots,U_n}[z_1,\ldots,z_n] =$$

$$\sum_{k_1=0}^{[V_1/U_1]} \cdots \sum_{k_n=0}^{[V_n/U_n]} \frac{(-V_1)_{U_1 k_1} \cdots (-V_n)_{U_n k_n}}{k_1! \ldots k_n!} \times$$

$$\times A[V_1,k_1;\ldots;V_n,k_n]\, z_1^{k_1} \ldots z_n^{k_n} \qquad (4)$$

$$V_i = 0,1,2,\ldots \quad ; i = 1,\ldots,n$$

where $A\ [V_1,k_1\ ;...;\ V_n,k_n\ ]$ are arbitrary constant coefficients.

(iii) For the definitions of Fox's H-function, *viz.*

$$H[x] = H_{p,q}^{m,n}\left[x \middle| \begin{matrix} (a_j,\alpha_j)_{1,p} \\ (b_j,\beta_j)_{1,q} \end{matrix} \right] \quad (5)$$

and H-function of several variables, *viz.*

$$H\begin{bmatrix} x_1 \\ \vdots \\ x_r \end{bmatrix} = H_{A,C:B',D';...;B^{(r)},D^{(r)}}^{0,\ell:m',n';...;m^{(r)},n^{(r)}} \times$$

$$\times \left[\begin{matrix} x_1 \\ \vdots \\ x_r \end{matrix} \middle| \begin{matrix} (a_j;\alpha'_j,..,\alpha_j^{(r)})_{1,A}\,(c'_j,\gamma'_j)_{1,B'};..; \\ (b_j;\beta'_j,..,\beta_j^{(r)})_{1,C}\,(d'_j,\delta'_j)_{1,D'};..; \end{matrix} \right.$$

$$\times \left. \begin{matrix} (c_j^{(r)},\gamma_j^{(r)})_{1,B^{(r)}} \\ (d_j^{(r)},\delta_j^{(r)})_{1,D^{(r)}} \end{matrix} \right] \quad (6)$$

and for their conditions of existence, etc., we refer to Srivastava *et al*[4]. In case $r = 2$, it reduces to the H-function of two variables.

(iv) The Riemann-Liouville fractional derivative of a function $\phi\ (z)$ is defined and represented as

$$D_z^q\ \phi(z) = \frac{1}{\sqrt{(-q)}} \int_0^z (z-t)^{-q-1}\ \phi(t)\,dt,\ ;$$

for $q<0$

$$= D_z^n\left[D_z^{q-n}\ \phi(z)\right],\ q \geq 0\ ,$$

n being a positive integer such that $n>q$ ... (6 a)

(v) For all q Agal[5]

$$D_z^q\left\{ z^{\lambda}\,e^{bz^k}\ H\begin{bmatrix} k_1 z^{h_1} \\ \vdots \\ k_r z^{h_r} \end{bmatrix} \right\} =$$

$$z^{\lambda-q}\ H_{A+1,C+1:*;0,1}^{0,\ell+1\ :*;1,0} \times$$

$$\times\left[\begin{matrix} E:*;...; \\ F:*;...; \end{matrix}\ k_1 z^{h_1},...,k_r z^{h_r},-bz^k \right] \quad (7)$$

where

$$E \equiv [-\lambda : h_1,...,h_r\ ,k]\ ,$$

$$[a_j\ ;\alpha'_j\ ,...,\alpha_j^{(r)}\ ,0]_{1,A}$$

$$F \equiv [b_j\ :\beta'_j\ ,...,\beta_j^{(r)},0]_{1,c}\ ,$$

$$[-\lambda+q:h_1,...,h_r\ ,k]$$

provided that $b>0,\ k\geq 0,\ h_i>0$,

$$\mathrm{Re}\left(1+\lambda+\sum_{i=1}^{r} h_i\ \frac{d_j^{(i)}}{\delta_j^{(i)}} \right) > 0$$

$$(\ i=1,\ldots,r\ ;\ j=1,\ldots,\ m^{(i)})$$

where $D_z^q\ [f(x)]$ represents the fractional derivative of $f(x)$ of order q.

The appearance of * indicates that the parameters at these places are the same as in the multivariable H-function on right hand side of (6) at the corresponding places.

Main Results

The following results are established here:

Let γ be an arbitrary complex number and let $t > 0$, $t_i > 0$, $(i = 1,\ldots,r)$. Also let

$$y(z,\eta) = exp\left(\frac{z}{z_0}(\eta+\gamma)\right) \times$$

$$\times \left(\frac{z-z_0}{z_0}\right)^{\eta+\gamma} / \Gamma(\eta+\gamma+1)$$

Then, for all z on the closed curve C given by

$$\left|(z-z_0)\exp\left(\frac{z}{z_0}\right)\right| = |z_0|$$

we have

(i) $$\sum_{k=0}^{[v/u]} \frac{(-v)_{uk}}{k!} A_{v,k}(z_0)^k \times$$

$$\times \int_{-\infty}^{\infty} y(z,\eta) H^{0,1:m,n;1,0}_{1,1:\ p,q;\ 0,1} \times$$

$$\times \left[\begin{array}{c|l} xz_0^t & (-\mu-k;t,1) \quad :(a_j,\alpha_j)_{1,p};\ - \\ \eta+\gamma & (-\mu-k+\eta+\gamma;t,1):(b_j,\beta_j)_{1,q};(0,1)\end{array}\right] d\eta$$

$$= \left(\frac{z}{z_0}\right)^{\mu-1} H^{m,n}_{p,q}\left[xz^t \left| \begin{array}{l}(a_j,\alpha_j)_{1,p}\\(b_j,\beta_j)_{1,q}\end{array}\right.\right] S^u_v[z] \qquad (8)$$

provided that

$$\min Re\left[(\mu+t\left(\frac{b_j}{\beta_j}\right)+1\right] > 0,\ 1\le j\le m.$$

(ii) $$\sum_{k=0}^{[v/u]} \frac{(-v)_{uk}}{k!} A_{v,k}(z_0)^k \times$$

$$\times \int_{-\infty}^{\infty} y(z,\eta) H^{0,n_1+1\ \ :*;1,0}_{p_1+1,q_1+1:*;0,1} \times$$

$$\times \left[\begin{array}{c|l} x_1z_0^{t_1} & (-\mu-k;t_1,t_2,1),(a_j;\alpha_j,A_j,0)_{1,p_1}\ ;*;\ - \\ x_2z_0^{t_2} & \\ \eta+\gamma & (-\mu-k+\eta+\gamma;t_1,t_2,1),(b_j,\beta_j,B_j,0)_{1,q_1};*;(0,1)\end{array}\right] d\eta$$

$$= \left(\frac{z}{z_0}\right)^{\mu-1} H^{0,n_1:*}_{p_1,q_1:*}\left[\begin{array}{c} x_1z^t \\ x_2z^t\end{array}\right] S^u_v[z] \qquad (9)$$

provided

$$Re\left[(\mu + t_1\left(\frac{d_i}{\delta_i}\right) + t_2\left(\frac{f_j}{F_j}\right)+1\right] > 0,$$

$$1 \le i \le m_2, 1 \le j \le m_3.$$

(iii) $$\sum_{k_1=0}^{[v_1/u_1]} \cdots \sum_{k_r=0}^{[v_r/u_r]} \frac{(-v_1)_{u_1k_1}\cdots(-v_r)_{u_rk_r}}{k_1!\ \ldots\ k_r!} \times$$

$$\times A[v_1,k_1;\ldots;v_r,k_r] \prod_{i=1}^{r} c_i^{k_i}(z_0)^{\sum_{i=1}^{r} k_i}$$

$$\times \int_{-\infty}^{\infty} y(z,\eta) H^{0,n+1\ \ :*;\ldots;*;1,0}_{p+1,q+1:*;\ldots;*;0,1} d\eta \times$$

$$\times \left[\begin{array}{c|c} x_1 z_0^{t_1} & E_1 : * ;...; * ; - \\ \vdots & \\ x_r z_0^{t_r} & F_1 : * ;...; * ;(0,1) \\ \eta+\gamma & \end{array} \right] = \left(\frac{z}{z_0} \right)^{\mu-1}$$

$$H \left[\begin{array}{c} x_1 z^{t_1} \\ \vdots \\ x_r z_r^{t_r} \end{array} \right] S_{v_1,...,v_r}^{u_1,...,u_r} [c_1 z,...,c_r z] \qquad (10)$$

where

$$E_1 \equiv (-\mu_1 - k_1 ... k_r \; ; t_1,...,t_r, 1) \, ,$$

$$(a_j \, ; \alpha'_j \, ,..., \alpha_j^{(r)}, 0)_{1,p}$$

$$F_1 \equiv (b_j \, ; \beta'_j \, ,..., \beta_j^{(r)}, 0)_{1,q} \, ,$$

$$(\mu - k_1 ... - k_r + \eta + \gamma \; ; t_1,...,t_r, 1)$$

provided $\min \text{Re} \left[(\mu + \sum_{i=1}^{r} t_i \left(\frac{d_j^{(i)}}{\delta_j^{(i)}} \right) + 1 \right] > 0,$

$$j = 1,...,m_v \; ; v = 1,...,r.$$

Method of Derivation

We choose in (2)

$$\theta(z) = (z - z_0) \, e^{\frac{z}{z_0}} \qquad (11)$$

and $f(z) = z^{\mu-1} H_{p,q}^{m,n} \left[xz^t \left| \begin{array}{l} (a_j,\alpha_j)_{1,p} \\ (b_j,\beta_j)_{1,q} \end{array} \right. \right] S_v^u \, [z]$

so that

$\theta'(z) = \frac{z}{z_0} e^{\frac{z}{z_0}}$ and $q(z) = e^{\frac{z}{z_0}}$, then use (7) to arrive at (8).

Similarly (9) and (10) are derived by taking $\theta(z)$ as in (11)

$$f(z) = z^{\mu-1} H_{p_1,q_1:p_2,q_2\,;\,p_3,q_3}^{0,n_1:m_2,n_2;m_3,n_3} \times$$

$$\times \left[\begin{array}{c|l} x_1 z^{t_1} & (a_j,\alpha_j,A_j)_{1,p_1} : (c_j,\gamma_j)_{1,p_2} ; (e_j,E_j)_{1,p_3} \\ x_2 z^{t_2} & (b_j,\beta_j,B_j)_{1,q_1} : (d_j,\delta_j)_{1,q_2} ; (f_j,F_j)_{1,q_3} \end{array} \right] S_v^u [z]$$

and

$$f(z) = z^{\mu-1} H_{p,q:p_1,q_1\,;...;\,p_r,q_r}^{0,n\,:m_1,n_1;...;\,m_r,n_r} \times$$

$$\times \left[\begin{array}{c|l} x_1 z^{t_1} & (a_j,\alpha'_j,...,\alpha_j^{(r)})_{1,p} : (c'_j,\gamma'_j)_{1,p_1} ;...; (c_j^{(r)},\gamma_j^{(r)})_{1,p_r} \\ \vdots & \\ x_r z^{t_r} & (b_j,\beta'_j,...,\beta_j^{(r)})_{1,q} : (d'_j,\delta'_j)_{1,q_1} ;...; (d_j^{(r)},\delta_j^{(r)})_{1,q_r} \end{array} \right] \times$$

$$\times S_{v_1,...,v_r}^{u_1,...,u_r} \, [c_1 z,...,c_r z]$$

respectively.

Series of Fourier Transform Pairs

The sum of three series of Fourier transforms of H-function of two, three and $(r+1)$ variables are established here:

Let ω be any real number and let $t > 0$, $t_i > 0$ $(i = 1,2,...,r)$

(i) $\sum_{k=0}^{[v/u]} \frac{(-v)_{uk}}{k!} A_{v,k} \, z_0^k \int_{-\infty+i\omega}^{\infty+i\omega} H_{1,1:\;p,q\,;\,0,1}^{0,1:\,m,\,n;1,0} \times$

$$\times \left[\begin{array}{c|l} x z_0^t & (-\mu-k;t,1) \quad : (a_j,\alpha_j)_{1,p};\ - \\ \eta & (-\mu-k+\eta+\gamma;t,1) : (b_j,\beta_j)_{1,q};(0,1) \end{array} \right] \times$$

$$\times \exp(-i\eta\phi)/\Gamma(\eta+1)\,d\eta$$

$$= \left(\frac{z}{z_0}\right)^{\mu-1} H_{p,q}^{m,n}\left[xz^t \left| \begin{array}{l} (a_j,\alpha_j)_{1,p} \\ (b_j,\beta_j)_{1,q} \end{array} \right. \right] S_v^u[z] \qquad (12)$$

provided

$$\text{Re}\left[\mu + t\left(\frac{b_j}{\beta_j}\right) + 1 \right] > 0,\ 1 \le j \le m.$$

(ii) $$\sum_{k=0}^{[v/u]} \frac{(-v)_{uk}}{k!} A_{v,k}\, z_0^k \int_{-\infty+i\omega}^{\infty+i\omega} H_{p_1+1,q_1+1:\,*;\,0,1}^{0,n_1+1\ :\ *;1,0} \times$$

$$\times \left[\begin{array}{c|l} x_1 z_0^{t_1} & (-\mu-k;t_1,t_2,1),(a_j;\alpha_j,A_j,0)_{1,p_1}\ ;*;\ - \\ x_2 z_0^{t_2} & \\ \eta & (-\mu-k-\eta;t_1,t_2,1),(b_j,\beta_j,B_j,0)_{1,q_1};*;(0,1) \end{array} \right] \times$$

$$\times \exp(-i\eta\phi)/\Gamma(\eta+1)\,d\eta$$

$$= \left(\frac{z}{z_0}\right)^{\mu-1} H_{p_1,q_1:*}^{0,n_1\ :*} \left[\begin{array}{c} x_1 z^{t_1} \\ x_2 z^{t_2} \end{array} \right] S_v^u[z] \qquad (13)$$

$$\text{provided Re}\left[\mu + t_1\left(\frac{d_i}{\delta_i}\right) + t_2\left(\frac{f_j}{F_j}\right) + 1 \right] > 0,$$

$$1 \le i \le m_2,\ 1 \le j \le m_3.$$

(vi) $$\sum_{k_1=0}^{[v_1/u_1]} \cdots \sum_{k_r=0}^{[v_r/u_r]} \frac{(-v_1)_{u_1k_1} \ldots (-v_r)_{u_rk_r}}{k_1! \ \ldots \ k_r!} \times$$

$$\times A[v_1,k_1;\ldots;v_r,k_r] \prod_{i=1}^{r} c_i^{k_i}\,(z_0)^{\sum_{i=1}^{r} k_i} \times$$

$$\times \int_{-\infty+i\omega}^{\infty+i\omega} H_{p+1,q+1:*;\ldots;*\ ;0,1}^{0,n+1\ \ :*;\ldots;*;1,0} \times$$

$$\times \left[\begin{array}{c|l} x_1 z_0^{t_1} & E_1 : *;\ldots;*;\ - \\ \vdots & \\ x_r z_0^{t_r} & F_1 : *;\ldots;*;(0,1) \\ \eta & \end{array} \right] \times$$

$$\times \exp(-i\eta\phi)/\Gamma(\eta+1)\,d\eta$$

$$= \left(\frac{z}{z_0}\right)^{\mu-1} H \left[\begin{array}{c} x_1 z^{t_1} \\ \vdots \\ x_r z_r^{t_r} \end{array} \right] S_{v_1,\ldots,v_r}^{u_1,\ldots,u_r} [c_1 z,\ldots,c_r z] \qquad (14)$$

E_1, F_1 are same as mentioned in (10)

$$\text{provided min Re}\left[\mu + \sum_{i=1}^{r} t_i \left(\frac{d_j^{(i)}}{\delta_j^{(i)}}\right) + 1 \right] > 0$$

$$j = 1,\ldots,m_v\ ;\ v = 1,\ldots,r.$$

where, by taking

$$(z-z_0)\exp\left(\frac{z}{z_0}\right) = z_0 \exp(-i\phi),\ |\phi| < \pi \qquad (15)$$

in $y(z,\eta)$

Method of Derivation

The results in (12), (13) and (14) are derived from (8), (9) and (10) respectively by taking $\gamma = 0$ in these equations and using (15).

Particular Cases :

(i) If in (8), we take

$$u = 1,\ A_{v,k} = \binom{v+\alpha}{v} \frac{(\alpha+\beta+v+1)_k}{(\alpha+1)_k}$$

so that $S_v^1[z] \to P_v^{(\alpha,\beta)}(1-2z)$, then it yields the following:

$$(i)\ \sum_{k=0}^{v} \frac{(-v)_k}{k!}\binom{v+\alpha}{v}\frac{(\alpha\beta+v+1)_k}{(\alpha+1)_k}\times$$

$$\times (z_0)^k \int_{-\infty}^{\infty} y(z,\eta)\, H\left[\begin{matrix} x z_0^t \\ \eta+\gamma \end{matrix}\right] d\eta$$

$$= \left(\frac{z}{z_0}\right)^{\mu-1} H_{p,q}^{m,n}\left[xz^t \left| \begin{matrix} (a_j,\alpha_j)_{1,p} \\ (b_j,\beta_j)_{1,q} \end{matrix} \right.\right] \times$$

$$\times P_v^{(\alpha,\beta)}(1-2z) \qquad (16)$$

where $P_v^{(\alpha,\beta)}(1-2z)$ is the Jacobi polynomial.

(ii) If in (8), we take $u = 1$, $A_{v,k} = \binom{v+\alpha}{v}\frac{1}{(\alpha+1)_k}$ so that $S_v^1[z] \to L_v^{(\alpha)}(z)$, then it yields the following:

$$\sum_{k=0}^{v} \frac{(-v)_k}{k!}\binom{v+\alpha}{v}\frac{1}{(\alpha+1)_k}(z_0)^k \times$$

$$\times \int_{-\infty}^{\infty} y(z,\eta)\, H\left[\begin{matrix} x z_0^t \\ \eta+\gamma \end{matrix}\right] d\eta$$

$$= \left(\frac{z}{z_0}\right)^{\mu-1} H_{p,q}^{m,n}\left[xz^t\right] {}_{v}^{(\alpha)}(z) \qquad (17)$$

where $L_v^{(\alpha)}(z)$ is the Laguerre polynomial.

(iii) If in (16), we take $\alpha = 0$, $\beta = 0$ so that $P_v(z) = P_v^{(0,0)}(z)$, then it yields the following:

$$\sum_{k=0}^{v} \frac{(-v)_k}{k!}\frac{(v+1)_k}{k!}(z_0)^k \times$$

$$\times \int_{-\infty}^{\infty} y(z,\eta)\, H\left[\begin{matrix} x z_0^t \\ \eta+\gamma \end{matrix}\right] d\eta$$

$$= \left(\frac{z}{z_0}\right)^{\mu-1} H_{p,q}^{m,n}\left[xz^t\right] P_v(1-2z) \qquad (18)$$

where $P_v(1-2z)$ is the familiar Legendre polynomial.

If we take $v = 0$, the above results reduce to known results by Arora[6].

References

1. Osler, T.J. (1972) *Math. Comp.* **26** : 450.
2. Srivastava, H.M. & Singh, N.P. (1983) *Rend. Circ. Mat. Palermo. Serie_II.* Tomo XXXII : 158.
3. Srivastava, H.M. (1985) *Pacific J. Math.* **117** : 184.
4. Srivastava, H.M., Gupta, K.C. & Goyal, S.P. (1982) *The H-functions of One and Two Variables with Applications*, South Asian Publishers, New Delhi.
5. Agal, S.N. & Koul, C.L. (1984) *Indian J. Pure Appl. Math.* **15** (7) : 766.
6. Arora, A.K. & Koul, C.L. (1987) *Indian J. Pure Appl. Math.* 18 (10) : 933.

PROC. NAT. ACAD. SCI. INDIA, 75 (A), I, 2005

Certain transformations involving q-series

SATYA PRAKASH SINGH

Department of Mathematics T.D.P.G. College, Jaunpur-222 002, India.

Received January 27, 2004, Accepted March 13, 2004.

Abstract

In this paper, certain transformations for basic hypergeometric series have been established by making use of a known identity.

(Keywords : hypergeometric functios/ summation/ transformation/ polybasic).

Introduction, Definitions and Preliminaries

In the following identity

$$\sum_{m=0}^{n}\delta_m \sum_{r=0}^{m}\alpha_r =$$

$$\sum_{r=0}^{n}\alpha_r \sum_{m=0}^{n}\delta_m - \sum_{r=0}^{n-1}\alpha_{r+1} \sum_{m=0}^{r}\delta_m , \qquad (1)$$

[Srivastava [1]; (4.3)]

if we take α_j z^j, (1) takes the following form :

$$\sum_{m=0}^{n}\delta_m z^m = z^n \sum_{m=0}^{n}\delta_m + (1-z)\sum_{r=0}^{n-1} z^r \sum_{m=0}^{r}\delta_m \qquad (2)$$

In this paper, an attempt has been made to establish certain transformation formulae for basic hypergeometric series by making use of the identity (2).

For real of complex $q(|q|<1)$, put

$$(\lambda ;q)_\infty = \prod_{j=0}^{\infty}(1-\lambda q^1) \qquad (3)$$

and let $(\lambda; q)_\mu$ be defined by

$$(\lambda;q)_\mu = \frac{(\lambda;q)_\infty}{(\lambda q^u;q)_\infty} \qquad (4)$$

for arbitrary parameters λ and μ, so that

$$(\lambda;q)_\mu = \begin{cases} 1, & n=0 \\ (1-\lambda)(1-\lambda q)..(1-\lambda q^{n-1}), & n\in(1,2,3,..). \end{cases}$$

A truncated basic hypergeometric series is defined as

$${}_r\Phi_s \left[\begin{matrix} a_1, a_2 ...., a_r; q; z \\ b_1, b_2, ..., b_s \end{matrix}\right]_N = \sum_{n=0}^{N} \frac{\prod_{j=1}^{r}[a_j;q]_n z^n}{\prod_{j=1}^{s}[b_j;q]_n [q;q]_n}, \qquad (6)$$

where $|q|<1$, $|z|<1$ and no zero appear in the denominator.

The truncated polybasic hypergeometric series of one variable is defined as

$${}_r\Phi_s \left[\begin{matrix} a_1, a_2 .., a_r; c_{1,1}, .. c_{1,r1}; .. ; c_{m,1}, .., c_{m}, r_m; q, q_1, . q_m; z \\ b_1, b_2, .. b_s; d_{1,1}, .. d_{1s1}; .. ; d_{m,1}, ... d_m, s_m; \end{matrix}\right]_N$$

$$= \sum_{n=0}^{N} \frac{[a_1, a_2, ..., a_r; q]_n z^n}{[q, b_1, b_2, ..., b_s; q]_n} \prod_{j=1}^{m} \frac{[c_{j,1}, ..., c_{j,rj}; q_j]_n}{[d_{j,1}, ..., d_{j,sj}; q]_n}. \qquad (7)$$

The series (7) converges for $|q|$, $|q_1|,\ldots,|q_m|<1$, $|z|<1$.

The other notations appearing in this paper shall stand for their usual meaning.

We shall use the following summations of truncateds series in our abalysis.

$$ {}_2\Phi_1\begin{bmatrix} a,y;q \\ ayq \end{bmatrix}_n = \frac{[aq,yq;q]_n}{[q,ayq;q]_n} \tag{8}$$

[Agarwal[2]; App. II (8)]

$$ {}_4\Phi_3\begin{bmatrix} a,q\sqrt{a},-q\sqrt{a},e;q;1/e \\ \sqrt{a},-\sqrt{a},aq/e \end{bmatrix}_n = \frac{[aq,eq;q]_n}{[q,aq/e;q]_n e^{n}}. \tag{9}$$

[Agarwal[2]; App. II (23)]

$$ {}_6\Phi_5.\begin{bmatrix} a,q\sqrt{a},-q\sqrt{a},b,c,d;q;q \\ \sqrt{a},-\sqrt{a},aq/b,aq/c,aq/d \end{bmatrix}_n = \frac{[aq,bq,cq,dq;q]_n}{[q,aq/b,aq/c,aq/d;q]_n}, \tag{10}$$

provided $a=bcd$

[Agarwal[2]; App. II (25)]

$$\sum_{k=0}^{n}\frac{(1-ap^kq^k)[a;p]_k[c;q]_k c^{-k}}{(1-a)[q;q]_k[ap/c;p]_k} = \frac{[ap;p]_n[cq;q]_n c^{-n}}{[q;q]_n[ap/c;p]_n}. \tag{11}$$

[Gasper and Rahman[3]; App. II (34)]

$$\sum_{k=0}^{n}\frac{(1-ap^kq^k)[1-bp^kq^{-k}][a,b;p]_k[c,a/bc;q]_k q^k}{(1-a)(1-b)[q,aq/b;q]_k[ap/c;bcp;p]_k}$$

$$= \frac{[ap,bp;p]_n[cq,aq/bc;q]_n}{[q,aq/b;q]_n[ap/c,bcp;p]_n}. \tag{12}$$

[Gasper and Rahman[3]; App. II (35)]

$$\sum_{k=0}^{n}\frac{(1-adp^kq^k)\left[1-\frac{b}{d}p^kq^{-k}\right][a,b;p]_k[c,ad^2/bc,q]_k q^k}{(1-ad)(1-b/d)[dq,adq/b;q]_k[adp/c;bcp/d;p]_k}$$

$$= \frac{(1-a)(1-b)(1-c)(1-ad^2/bc)}{d(1-ad)(1-b/d)(1-c/d)(1-ad/bc)}\times$$

$$\times\left[\frac{[ap,bp;p]_n[cq,ad^2q/bc;q]_n}{[dq,adq/b;q]_n[adp/c,bcp/d;p]_n}\right.$$

$$\left.-\frac{(b-ad)(c-ad)(d-bc)(1-d)}{d(1-a)(1-b)(1-c)(bc-ad^2)}\right] \tag{13}$$

which is $m=0$ case of [Gasper and Rahman[3]; App. II (36)]

$$\sum_{k=0}^{n}\frac{(1-adp^kq^kP^kQ^k)\left(1-\frac{dP^kQ^k}{cp^kq^{-k}}\right)\left(1-\frac{bp^kP^k}{dq^kQ^k}\right)\left(1-\frac{adP^kQ^k}{bcq^kp^k}\right)}{(1-ad)(1-d/c)(1-b/d)(1-ad/bc)}$$

$$\times\frac{[a;p^2]_k[c;q^2]_k[b;P^2]_k[ad/bc;Q^2]_k q^{2k}}{\left[d\frac{qPQ}{p};\frac{qPQ}{p}\right]_k\left[\frac{ad}{c}\frac{pRQ}{q};\frac{pRQ}{q}\right]_k\left[\frac{ad}{b}\frac{pqQ}{p};\frac{pqQ}{p}\right]_k\left[\frac{bc}{d}\frac{pqP}{Q}\frac{pqP}{Q}\right]_k}$$

$$= \frac{(1-a)(1-b)(1-c)(1-ad^2/bc)}{(1-ad)(c-d)(1-b/d)(1-ad/bc)}\times$$

$$\times\left[\frac{[ap^2;p^2]_n[cq^2;q^2]_n[bp^2;P^2]_n}{\left[d\frac{qPQ}{p};\frac{qPQ}{p}\right]_n\left[\frac{ad}{c}\frac{pPQ}{q};\frac{pPQ}{q}\right]_n} \frac{\left[\frac{ad^2}{bc}Q^2;Q^2\right]_n}{\left[\frac{ad}{b}\frac{pqQ}{P};\frac{pqQ}{P}\right]_n\left[\frac{bc}{d}\frac{pqP}{Q};\frac{pqP}{Q}\right]_n}\right.$$

$$\left.-\frac{(b-ad)(c-ad)(d-bc)(1-d)}{d(1-a)(1-b)(1-c)(bc-ad^2)}\right], \qquad (14)$$

which is m=0 case of [Agarwal *et al.* [4]; (18) p. 89]

Main Results

If we take $\delta_m = \frac{[a,y;q]_m q^m}{[q,ayq;q]_m}$ in (2) and make use of (8) we get

$${}_2\Phi_1\left[\begin{matrix}a,y;q;qz\\ayq\end{matrix}\right]_n = \frac{z^n[aq,yq;q]_n}{[q,ayq;q]_n}+$$

$$(1-z){}_2\Phi_1\left[\begin{matrix}aq,yq;q;\\ayq\end{matrix}\right]_{n-1} \quad |z|<1. \qquad (15)$$

As $n\to\infty$, (15) yields the following transformation

$${}_2\Phi_1\left[\begin{matrix}a,y;q;qz\\ayq\end{matrix}\right] = (1-z){}_2\Phi_1\left[\begin{matrix}aq,yq;q;z\\ayq\end{matrix}\right], |z|<1 \qquad (16)$$

Taking $\delta_m = \frac{[a,q\sqrt{a},-q\sqrt{a},e;q]_m}{[q,\sqrt{a},-\sqrt{a},aq/e;q]_m e^m}$ in (2) and making use of (9) we get

$${}_4\Phi_3\left[\begin{matrix}a,q\sqrt{a},-q\sqrt{a},e;z/e\\\sqrt{a},-\sqrt{a},aq/e\end{matrix}\right]_n$$

$$= \frac{z^n[aq,eq;q]_n}{e^n[e,aq/e;q]_n}+(1-z){}_2\Phi_1\left[\begin{matrix}aq,eq;q;z/e\\aq/e\end{matrix}\right]_{n-1} \qquad (17)$$

For $|z|<1$ and $|e|>1$, (1) yields the following transformation, when $n\to\infty$,

$${}_4\Phi_3\left[\begin{matrix}a,q\sqrt{a},-q\sqrt{a},e;z;/e\\\sqrt{a},-\sqrt{a},aq/e\end{matrix}\right]=$$

$$(1-z){}_2\Phi_1\left[\begin{matrix}aq,eq;q;z/e\\aq/e\end{matrix}\right]. \qquad (18)$$

Taking

$$\delta_m = \frac{[a,q\sqrt{a},-q\sqrt{a},b,c,a/bc;q]_m q^m}{[q,\sqrt{a},-\sqrt{a},aq/b,aq/c,bcq;q]_m}$$

in (2) and making use of (10) we get

$${}_6\Phi_5\left[\begin{matrix}a,q\sqrt{a},-q\sqrt{a},b.c.a/bc;q;zq\\q,\sqrt{a},-\sqrt{a},aq/b,aq/c,bcq\end{matrix}\right]_n$$

$$\frac{[aq,bq,cq,aq/bc;q;z]_n z^n}{[q,aq/b,aq/c,bcq;q]_n}+$$

$$(1-z){}_4\Phi_3\left[\begin{matrix}aq,bq,cq,aq/bc;q;z\\aq/b,aq/c,bcq\end{matrix}\right]_{n-1}, |z|<1. \qquad (19)$$

As $n\to\infty$, (19) yields the following transformation

$$ {}_6\Phi_5\left[\begin{matrix} a, q\sqrt{a}, -q\sqrt{a}, b.c.a/bc; q; zq \\ q, \sqrt{a}, -\sqrt{a}, aq/b, aq/c, bcq \end{matrix}\right] $$

$$ = (1-z)_4\Phi_3\left[\begin{matrix} aq, bq, cq, aq/bc; q; z \\ aq/b, aq/c, bcq \end{matrix}\right]. \qquad (20) $$

Taking $\delta_m = \dfrac{[apq; pq]_m [a; p]_m [c; q]_m c^{-m}}{[a; pq]_m [q; q]_m [ap/c; p]_m}$ in (2) and making use of (11), we get

$$ {}_3\Phi_2\left[\begin{matrix} c; a; apq; q, p, pq; z/c \\ -; ap/c; a; \end{matrix}\right]_n $$

$$ = \frac{z^n [ap; p]_n [cq; q]_n}{c^n [q; q]_n [ap/c; p]_n} + $$

$$ (1-z)_2\Phi_1\left[\begin{matrix} cq; ap; q, p; z/c \\ -; ap/c \end{matrix}\right]_{n-1} \qquad (21) $$

For $|z| < 1$, $|c| > 1$ and $n \to \infty$, (21) yields

$$ {}_3\Phi_2\left[\begin{matrix} c; a; apq; q, p, pq; z/c \\ -; ap/c; a; \end{matrix}\right] $$

$$ = (1-z)_2\Phi_1\left[\begin{matrix} cq; ap; q, p; z/c \\ -; ap/c \end{matrix}\right]_n \qquad (22) $$

Taking

$$ \delta_m = \frac{[apq, pq]_m [bp/q; p/q]_m [a, b; p]_m [c, a/bc; q]_m q^m}{[a; pq]_m [b; p/q]_m [q, aq/b; q]_m [ap/c, bcp; p]_m} $$

in (2) and making use of (12), we get

$$ {}_6\Phi_5\left[\begin{matrix} c, a/bc; a, b; apq; b\frac{p}{q}; q, p, pq, \frac{p}{q}; z \\ aq/b; ap/c, bcp; a; b \end{matrix}\right]_n $$

$$ = \frac{[aq, bp, p]_n [cq, aq/bc; q]_n z^n}{[q, aq/b; q]_n [ap/c, bcp; p]_n} $$

$$ + (1-z)_4\Phi_3\left[\begin{matrix} cq, aq/bc; ap, bp; q, p; z \\ aq/b; ap/c, bcp \end{matrix}\right]_{n-1}, |z| < 1. \qquad (23) $$

As $n \to \infty$, (23) yields the following transformation

$$ {}_6\Phi_5\left[\begin{matrix} c, a/bc; a, b; apq; b\frac{p}{q} q, p, pq, \frac{p}{q} z \\ aq/b, aq/c, bcp; a; b \end{matrix}\right] $$

$$ = (1-z)_4\Phi_3\left[\begin{matrix} cq, aq/bc; ap, bp; q, p; z \\ aq/b; ap/c, bcp \end{matrix}\right]. \qquad (24) $$

Taking

$$ \delta_m = \frac{[[adpq; pq]_m \left[\frac{b}{d}\frac{p}{q}; \frac{p}{q}\right]_m [a, b; p]_m \left[c, \frac{ad^2}{bc}; q\right]_m q^m}{[a; pq]_m \left[\frac{b}{d}; \frac{p}{q}\right]_m [q, aq/b; q]_m \left[\frac{adp}{c}, \frac{bcp}{d}; p\right]_m} $$

in (2) and making use of (13), we get

$$ {}_7\Phi_6\left[\begin{matrix} c, ad^2/bc, q; a, b; adpq, bp/dq, q, p, pq, p/q; zq \\ dq, adq/b; adp/c, bcp/d; ad; b/d \end{matrix}\right]_n $$

$$ = \frac{z^n (1-a)(1-b)(1-c)(1-ad^2/bc)[ap, bp; p]_n [cq, ad^2q; q]_n}{d(1-ad)(1-b/d)(1-c/d)(1-ad/bc)[dq, adq/b; q]_n [adp/c, bcp/d; p]_n} $$

$$-\frac{(1-ad)(c-ad)(d-bc)(1-d)}{bcd^2(1-ad)(1-b/d)(1-c/d)(1-ad/bc)}$$

$$+ (1-z)\frac{(1-a)(1-b)(1-c)(1-ad^2/bc)}{d(1-ad)(1-b/d)(1-c/d)(1-ad/bc)}\times$$

$$\times {}_5\Phi_4\left[\begin{matrix} cq, ad^2q/bc, q; ap, bp; q, p; z \\ dq, adq/b; adp/c, bcp/d \end{matrix}\right]_{n-1}, \quad |z|<1. \tag{25}$$

As $n\to\infty$, (25) yields

$${}_7\Phi_6\left[\begin{matrix} c; ad^2/bc, q; a, b; adpqbp/dq, q, p, pq, p/q; zq \\ dq, adq/b; adp/c, bcp/d; ad; b/d \end{matrix}\right]$$

$$= (1-z)\frac{(1-a)(1-b)(1-c)(1-ad^2/bc)}{d(1-ad)(1-b/d)(1-c/d)(1-ad/bc)}\times$$

$$\times {}_5\Phi_4\left[\begin{matrix} cq, ad^2q/bc, q; ap, bp; q, p; z \\ dq, adq/b; adp/c, bcp/d \end{matrix}\right]_n$$

$$-\frac{(1-ad)(c-ad)(d-bc)(1-d)}{bcd^2(1-ad)(1-b/d)(1-c/d)(1-ad/bc)} \tag{26}$$

References

1. Srivastava, A.K. (1997) *Proc. Indian Acad. Sci.* **107** : 12.
2. Agarwal, R.P. *Generalized hypergeometric series and its application to the theory of combinatorial analysis and partition theory* (Unpublished monograph).
3. Gasper, G. & Rahman, M. (1990) : *Basic hypergeometric series,* Cambridge University Press.
4. Agarwal, R.P., Manocha, H.L. & Rao, K.Srinivasa (2001) *Selected topics in special function,* Allied Publishers Limited, New Delhi.

PROC. NAT. ACAD. SCI. INDIA, 75 (A), I, 2005

Unsteady flow and heat transfer along a porous vertical surface bounded by porous medium

P.R. SHARMA and UPENDRA MISHRA

Department of Mathematics, University of Rajasthan, Jaipur-302 004, India.

Received December 10, 2001; Revised May 6, 2003; Accepted March 19, 2004

Abstract

Unsteady flow and heat transfer along a porous vertical surface bounded by porous medium in the presence of variable free stream and permeability is investigated. The expressions of velocity and temperature distributions are derived, discussed numerically and shown through graphs. The expressions for skin-friction coefficient and rate of heat transfer in terms of Nusselt number at the surface are derived, discussed numerically and their values are presented through Table 1.

(**Keywords :** unsteady/ free convective flow/ porous medium/ skin-friction coefficient/ Nusselt number.)

Introduction

The study of free convective flow through a porous medium under the influence of temperature differences is one of the most contemporary subject, because it has great applications in geothermy, geophysics and technology. Also its numerous scientific and engineering applications, *viz.* are in the fields of agricultural engineering to study the underground water resources; in petroleum technology to study the movements of natural gas, oil and water through the oil reservoirs, in chemical engineering for filteration and purification processes.

Steady/unsteady flow and heat transfer through a porous medium have been studied by several researchers[1-11].

In the present text unsteady flow and heat transfer along a porous vertical surface bounded by porous medium in the presence of variable free stream and permeability is investigated.

Governing Equations of Motion

The porous infinite surface is placed along x-axis in upwards direction and y-axis is taken normal to it. The fluid is sucked through the surface at constant rate. All fluid properties are taken constant except that the influence of the density variation with temperature is considered in the body force term. Temperature of the surface is fluctuated and free stream velocity vibrates about a mean constant value.

The governing equations of motion and energy for unsteady flow and heat transfer of an incompressible viscous fluid along a porous surface bounded by a porous medium in non-dimensional form are

$$\frac{\partial u}{\partial t}-\frac{\partial u}{\partial y}=\frac{dU(t)}{dt}+Gr\,T+\frac{\partial^2 u}{\partial y^2}+\frac{(U(t)-u)}{K(t)}, \quad \text{and} \tag{1}$$

$$\frac{\partial T}{\partial t}-\frac{\partial T}{\partial y}=Pr^{-1}\frac{\partial^2 T}{\partial y^2}+Ec\left(\frac{\partial u}{\partial y}\right)^2, \tag{2}$$

where u is the fluid velocity along x-axis, T the fluid temperature, t the time, ω the frequency, Gr the Grashoff number, K the permeability parameter, Pr the Prandtl number and Ec the Eckert number.

The boundary conditions in non-dimensional form are

$$y=0: \quad u=0,\ T=1+\varepsilon e^{i\omega t},$$

$$y\to\infty\ :\ u\to 1+\varepsilon e^{i\omega t}\ ,\ T=0 \tag{3}$$

Method of Solution

Assuming

$$u(y,\ t)=u_0(y)+\varepsilon u_1(y)\,e^{i\omega t},$$

$$T(y,\ t)=T_0(y)+\varepsilon T_1(y)\,e^{i\omega t},\ \text{and}$$

$$U(t)=1+\varepsilon\ e^{i\omega t} \tag{4}$$

and using into the equations (1) and (2), the boundary conditions (3), and equating the coefficients of o(ε), we get

Zeroth-order equations

$$u_0'' + u_0' - \frac{1}{K_0}u_0 = -\frac{1}{K_0} - Gr\,T_0\ ,\ \text{and} \tag{5}$$

$$T_0'' + Pr\,T_0' + Pr\,Ec\,u_0'^2 = 0\ . \tag{6}$$

First-order equations

$$u_1'' + u_1' - \left(i\omega + \frac{1}{K_0}\right)u_1 = -\frac{1}{K_0}u_0 - i\omega - Gr\,T_1\ ,$$

and (7)

$$T_1'' + Pr\,T_1' - i\omega Pr\,T_1 = -2Pr\,Ec\,u_0'\,u_1', \tag{8}$$

and the corresponding boundary conditions are as follows

$$y=0\ :\ u_0=0=u_1,\ T_0=1=T_1,$$

$$y\to\infty\ :\ u_0=1=u_1,\ T_0=0=T_1. \tag{9}$$

The equations (5) to (8) are ordinary coupled differential equations. Since the Eckert number Ec is very small for incompressible fluid flows, therefore fluid velocity and temperature can be expanded in the powers of Ec as given below

$$F = F_0 + Ec\,F_1 + o\,(Ec^2)\ , \tag{10}$$

where F stands for u_0, u_1, T_0 or T_1 .

Using (10) into the equations (5) to (8), the boundary conditions (9), and equating the coefficients of like powers of Ec, we get a set of ordinary differential equations with the corresponding boundary conditions. Through straight forward algebra, the solutions of u_{00}, u_{01}, u_{10}, u_{11}, T_{00}, T_{01}, T_{10} and T_{11} are known and finally the expressions of velocity and temperature distributions are obtained in the following form

$$u\,(y,\ t)=F_6\,(y)+Ec\,F_7\,(y)+$$
$$\varepsilon\,[\{F_8\,(y)+Ec\,F_{10}\,(y)\}\cos\omega t$$
$$-\{F_9\,(y)+Ec\,F_{11}\,(y)\}\sin\omega t], \tag{11}$$

$$T\,(y,\ t)=e^{-Pr\,y}+Ec\,F_1\,(y)+$$
$$\varepsilon\,[\{F_2\,(y)+Ec\,F_4\,(y)\}\cos\omega t$$
$$-\{F_3\,(y)+Ec\,F_5\,(y)\}\sin\omega t]. \tag{12}$$

Here, the expressions of $F_1(y)$ to $F_{11}(y)$ are not included for the sake of brevity.

Skin-Friction

The skin-friction coefficient at the surface is given by

$$C_f = \frac{\tau_w}{\rho U v_0} = (C_1 + E_c C_2) + \varepsilon\{(C_3 + E_c C_4)$$

$$\cos \omega t + (C_5 + Ec\, C_6) \sin \omega t\} \quad (13)$$

where τ_w is the shear stress at the surface, ρ the density, U the mean free stream velocity and v_0 the cross-flow fluid velocity.

Nusselt Number

The rate of heat transfer in terms of Nusselt number at the surface is given by

$$Nu = \frac{q \upsilon}{\kappa v_0 (T_w - T_\infty)}$$

$$= Pr + Ec\, C_7 + \varepsilon\{(C_8 + Ec\, C_9) \cos \omega t$$

$$+ (C_{10} + Ec\, C_{11}) \sin \omega t\} \quad (14)$$

Here C_1 to C_{11} are constants and their expressions are not presented for the sake of brevity.

Numerical results for the velocity and temperature distributions and values of skin-friction coefficient and Nusselt number at the surface are carried out on Intel Pentium-III Computer using C++ language.

Results and Discussion

It is observed from Fig. 1 that fluid velocity increases due to increase in Grashoff number or permeability parameter, while it decreases due to increase in Prandtl number, phase angle, Eckert number or frequency. It is noted from Fig. 2 that fluid temperature decreases due to increase in Prandtl number, permeability parameter, Grashoff number, Eckert number, frequency or phase angle.

It is seen from Table 1 that skin-friction coefficient at the surface increases with the increase in Grashoff number or permeability parameter, while it decreases due to increase in Prandtl number, phase angle, frequency or Eckert number. The Nusselt number at the surface increases due to increase in Prandtl number, permeability parameter, Grashoff number or Eckert number, while it decreases due to increase in frequency or phase angle.

Table 1– Values of skin-friction coefficient and Nusselt number at the surface.

Gr	Pr	Ec	ε	K_0	ω	ωt	C_f	Nu
3.0	0.71	0.01	0.0	1.0	-	-	3.822372	0.798385
3.0	0.71	0.01	0.25	1.0	5.0	$\pi/4$	4.170936	0.878249
3.0	0.71	0.01	0.25	1.0	5.0	$\pi/3$	3.998218	0.73811
3.0	0.71	0.01	0.25	1.0	10.0	$\pi/4$	4.076478	0.869563
3.0	0.71	0.01	0.25	3.0	5.0	$\pi/4$	4.279303	1.118067
3.0	0.71	0.02	0.25	1.0	5.0	$\pi/4$	4.125833	0.975382
3.0	7.0	0.01	0.25	1.0	5.0	$\pi/4$	2.16895	7.770732
5.0	0.71	0.01	0.25	1.0	5.0	$\pi/4$	5.733157	1.006683
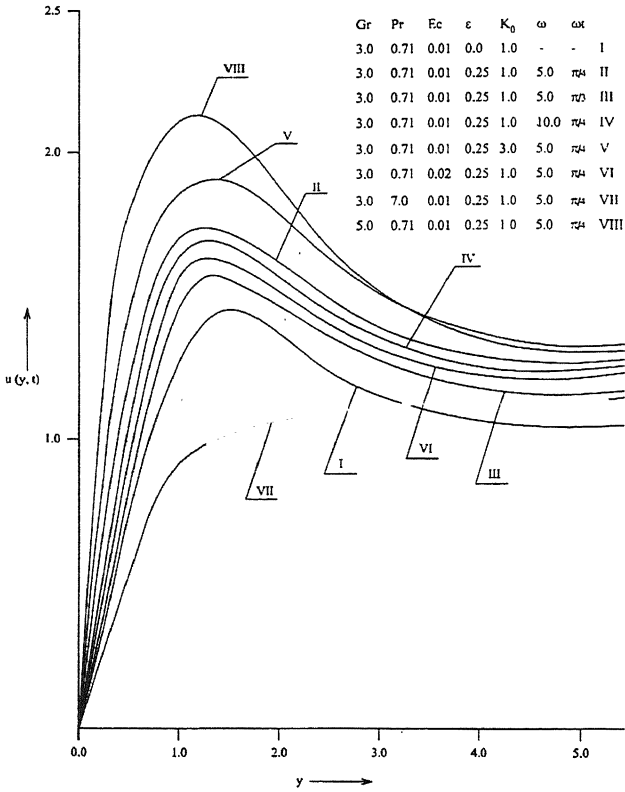
Fig. 1– Velocity distribution *vs.* *y*
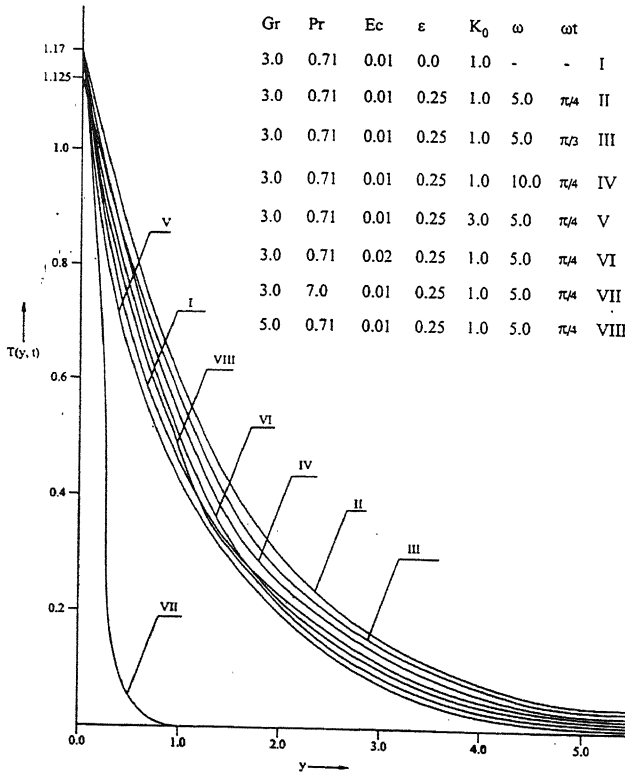
Fig. 2– Temperature distribution *vs.* *y*

Acknowledgement

First author thanks the CSIR for providing financial help through major research project.

References

1. Yamamoto, K. & Iwamura, N. (1976) *J. Engng. Maths.* **10** : 41.
2. Raptis, A., Perdikis, C. & Tzivanidis, G. (1981) *J. Phys D: Appl. Phys.* **14** : L99.
3. Raptis, A., Tzivanidis, G. & Kafousias, N. (1981) *Lett. Heat Mass Transfer* **8** : 417.
4. Raptis, A., Kafousias, N. & Massalas, C. (1982) *ZAMM* **62** : 489.
5. Raptis, A. (1983) *Int. J. Engng. Sci.* **21** : 345.
6. Raptis, A. A. & Perdikis, C. (1985) *Int. J. Engng. Sci.* **23** : 51.
7. Ingham, D.B. & Pop, I. (1987) *Int. J. Engng. Sci.* **25** : 373.
8. Sharma, P.R. (1992) *J. Phys D: Appl. Phys (UK)* **25** : 162.
9. Sharma, P.R. & Kumar, H. (1993) *Indian J. Theo. Phys.* **41** : 181.
10. Sattar, M.A. (1994) *Indian J. Pure Appl. Math.* **25** : 7.
11. Sharma, P.R., Gaur, M. & Gaur, Y.N. (1999) *Bull. Pure Appl. Sciences* **18E** : 25.

PROC. NAT. ACAD. SCI. INDIA, 75 (A), I, 2005

Hill's stability problem criteria in the oblate restricted three-body problem

L.M. SAHA[a], TIL PRASAD SARMA[b], G.H. ERJAEE[c] and PURNIMA DIXIT[d]

[a]*Department of Mathematics, Zakir Husain College, University of Delhi, J.L.N. Marg, New Delhi-110 002, India.*

[b]*Amity School of Engg. & Technology, G.G.S. I. P. University, New Delhi-110 061, India.*

[c]*Mathematics Department, College of Science, Shiraz University, Shiraz, Iran*

[d]*Department of Mathematics, University of Delhi, Delhi-110 007, India,*

Received October 4, 2002; Revised December 20, 2003; Accepted March 19, 2004.

Abstract

Hill's problem on stability criteria of outer planetary orbit encircling binary stars has been investigated. The result for restricted problem, when one of the primaries is an oblate spheroid body has been discussed through Hill's analytical method by varying the mass parameters $\mu=\frac{m_2}{(m_1+m_2)}$, $0 \leq \mu \leq 0.5$.

(**Keywords** : planetary orbits / Hill's stability)

Introduction

Orbital stability can be investigated in triple star systems, perturbed satellite's orbits and planetary orbits. Such studies are helpful to predict the exact location of the orbit and its type in the planetary systems. Several authors[1-4] have discussed Hill's criteria of stability in binary stars systems.

Now, it is evident that majority of the stars occurring in the sky are binary systems. Because of this, scientists working in the area of orbital stability prefer to choose binary systems. The outer planetary stability can be explained for a binary system with masses m_1 and m_2, $(m_1 > m_2)$, if the outer planet is far enough from the binary, (cf. Szebehely[5]). In such a case the planets orbit will not be distrubed by the perturbation due to the binary implying that the orbit is stable. On the other hand, if the size of the outer planetary orbit is below the limit of stability then the orbit would be disturbed by the binary. If the orbit of the planet lie very far away from the binary then it might be perturbed by other members of the galactic system and the binary could lose the planet.

The objective of the present work is to study the stability of the outer planetary orbits by considering the first case discussed above. The mathematical model is that of the restricted three-body problem assuming one of the primaries is an oblate body and the outer planet encloses both the primaries. Here we have adopted the Hill's stability criteria, based on the zero velocity curve, on the Earth-Moon system where the Earth has been treated as an oblate body. The existence of the Jacobian integral is most significant in such stability problem.

Description of the Problem

In a rotating, barycentric dimensionless coordinate system with two bodies on the x-axis, the equations of motion for the restricted three body problem when one of the primaries is an oblate spheroid body are given by

$$\ddot{x}-2n\,\dot{y} = \frac{\partial\Omega}{\partial x}, \qquad \ddot{y}+2n\,\dot{x} = \frac{\partial\Omega}{\partial y}, \qquad (1)$$

where

$$\Omega = \frac{1}{2}\,n^2 \times$$
$$\times\left[(1-\mu)r_1^2+\mu r_2^2\right]+\frac{1-\mu}{r_1}+\frac{\mu}{r_2}+\frac{(1-\mu)A_1}{2r_1^3}, \qquad (2)$$

$$n = 1+\frac{3}{4}A_1, \qquad A_1 = \frac{\mathrm{AE}^2-\mathrm{AP}^2}{5R^2} \qquad (3)$$

$$r_1^2 = (x-\mu)^2+y^2, \qquad r_2^2 = (x+1-\mu)^2+y^2. \qquad (4)$$

Here AE, AP are equatorial and polar radii of primaries and R is the distance between primaries. μ is the ratio of the mass of the smaller primary to the total mass of the primaries and $0 \leq \mu \leq \frac{1}{2}$. The variable (x,y) are the coordinate of the third body in the circular orbit.

Stability Analysis

For the stability analysis, we solve the equations

$$\frac{\partial\Omega}{\partial x} = \frac{\partial\Omega}{\partial y} = 0 \qquad (5)$$

In the rotating system the origin is located at the centre of mass of the primaries, the primary with the larger mass is located at the right side of the origin of the system at $x = \mu$, and the primary with the smaller mass is located at $x = \mu-1$. The collinear equilibrium points are obtained as the roots of the equation

$$\left(\frac{\partial\Omega}{\partial x}\right)_{y=0} = 0 \qquad (6)$$

The straight line solutions of (5) are denoted by the points L_1, L_2 and L_3. Then, if we consider the abscissa of L_1 as x_1, then the corresponding distances from the primaries to L_1 are $r_1 = \mu - x_1$ and $r_2 = \mu - x_1 - 1$. Then, x_1 is given by the equation

$$H(x_1,\mu) = n^2 x_1 +$$
$$\frac{1-\mu}{(x_1-\mu)^2}+\frac{\mu}{(x_1-\mu+1)^2}+\frac{3A_1(1-\mu)}{2(x_1-\mu)^4} = 0. \qquad (7)$$

This is a seventh order algebraic equation in x_1. We solve this equation numerically. For different μ we obtain different real values of x_1 shown in Table 1. For Hill's stability of the outer planetary orbit it is required that the Jacobian constant of the motion of the third body should be larger than or equal to the Jacobian constant at L_1. For the third body, the Jacobian constant is given by

$$C = 2\,\Omega - v^2. \qquad (8)$$

As explained by Kubala *et al*[4]. the approximately circular motion of the third body in the fixed system requires the dimensionless velocity $v_\alpha = 1/\sqrt{r}$ if the motion is clockwise and $v_\alpha = -1/\sqrt{r}$ if the motion is anti-clockwise. Also relative velocity of the third body w.r.t. the rotating system is

$$v = v_{rel} = v_\alpha - v_s = \pm\frac{1}{\sqrt{r}} - r\,. \qquad (9)$$

Here, $v_s = r$, is the velocity at distance r from the origin as the value of the angular velocity is one. From (8) and (9), we get

$$C = 2\,\Omega(r) + 2\,\sqrt{r} - r^2 - \frac{1}{r}. \qquad (10)$$

We calculate C, the Jacobian at L_1 from (5) and obtain

$$C = C_1 = 2\Omega[x_1(\mu), 0]. \qquad (11)$$

The functions $C_1(\mu)$, $x_1(\mu)$, which are of non-monotonic nature, are shown in Fig. 1. Here, with the notation of Kubala *et al.*[4], $C_1(\mu)$ represents the value of Jacobian constant at the equillibrium point L_1 and $x_1(\mu)$ is the location of L_1 relative to the centre of mass of the binary.

For a given value of μ, $C = C_1$, Equation (10) will be of degree seven in r. We have used iterations method to compute the values of r and are shown in Table 1. Since it is an approximate value, the function $\Omega(r)$ can be determined by two different methods. If the radius of the aproximately circular orbit is r, then ther wil be two points of intersection of this circle with the x-axis. In case $r_1 = r - \mu$ and $r_2 = r - \mu + 1$, the intersection will occur on the positive side of x-axis, and in case $r_1 = r + \mu$ and $r_2 = r + \mu - 1$, the intersection will occur on the nagative side of x-axis. In the first case, we have $r_2 = 1 + r_1$, while in the second case we have $r_1 = 1 + r_2$. The values of Jacobian constant corresponding to the above values of r_2 and r_1 are respectively given by C_R and C_L.

Table 1

μ	x_1	c_1	r_R	r_L	Δr	r_{ave}
0.01	-1.1467	3.1642	1.5910	1.5632	0.0278	1.5771
0.03	-1.2011	3.3072	1.8755	1.8456	0.0299	1.8605
0.05	-1.2280	3.4019	2.0395	2.0094	0.0301	2.0244
0.07	-1.2447	3.4740	2.1539	2.1238	0.0301	2.1388
0.09	-1. 2556	3.5318	2.2386	2.2086	0.0299	2.2236
0.11	-1.2629	3.5793	2.3028	2.2730	0.0297	2.2879
0.13	-1.2676	3.6188	2.3517	2.3221	0.0295	2.3369
0.15	-1.2703	3.6518	2.3885	2.3592	0.0293	2.3738
0.17	-1.2715	3.6794	2.4154	2.3864	0.0290	2.4009
0.19	-1.2714	3.7024	2.4342	2.4055	0.0286	2.4198
0.21	-1.2704	3.7213	2.4458	2.4176	0.0282	2.4317
0.23	-1.2684	3.7366	2.4515	2.4237	0.0277	2.4376
0.25	-1.2658	3.7487	2.4517	2.4246	0.0271	2.4381
0.27	-1. 2626	3.7577	2.4473	2.4208	0.0264	2.4340
0.29	-1.2588	3.7641	2.4386	2.4130	0.0256	2.4258
0.31	-1.2545	3.7680	2.4262	2.4015	0.0246	2.4138
0.33	-1.2498	3.7696	2.4102	2.3867	0.0235	2.3985
0.35	-1.2448	3.7690	2.3911	2.3690	0.0221	2.3800
0.37	-1.2394	3.7664	2.3691	2.3486	0.0205	2.3588
0.39	-1.2337	3.7618	2.3444	2.3258	0.0185	2.3351
0.41	-1.2278	3.7555	2.3170	2.3007	0.0163	2.3089
0.43	-1. 2216	3.7474	2.2873	2.2737	0.0136	2.2805
0.45	-1.2152	3.7377	2.2556	2.2447	0.0109	2.2502
0.47	-1.2086	3.7265	2.2209	2.2140	0.0068	2.2175
0.49	-1.2018	3.7137	2.1843	2.1818	0.0024	2.1830
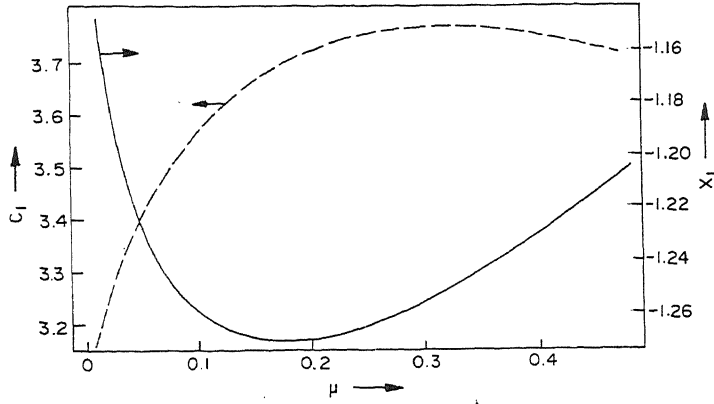
Fig. 1–Graphs of $C_1(\mu)$ and X_1 (μ). Continuous curve stands for C_1 (μ).

From equation (10) and (2), we obtain

$$C_R = n^2\ (r^2+\mu-\mu^2) + \frac{2(1-\mu)}{r-\mu} + \frac{2\mu}{r-\mu+1} + \frac{(2-\mu)A_1}{(r-\mu)^3} - \frac{1}{r} + 2\sqrt{r} - r^2 \quad (12)$$

and

$$C_L = n^2\ (r^2+\mu-\mu^2) + \frac{2(1-\mu)}{r-\mu} + \frac{2\mu}{r-\mu+1} + \frac{(2-\mu)A_1}{(r-\mu)^3} - \frac{1}{r} + 2\sqrt{r} - r^2 \quad (13)$$

The Jacobian constany for given values of r and μ differ by

$$\Delta C = C_R - C_L = 2\mu\ (1-\mu)\times \times\left\{2r(1-n^2) + \frac{2(2r^2-2\mu^2+2\mu-1)}{(r^2-\mu^2)(r^2-\mu^2+2\mu+1)} + \frac{A_1(\mu^3+3r^2)}{2(r^2-\mu^2)^3}\right\} \quad (14)$$

This difference is zero, when μ = 0,1. We have calculated x_1, c_1, r_1, r_2 from the relations (7), (11), (12) and (13) respectively. To get the value of n we have substituted equatorial radius, AE=6378.140 km, polar radius, AP=6356.757 km and distance between earth and moon, R = 384400.00 km in equation (3). We have obtained at μ=0.01, C_1=3.16422 and with $C_1=C_R$ the value of r as $r \in rR$ =1.59109. For the same value of μ, the relation $C_1=C_L$ provides the value of r as $r=r_L$=1.56320. Table 1 shows the value of x_1, C_1, r_R, r_L. Δr and r_{ave} for various values of μ, where $\Delta r=r_R-r_L$ and r_{ave}=(1/2) (r_R+r_L). Δr is obtained below 1.13%. The curves r_R (μ), r_L (μ) are drawn in Fig. 2.
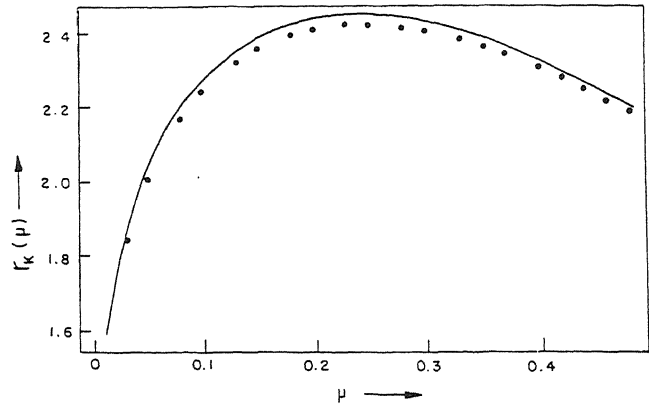
Fig. 2–Graphs of r_K (μ). (K=R,L). Comparison of Stability Curves r_R (μ) and r_L (μ); continuous curve representing r_R (μ) and dotted curve representing r_L (μ)

The multiple roots of the algebraic equations (7), (12) and (13) do not create problem as only real roots are of our interest and we ignore any solution that do not satisfy x_1 <0 and r>l. If there are more roots satisfying the conditions r>l, we select only the largest root.
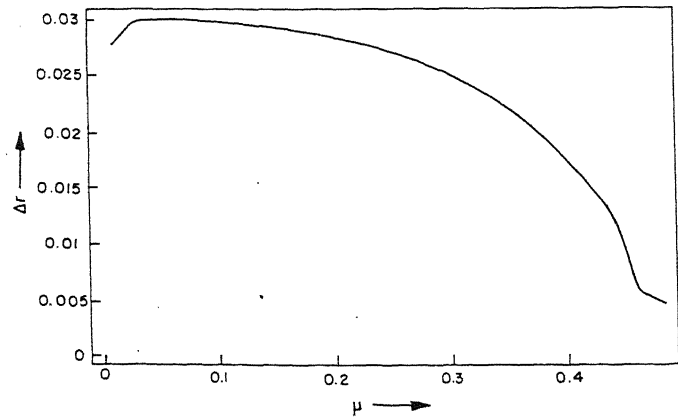
Fig. 3– Variation of Δr with μ

Discussion

If in Hill's stability problem, one takes one of the primaries as an oblate body, then the results obtained are significantly different. In this present case the maximum value of C_1 is 3.76963 when μ=0.33 and minimum value of $x_1 = -1.27163$ when μ=0.17894; these are the same as in their case. However, due to oblateness of one of the primaries, we see significant change in the stability curves (Fig. 2). In our case, we have obtained a difference between r_R and r_L as 1.13% which is less than that of Kubala *et al*[4]. They obtained this difference as 1.18%. A variation of Δr with μ is shown in Fig. 3.

References

1. Szebehely, V. (1967) *Theory of Orbits*, Academic Press, New York.
2. Szebehely, V. (1980) *Celest. Mech.* **22** : 7
3. Szebehely, V. & McKenzie, R. (1981) *Celest. Mech.* **23** : 3
4. Kubala, A., Black, D. & Szebehely, V. (1993) *Celest. Mech.* **56** : 51
5. Szebehely, V. (1984) *Celest. Mech.* **34** : 49

PROC. NAT. ACAD. SCI. INDIA, 75 (A), I, 2005

Projective motion admitting recurrent vector in flat Finsler space

J. K. SAHU

Department of Mathematics, Gangadhar Meher College, Sambalpur-768 004, India

Received January 27, 2004; Accepted June 2, 2004

Abstract

The vector field $v^i(x^i)$ has an important role in the infinitesimal transformation in Riemannian as well as Finsler space which gives rise to lie derivative. The vector field v^i in both spaces is considered as a function of position. Yano has treated the various possibilities of covariant derivative of v^i in non-Reiemannian spaces and they are named contra-vector field, recurrent vector field and concircular vector field. Okumura generalizes the idea of concircular vector field which he called as torse-forming vector field. The concepts of different types of recurrent vector of v^i in a flat Finsler space admitting projective motion has been introduced and explored certain results concerning it in this paper.

(**Keywords** : *V*-recurrent / *SV* recurrent /*PT* –recurrent / flat Finsler space)

Introduction

Let F_n be an n-dimensional Finsler space and G^i_{jk} being homogeneous of degree zero in the directional arguments satisfy

$$\text{(a) } G^i_{jk}x^j = 0, \text{ (b) } G^i_{jk}x^j = G^i_k \tag{1}$$

where $G^i_{jkh}x^j = \partial_j G^i_{kh}$ from a tensor field symmetric in all its covariant indices. With the help of this connection parameter, Berwald defines a covariant derivative of a tensor field $T^i_h(x, \dot{x})$ and second order covariant derivative of this tensor field gives rise to

$$2B_{[j}B_{k]}T^i_h = T^s_h H^i_{jks} - (\partial_s T^i_h)H^s_{jk} \tag{2}^*$$

where B_j stands for Berwald's covariant derivative and H^i_{jkh} is the curvature tensor field, skew symmetric in j, k and homogeneous function of degree zero in x^i's. Thus we have

$$H^i_{jkh}x^h = H^i_{jk} \tag{3}$$

The partial derivative $\dot{\partial}_j$ and Berwald's covariant derivative B_k commute according to

$$(\partial_j B_k - B_k \partial_j)\ T^i_h = T^s_h G^i_{jks} \tag{4}$$

The infinitesimal transformation

$$\bar{x}^i = x^i + \in v^i(x^j) \tag{5}$$

where ϵ is an infinitesimal constant and v^i is the vector field independent of the directional arguments, gives rise to the lie derivative £ of connection parameter by

$$£\, 2G^i_{jk} = B_j B_k v^i + v^h H^i_{jkh} + G^i_{jkh} B_m v^h x^m \tag{6}$$

Different type of recurrence of v^i : Similar to the definition of Takano[10], we call vector field v^i possesses the recurrent property in F_n if it satisfies

$$B_k v^i = \phi_k v^i, \text{ for a non-null vector } \phi(x, \dot{x}). \tag{7}$$

---

*The square brackets denote the skew symmetric part with respect to the indices enclosed therein.

Such a property of v^i is called *V*-recurrent in F_n.

Definition : A Finsler space is called flat if its curvature tensor field H^i_{jkh} vanishes in F_n :

$$H^i_{jkh} = 0. \tag{8}$$

It can be easily seen that the tensor field H^i_{jkh} also vanishes in flat F_n .

$$H^i_{jk} = 0. \tag{9}$$

Definition : The vector field v^i possesses SV-recurrent in F_n if v^i satisfies

(i) $B_j v^i = \phi_j v^i$,

(ii) $B_j \dot{\phi} = \phi_j \phi_,$. (10)

Projective Motion Admitting SV-Recurrent in F_n :

In this section, we want to investigate the conditions for projective motion which reduces to an affine motion in the space of our consideration. The necessary and sufficient conditions for the projective motion in F_n is that the lie derivative of G^i_{jk} is expressed by

$$£\ G^i_{jk} = 2\delta^i_{(jP_k)} + \dot{x}^i p_{jk} \tag{11}$$

where $p_j = \dot{\partial}_j$ and $p_{jk} = \dot{\partial}_j p_k$

The function p_j is homogeneous of degree zero in $\dot{x}^i$'s. Due to this property of p_j, we have

$$p_{jk}\ \dot{x}^j = 0. \tag{12}$$

It can be easily seen that the vanishing of p_j reduces the projective motion into affine motion in F_n.

Theorem : The projective motion admitting SV-recurrent satisfies

$$£\, G^i_{jk} = \frac{v^h}{n+1}\left\{ 2H^m{}_{hm(k}\delta^i{}_{j)} + \dot{x}^i H^m_{hmjk} \right\} \tag{13}$$

Proof: Using (6) and (7) in (11), we obtain

$$2\delta^i_{(jP_k)} + \dot{x}^i p_{jk} = (B_j \phi_j \phi_k) v^i$$

$$+ v^h H^i_{hjk} + G^i_{jkh} v^h \phi_m \dot{x}_m$$

Transvecting the above relation by $\dot{x}^k$ by the help of (1 a), (10) and (12), we get

$$\delta^i_j p_k \dot{x}^k + \dot{x}^i p_j = v^h H^i_{hj}.$$

On substituting $i = j$, the scalar function is given by

$$p = \frac{v^h}{n+1} H^i_{hi} \tag{14}$$

The partial derivative of (14) with respect to $\dot{x}^j$ yields p_j and on further differentiation gives p_{jk}. Substituting in the values of p_j and p_{jk} in (11), the result is obtained.

Corollary : The projective motion admitting *SV*-recurrent in flat F_n becomes an affine motion.

PT-recurrent of v^i in a Flat F_n : Okumara[1] generalizes the concept of concircular vector field in non-Riemannian space by considering vector field ϕ_k as non-gradient vector. We call such a vector field as torse forming vector in the space of our consideration. Misra and Meher[5,6] have considered a special type of torse-forming vector in the Finsler space admitting affine and projective motions. In this section, we have considered a particular type of this vector field which is different from literature[5,6].

Definition : The vector field v^i is called torse forming vector field in F_n if it satisfies

$$B_k v^i = \delta^i_k \rho + \phi_k v^i \quad (15)$$

for a scalar function $\rho(x, \dot{x})$ and a vector field $\phi_k (x, \dot{x})$.

In Misra and Meher[5,6], the torse-forming vector field is defined as a special kind of this vector if (15) also satisfies $B_{|j}\phi_{k|} = 0$.

Definition : The torse-forming vector field is characterized by

$$\text{(i) } B_k v^i = \delta^i_k \rho + \phi_k v^i \quad \text{(ii) } B_k \rho = 0; \quad (16)$$

is called PT-recurrent of v^i in F_n.

Theorem.: In a flat F_n, the PT-recurrent of v^i satisfies

$$\text{(a) } \rho = 0, \quad \text{(b) } v^k \phi_k = 0 \text{ for } n>1. \quad (17)$$

Proof : Covariant derivative of (16) with respect to x^j and taking the skew-symmetric part of this relation, in view of (2) and (16) reduces to

$$) \; v_h H^i_{jkh} = 2\{\delta^i_{|j}\rho\phi_{k|} + v^i B_{|j}\phi_{k|}\} \quad (18)$$

where the independent property of v^i in $\dot{x}^i$'s is taken into consideration.

For a flat F_n, the above relation reduces to

$$v^i B_{|k}\phi_{j|} = \rho\delta^i_{|j}\phi_{k|} \quad (19)$$

Contracting the above relation on i,j and multiplying this relation by v^k, we obtain

$$) \; \rho v^k \phi_k = 0, \text{ for } n>1. \quad (20)$$

Hence either $\rho = 0$

or $v_k \phi_k = 0$, for $n>1$.

Corollary : The PT-recurrent of v^i admitting llat F_n becomes a recurrent field provided $v^j \phi_j \neq 0$.

Theorem : If the PT-recurrent of v^i is admitted in Flat F_n along with $\rho = 0$, then the vector field reduces to contra-field in the same space.

Proof: Covariant derivative of 17(b) yields

$$v^i B_j \phi_k + \rho\phi_j = 0, \quad (21)$$

where (16) and (17(b)) are taken into consideration.

Taking covariant derivative of (21) with respect to x^h in view of (16) and (21), we obtain

$$v^k B_h B_j \phi_k + \rho(B_j\phi_h - B_h\phi_j) - \rho\phi_j\phi_h = 0$$

The skew symmetric part of the above relation yields,

$$v^k B_{|h} B_{j|}\phi_k + 2B_{|j}\phi_{h|} = 0.$$

Using (2), we obtain

$$-v^k \{\phi_s H^s_{hjk} + (\dot{\partial}_s \phi_k) H^s_{hj}\} + 2B_{|j}\phi_{k|} = 0.$$

The space under our discussion is flat, hence the relation (8) and (9) holds. Also the skew symmetric part on $B_j \phi_k$ vanishes.

Thus we get $\rho\delta^i_{|j}\phi_{h|} = 0$, which on contraction yields the required result.

References

1. Okumura, M. (1962) *Tensor (N.S.)* **12** : 33.
2. Meher, F.M. (1973) *Tensor (N. S.)* **27** : 208.
3. Misra, R.B. & Meher, F. M (1972) *Indian J. Pure and Appl. Math.* **3** : 219.
4. Misra, R.B. & Meher, F. M (1971) *Act. Math Acad. Sci. Hungarica* **22** : 423.
5. Misra, R.B. & Meher, F. M (1972) *Tensor (N.S.)* **24** : 288.
6. Misra, R.B. & Meher, F. M (1975) *Indian J. Appl. Math.* **6** : 522.
7. Sinha, R.S. (1969) *Tensor* (N.S.) **20** : 261.
8. Singh, S. P (2001) *Istanbul Univ. Fen. Fek. Mat. Der.* **60** : 85.
9. Rund, H (1959) *Springer Verlag,*
10. Takano, K. (1961) *Tensor* (N.S.) **11** : 137,174, 245, 270.
11. Takano, K. & Okumara, M. (1961) *Affine motion in non-Riemannian K-spaces* II, **11** : 161.
12. Yano, K. (1940) *Proc. Acad. Tokyo* **16** : 195, 354, 442, 505.

PROC. NAT. ACAD. SCI. INDIA, 75 (A), I, 2005

Axial symmetric translational motion of a half submerged sphere in a liquid with a surfactant layer

SUNIL DATTA and NIDHI PANDYA

Department of Mathematics and Astronomy, Lucknow University, Lucknow-226 007, India.

Received April 30, 2002, Revised March 2, 2003, Re-Revised February 26, 2004; Accepted June 14, 2004.

Abstract

In this paper, we study the translational motion of a half - submerged sphere in viscous fluid bounded by a plane surface covered by a monomolecular layer of sufactant fluid. The Stokes flow solution is presented for the quasistatic case and the effect of surfactant layer on the drag determined and discussed. Numerical results in tabular and graphical forms reveal that in general the effect of surfactant layer is to increase the values of drag over those of O'Neill *et al.*

(**Keywords** : surfactant layer/slip condition/Stokes equation)

Introduction

In 1986 O'Neill *et al.*[1] studied the motion of a translating - rotating sphere in a semi- infinite viscous fluid when the bounding free surface bisects the sphere. They removed the singularity present at the corner between the plane free surface and the hemi - spherical immersed part by using slip condition introduced by Basset[2]. The conditions of zero normal velocity at the surface of the sphere and at the boundary plane, and vanishing of tangential stress condition are also satisfied. Now, when the adsorbed monomolecular layer of surfactant fluid is present at the free surface, the zero tangential stress has to be modified to incorporate the effect of surface shear viscosity ε and surface dilational viscosity κ present in the surfactant layer. The boundary condition at the surfactant layer is derived from the work of Scriven[3], who studied the motion of a thin fluid interface between two bulk fluids of different viscosities.

In the present paper, we have considered the quasistatic situation when Reynolds number is vanishingly small so that steady - state Stokes equations are applicable.

Formulation of the Problem

A sphere of radius a is exactly half - submerged in a semi - infinite expense of viscous fluid of density ρ, viscosity μ and bounded by a surfactant layer of surface shear viscosity ε and surface dilational viscosity κ. Here, we study the motion when the sphere starts moving parallel to the normal to the surfactant layer, with velocity U. Obviously the motion is axisymmetric with the normal as the axis of symmetry. A spherical polar coordinate system, with the pole in the surfactant layer and coordinates (r,θ) in the meridional plane containing the axis of symmetry $\theta = 0$ is set up. It will be found convenient to non-dimensionalise space coordinates by sphere radius a, the velocity by U and the pressure by $(\rho\nu U/a)$. The motion may be taken as quasi-static and governed by the Stokes equation

$$\nabla^2 v = \nabla p, \tag{1}$$

and the continuity equation

$$\nabla.v = 0. \tag{2}$$
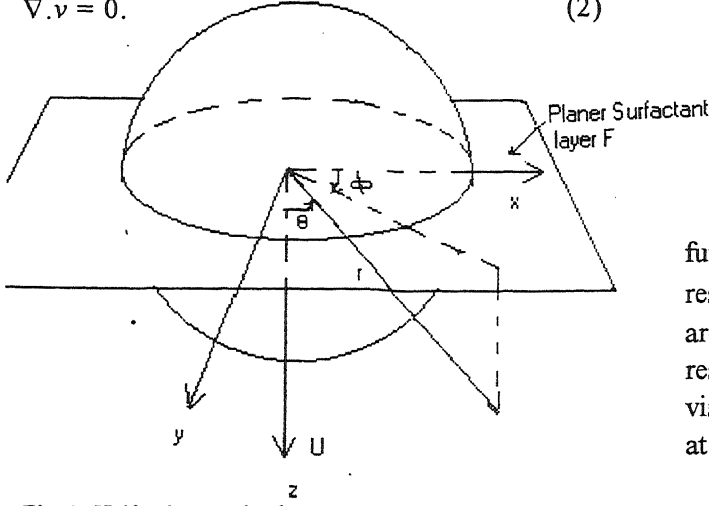
Fig. 1–Half submerged sphere penetrating a planar surfatant layer F bounding a semi-infinite fluid

From axial symmertic nature of the flow, it follows that azimuthal component of veloctiy $u_\Phi = 0$ and that (u_r, u_θ) componenents are expressible in terms of the Stokes stream function ψ as

$$u_r = -\frac{1}{r^2 \sin\theta}\frac{\partial\psi}{\partial\theta}, \tag{3}$$

$$u_\theta = \frac{1}{r\sin\theta}\frac{\partial\psi}{\partial r}, \tag{4}$$

so that the equation of continuity is identically satisfied. Further equation (1) leads to

$$E^4\,\psi = 0, \tag{5}$$

where

$$E^2 = \frac{\partial^2}{\partial r^2} + \frac{\sin\theta}{r^2}\frac{\partial}{\partial\theta}\left(\frac{1}{\sin\theta}\frac{\partial}{\partial\theta}\right). \tag{6}$$

The solution of equation (5), which is finite everywhere in the fluid region may be expressed (ref. 4. p. 133-138) as

$$\psi = A_0\, cos\theta + \sum_{n=1}^{\infty}\left(\frac{A_n}{r^{2n}} + \frac{B_n}{r^{2n-2}}\right)P'_{2n}(\cos\theta)\sin^2\theta$$

$$+ \left(\lambda+\bar{\lambda}\right)\sum_{n=0}^{\infty}\left(\frac{C_n}{r^{2n+1}} + \frac{D_n}{r^{2n-1}}\right)P'_{2n+1}(\cos\theta)\sin^2\theta$$

$$+ \left(\lambda+\bar{\lambda}\right)\sum_{n=1}^{\infty}\left(\frac{E_n}{r^{2n}} + \frac{F_n}{r^{2n-2}}\right)P'_{2n}(\cos\theta)\sin^2\theta. \tag{7}$$

Here P_{2n+1} (cosθ) and P_{2n} (cosθ) are Legendre's function, accent represents differentiation with respect to the argument and $\lambda = \in'\mu a$, $\bar{\lambda} = \kappa'\mu a$ are dimensionless parameters representing respectively the surface shear and dilational viscosity ratios; also a is the radius of body section at the boubdary surface $\theta = \pi/2$.

Next we shall evaluate the value of unknown constants A_n, B_n, C_n, D_n, E_n and F_n from the following boundary conditions:

i. The impenetrability of the sphere (r = 1 in the non-dimensional variables) surface by the fluid provides the kinematical boundary condition

$$u_r = \cos\theta, \qquad \text{on } r = 1, \tag{8}$$

or using (3) and (4),

$$\psi = \frac{1}{2}\cos^2\theta, \qquad 0 \le \theta < \frac{\pi}{2}$$

ii. The normal velocity at the surfactant layer F vanishes i.e.

$$u_\theta = 0, \qquad \text{on } F\ (\theta = \frac{\pi}{2}) \tag{9}$$

or

$$\psi(r, \theta = \frac{\pi}{2}) = 0, \qquad \text{for } r \ge 1.$$

iii. Surfactant layer condition : This may be achieved by considering the thin mono-molecular motion of surfactant layer as a surface flow governed by two-dimensional Riemannian metric. Equations of mass conservation, momentum and

constitutive equations may thus be derived for the surface flow. Next the dynamical tensor quantities for the interface are linked with those for the surroundings. The derivation involves lengthy algebra which was erected by Scriven[3] and we, omitting the details, reproduce below his final results as

$$\frac{1}{r^3}\frac{\partial^2\psi}{\partial\theta^2} = \left(\lambda+\bar{\lambda}\right)\frac{\partial}{\partial r}\left[\frac{1}{r^2}\frac{\partial}{\partial r}\left(\frac{\partial\psi}{\partial\theta}\right)\right]$$

$$\text{at } \theta = \frac{\pi}{2},\ r \geq 1. \tag{10}$$

iv. The slip condition corresponds to the Basset's[2] condition and may be taken as

$$\beta\ (u_\theta + \sin\theta) = \frac{1}{r}\frac{\partial u_r}{\partial\theta} + r\frac{\partial}{\partial r}\frac{u_\theta}{r},\ \text{at } r = 1.$$

Here the coefficient β of sliding friction is a measure of the degree of slip existing between the fluid and the surface of the sphere; $\beta\to\infty$ corresponds to the no-slip condition and $\beta\to 0$ to the free surface condition of perfect slip.

Upon using (3) (4) and (8), above condition provides

$$(\beta+1)\ \frac{\partial\psi}{\partial r} + (\beta+1)\sin^2\theta = \frac{\partial}{\partial r}\left(\frac{1}{r}\frac{\partial\psi}{\partial r}\right),\ \text{at } r = 1. \tag{11}$$

v. The condition that the fluid be at rest at infinity provides

$$\frac{\psi}{r^2}\to 0 \quad \text{as } r\to\infty, \qquad 0 \leq \theta < \frac{\pi}{2}.$$

The pressure p $(r,\ \theta)$ for axisymmetric translational motion is obtained by integration of the Stokes equations (1). The r and θ components of equations (1) in terms of $\psi(r,\ \theta)$ are expressible as

$$\frac{\partial p}{\partial r} = -\frac{1}{r^2\sin\theta}\frac{\partial}{\partial\theta}(E^2\psi), \tag{13}$$

$$\frac{\partial p}{\partial\theta} = \frac{1}{\sin\theta}\frac{\partial}{\partial\theta}(E^2\psi). \tag{14}$$

Therefore by using (6) and (7) in equations (13) and (14), we get on integration

$$p = -\sum_{m=1}^{\infty}4m(4m-1)\frac{B_m}{r^{2m+1}}P_{2m}(\cos\theta)$$

$$-\left(\lambda+\bar{\lambda}\right)\left[\sum_{m=1}^{\infty}4m(4m-1)\frac{F_m}{r^{2m+1}}P_{2m}(\cos\theta)\right.$$

$$-\left.\left(\lambda+\bar{\lambda}\right)\sum_{m=0}^{\infty}2m(4m+1)(2m+1)\frac{D_m}{r^{2m+2}}P_{2m+1}(\cos\theta)\right].$$

Evaluation of Constants

Next on using (7) in the boundary condition (9) and using the fact that $P'_{2n}(0) = 0$ for every positive integer n, we get

$$C_nP'_{2n+1}(0) + D_{n+1}P'_{2n+3}(0) = 0,\ \text{for every } n \geq 0.$$

Next making use of the result[5]

$$P'_{2n+1}(0) = \frac{(-1)^n(2n+1)!}{2^{2n}(n!)^2}$$

the above relation reduces to

$$D_{n+1} = \frac{2(n+1)}{(2n+3)}C_n, \qquad \text{for ever } n \geq 0. \tag{16}$$

Now using the function ψ as given by (7) in the boundary condition (10), neglecting squares of

small quantities $(\lambda+\bar{\lambda})$ and using the fact that $P'_{2n}(0) = 0$, we obtain

$$(2n+1)(2n+2)C_n P'_{2n+1}(0) + (2n+3)(2n+4)D_{n+1}P'_{2n+3}(0)$$

$$= -[(2n)^2(2n+1)(2n+3)P_{2n}(0)A_n$$

$$-(2n)(2n+2)(2n+3)^2 P_{2n+2}(0)B_{n+1}]$$

for every $n \geq 0$.

Now substituting the value of D_{n+1} from (16) in the above equation and using the values[5] of

$$\frac{P_{2n}(0)}{P'_{2n+1}(0)} = \frac{1}{2n+1} \quad \text{and}$$

$$\frac{P_{2n+2}(0)}{P'_{2n+1}(0)} = -\frac{1}{2(n+1)},$$

we get

$$C_n = \frac{n(2n+3)[2nA_n - (2n+3)B_{n+1}]}{(4n+5)},$$

for every $n \geq 0$. (17)

and then from (16)

$$D_n = \frac{2n(n-1)[2(n-1)A_{n-1} - (2n+1)B_n]}{4n+1},$$

for every $n \geq 0$. (18)

Next, using the boundary condition (8) with ψ given by (7), we obtain the values

$$A_0 = \frac{1}{2}, \qquad \text{for } \theta = 0,$$

and for $0<\theta<\pi/2$

$$\frac{1}{2}\cos^2\theta - \frac{1}{2}\cos\theta = \sum_{n=1}^{\infty}(A_n + B_n)P'_{2n}(\cos\theta)\sin^2\theta$$

$$+ (\lambda+\bar{\lambda})\sum_{n=0}^{\infty}(C_n + D_n)P'_{2n+1}(\cos\theta)\sin^2\theta$$

$$+ (\lambda+\bar{\lambda})\sum_{n=1}^{\infty}(E_n + F_n)P'_{2n}(\cos\theta)\sin^2\theta. \quad (19)$$

Multiplying both sides of the above equation by $P'_{2m}(x)$ ($x = \cos\theta$) and integrating from 0 to 1, on equating the coefficients of 1 and $(\lambda+\bar{\lambda})$, we get

$$A_m + B_m = \frac{t_m}{2r_m}, \qquad m \geq 1,$$

and

$$E_m + F_m = -(4m+1)P_{2m}(0)\sum_{n=0}^{\infty}p_{mn}(C_n + D_n)$$

for every $m \geq 1$, (21)

where

$$\left.\begin{aligned}
&\int_0^1 x^2 P'_{2m}(x)\,dx = 1 + t_m,\\
&\int_0^1 x P'_{2m}(x)\,dx = 1\\
&\int_0^1 (1-x^2)P'_{2m}(x)P'_{2n+1}(x)\,dx =\\
&\qquad 2m(2m+1)P_{2m}(0).p_{mn}, \text{ and}\\
&\int_0^1 (1-x^2)P'_{2m}(x)P'_{2n}(x)\,dx = \delta_{mn,}r_n
\end{aligned}\right\} \quad (22)$$

in which, δ_{mn}, is the Kronecker delta,

$$P_{2m}(0) = \frac{(-1)^m 2m!}{2^{2m}(m!)^2}$$

$$p_{mn} = \frac{(-1)^{n+1}(2n+1)!}{2^{2n}(2m-2n-1)(2m+2n+2)(n!)^2}, \quad (23)$$

$$t_m(0) = \frac{P_{2m}(0)}{(m+1)(2m-1)}$$

and

$$r_m = \frac{2m(2m+1)}{4m+1},$$

Next the slip boundary condition (11) with ψ given by (7) leads to

$$\sum_{n=1}^{\infty}\{2n(2n+3+\beta)A_n + 2(n-1)(2n+1+\beta)B_n\}\times \times P'_{2m}(\cos\theta)$$

$$+ (\lambda+\bar{\lambda})\sum_{n=0}^{\infty}\{2n(2n+1)(2n+4+\beta)C_n + (2n-1)(2n+2+\beta)D_n\}P'_{2n+1}(\cos\theta)$$

$$+ (\lambda+\bar{\lambda})\sum_{n=1}^{\infty}\{2n(2n+3+\beta)E_n + 2(n-1)(2n+1+\beta)F_n\}P'_{2n}(\cos\theta) = 1+\beta.$$

Now by using the identities (22) and the identity

$$\int_0^1 (1-x^2)P'_{2m}(x)dx = -m(2m+1)t_m,.$$

in the above equation, and equating the coefficient of 1 and $(\lambda+\bar{\lambda})$, we get

$$2m\,(2m+3+\beta)\,A_m + 2(m-1)\,(2m+1+\beta)\,B_n$$

$$= -m(2m+1)\,(1+\beta)\,\frac{t_m}{r_m},$$

for every $m \geq 1$, (24)

and

$$2m(2m+3+\beta)E_m + 2(m-1)(2m+1+\beta)F_m = -(4m+1)P_{2m}(0).$$

$$\sum_{n=0}^{\infty} p_{mn}\{(2n+1)(2n+4+\beta)C_n + (2n-1)(2n+2+\beta)D_n\}$$

for every $m \geq 1$ (25)

Equation (20) and (24) provide for $m \geq 1$

$$A_m = -\frac{(4m+1)t_m}{4m(4m+1+\beta)}\left[(2m-1) + \frac{(2m^2+2m-1)}{2m+1}\right], \quad (26)$$

and

$$B_m = -\frac{(4m+1)(m+1)(2+\beta)t_m}{2(2m+1)(4m+1+\beta)}, \quad (27)$$

Next by using (17) (18) (23) (26) and (27) the equations (21) and (25) may be written as (21).

$$E_m + F_m = (4m+1)P_{2m}(0)\times \sum_{n=1}^{\infty} \frac{f(n)}{(2m-2n-3)(2m-2n-1)(2m+2n+2)(2m+2n+4)}$$

$$= (4m+1)P_{2m}(0)\,S_f(m), \quad \text{for every } m \geq 1. \quad (28)$$

and

$$2m(2m+3+\beta)E_m + 2(m-1)(2m+1+\beta)F_m$$

$$= (4m+1)P_{2m}(0) \times \sum_{n=1}^{\infty} \frac{g(n)}{(2m-2n-3)(2m-2n-1)(2m+2n+2)(2m+2n+4)}$$

$$= (4m+1)P_{2m}(0)\, S_g(m),$$

$$\text{for every } m \geq 1. \qquad (29)$$

$$f(n) = \frac{n(2n+3)(64n^3+48n^2-4n+3\beta+3)\beta}{2\pi(n+1)(2n-1)(4n+1+\beta)(4n+5+\beta)} \left(\frac{\Gamma\left(n+\frac{1}{2}\right)}{\Gamma(n+1)} \right)^2, \qquad (30)$$

$$g(n) = (2n+1)(2n+4+\beta)f(n), \qquad (31)$$

$$S_f(m) = \sum_{n=1}^{\infty} \frac{f(n)}{(2m-2n-3)(2m-2n-1)(2m+2n+2)(2m+2n+4)}, \qquad (32)$$

and

$$S_g(m) = \sum_{n=1}^{\infty} \frac{(2n+1)(2n+4+\beta)f(n)}{(2m-2n-3)(2m-2n-1)(2m+2n+2)(2m+2n+4)} \qquad (33)$$

Now, by making use of Stirling's formula for the asymptotic expansion of the factorial frnction, we obtain

$$\frac{\Gamma\left(n+\frac{1}{2}\right)}{\Gamma(n+1)} \approx n^{-\frac{1}{2}}, \qquad (34)$$

Using the above asympotic expansion, we find that the nth terms of the series (28) (29) are respectively $O\left(\frac{1}{n^4}\right)$ and $\left(\frac{1}{n^2}\right)$, hence both the series are convergent.

In the sequel we shall see that the drag force comes out in terms of an infinite series involving the coefficients A_m, B_m, E_m, and F_m, A_m, and B_m, have already been derived, The existence of E_m, and F_m has been demonstrated above.

The explicit forms of E_m, and F_m as obtained from the equations (28) and (29) are

$$E_m = -\frac{(4m+1)P_{2m}(0)}{2(4m+1+\beta)} \sum_{n=1}^{\infty} f(n) \left[\frac{1}{(2m-2n-1)(2m+2n+4)} + \frac{\beta}{(2m-2n-1)(2m+2n+2)(2m+2n+4)} \right] \qquad (35)$$

$$F_m = \frac{(4m+1)P_{2m}(0)}{2(4m+1+\beta)} \sum_{n=1}^{\infty} f(n) \left[\frac{1}{(2m-2n-3)(2m+2n+4)} \right.$$

$$+\left.\frac{\beta}{(2m-2n-3)(2m+2n+2)(2m+2n+4)}\right] \quad (36)$$

Force on the Half-Sphere

Here we shall evaluate the force on the half-submerged sphere. This force as obtained by integrating surface stress over the sphere is

$$F = \int_0^{\frac{\pi}{2}} (p_{rr}\cos\theta - p_{r\theta}\sin\theta).\sin\theta d\theta, \quad \text{at } r = 1 \quad (37)$$

where normal stress

$$p_{rr} = -p+2\frac{\partial u_r}{\partial r}, \quad (38)$$

and tangential stress

$$p_{r\theta}= \frac{1}{r}\frac{\partial u_r}{\partial\theta}+r\frac{\partial}{\partial r}\left(\frac{u_\theta}{r}\right), \quad (39)$$

with pressure p given by (15).

Thus, by using (3) (4) (7) (15) (38) and (39), equation (37) provides

$$\frac{F}{2\pi} = -\sum_{m=1}^{\infty} 2m(4m-1)B_m t_m$$

$$-2\left(\lambda+\bar{\lambda}\right)\sum_{m=1}^{\infty} m(4m-1)F_m t_m -1$$

$$-4\sum_{m=1}^{\infty} m(2m+1)[\{(m+1)A_m+mB_m\}$$

$$+\left(\lambda+\bar{\lambda}\right)\{(m+1)E_m+mF_m\}t_m]$$

$$-2\beta\sum_{m=1}^{\infty} m(2m+1)\{mA_m+(m-1)B_m\}t_m$$

$$-2\beta\left(\lambda+\bar{\lambda}\right)\sum_{m=1}^{\infty} m(2m+1)[\{mE_m+,$$

$$(m-1)F_m\}t_m-\frac{2}{3}\beta \quad (40)$$

where we have used the value $A_0 = 1/2$ and the following identities[5] ·

$$\int_0^1 xP_{2m}(x)dx = \frac{1}{2}(1-p_m) = -\frac{1}{2}t_m,$$

$$\int_0^1 xP_{2m}(x)dx = \frac{1}{2}(1-p_m) = -\frac{1}{2}t_m, \quad (41)$$

$$\int_0^1 (1-x^2)P'_{2m+1}(x)dx = 0$$

Now with the help of equation (19) we see that the sum of series

$$\sum_{m=1}^{\infty} m(2m+1)[\{m+1)A_m+mB_m\}+$$

$$\left(\lambda+\bar{\lambda}\right)\{(m+1)E_m+mF_m\}]t_m \quad (42)$$

appearing on the right hand side of expression (40) is equal to

$$\sum_{m=1}^{\infty} m(2m+1)[\{mA_m+(m-1)B_m\}+.$$

$$\left(\lambda+\bar{\lambda}\right)\{(mE_m+(m-1)F_m\}]t_m+\frac{1}{12} \quad (43)$$

Substitute the above form of series (42) in equation (40) to obtain

$$-\frac{F}{\pi(\beta+2)} = X_0+\left(\lambda+\bar{\lambda}\right)X_1, \quad (44)$$

where

$$X_0 = \frac{4}{3} + 4\sum_{m=1}^{\infty} m(2m+1)\{mA_m + (m-1)B_m\}t_m$$

$$+\frac{1}{(\beta+2)}\sum_{m=1}^{\infty} 4m(4m-1)B_m t_m, \qquad (45)$$

$$X_1 = 4\sum_{m=1}^{\infty}\{h_1(m) + h_2(m) + h_3(m)\}. \qquad (46)$$

Here the expression (45) for X_0 is same as that of O'Neill *et al*[7]. It remains to establish the existence of the coefficients of $(\lambda+\bar{\lambda})$ i.e. X_1. Now, h_1, h_2 and h_3 may be expressed as following infinite series

$$h_1(m) = -\frac{m^2(2m+1)(4m+1)P_{2m}(0)t_m}{2(4m+1+\beta)}$$

$$\times \sum_{n=1}^{\infty} f(n)\left\{\frac{1}{(2m-2n-1)(2m+2n+4)} + \right.$$

$$\left.\frac{\beta}{(2m-2n-1)(2m+2n+2)(2m+2n+4)}\right\} \qquad (47)$$

$$h_2(m) = \frac{m(2m+1)(4m+1)(m-1)P_{2m}(0)t_m}{2(4m+1+\beta)}$$

$$\times \sum_{n=1}^{\infty} f(n)\left\{\frac{1}{(2m-2n-3)(2m+2n+2)} + \right.$$

$$\left.\frac{\beta}{(2m-2n-3)(2m+2n+2)(2m+2n+4)}\right\} \qquad (48)$$

and

$$h_3(\mathrm{m}) = \frac{m(4m-1)(4m+1)P_{2m}(0)t_m}{2(4m+1+\beta)(\beta+2)}$$

$$\times \sum_{n=1}^{\infty} f(n)\left\{\frac{1}{(2m-2n-3)(2m+2n+2)} + \right.$$

$$\left.\frac{\beta}{(2m-2n-3)(2m+2n+2)(2m+2n+4)}\right\} \qquad (49)$$

It may be seen that $h_1(m)$ and $h_2(m)$ are of the same type and that the convergence of $h_3(m)$ follows from that of $h_1(m)$. Thus it remains only to check the series $h_1(m)$ for convergence. Now for establishing the convergence of the series $h_1(m)$ we consider only the first of the constituent series since the convergence of the second will follow from that of the first. Thus, if $f(n)$ were a constant f_0 (say), then consider

$$g_0(m) = \sum_{n=1}^{\infty}\frac{f_0}{(2m-2n-1)(2m+2n+4)} \qquad (50)$$

$$= \sum_{n=1}^{\infty}\frac{1}{2(4m+1)}\left[\frac{-1}{(n-m+\frac{1}{2}} + \frac{1}{(n+m+2)}\right]f_0$$

$$= -\frac{1}{2(4m+1)}\left[-\psi\left(m-\frac{1}{2}\right) + \psi(m+3)\right]f_0$$

$$\sim \left[-\frac{7}{16}\frac{1}{m^2} + \frac{35}{64}\frac{1}{m^3} + \ldots\right]f_0 \qquad (51)$$

Here, we use the asymptotic expansion of digamma function[5] Ψ(Ref. 5, p. 264)

$$\Psi(z) = \frac{d}{dz}\log\Gamma(z) = \frac{\Gamma'(z)}{\Gamma(z)},$$

as

$$\Psi(m-\frac{1}{2}) \sim \log m - \frac{1}{m} - \frac{5}{24m^2} + \ldots,$$

$$\Psi(m+3) \sim \log m + \frac{5}{2m} - \frac{55}{12m^2} + \ldots,$$

But, here $f(n)$ is not a constant. We conjecture that an approximation will be obtained if, instead, we use the asymptotic expansion of $f(n)$, vis.,

$$f(n) \sim \frac{1}{\pi}\left[f_0 + f_1.\frac{1}{n} + f_2\frac{1}{n^2} + \ldots\right]$$

where

$$f_0 = 2\beta,\ f_1 = \left(\frac{1}{2}\beta - \beta^2\right),$$

$$f_2 = -\beta\left(8 + \frac{7}{2}\beta + \frac{\beta^2}{8}\right), \ldots.$$

Thus, expression (51) becomes

$$g_o(m) \sim \beta\left\{-\frac{7}{8}.\frac{1}{m^2} + \frac{35}{32}.\frac{1}{m^3} + \ldots.\right\}$$

We may also calculate in a similar way the terms g_1 and g_2 etc. corresponding to f_1, f_2 etc. Thus we have

$$g_1(m) = \sum_{n=1}^{\infty}\frac{f_2}{(2m-2n-1)(2m+2n+4)n^2}$$

$$\sim \beta((\frac{1}{2} - \beta)\left\{-\frac{\gamma}{4}.\frac{1}{m^2} + \frac{3}{16}.\frac{1}{m^3}\right\},$$

and

$$g_2(m) = \sum_{n=1}^{\infty}\frac{f_2}{(2m-2n-1)(2m+2n+4)n^2}$$

$$\sim -\frac{\pi^2}{24}\beta\left(8 + \frac{7}{2}\beta + \frac{1}{8}\beta^2\right).\frac{1}{m^2},$$

where γ is the Euler's constant. Thus, from the above the contribution of first series in $h_1(m)$ is given as

$$\sum_{n=1}^{\infty}\frac{f(n)}{(2m-2n-1)(2m+2n+4)}$$

$$\sim \beta \left[\left\{-\frac{(21+3\gamma+8\pi^2)}{24} + \frac{(12\gamma-7\pi^2)}{48}\beta - \frac{\pi^2}{192}\beta^2 + \ldots.\right\}\frac{1}{m^2} + \left\{\frac{19}{16} - \frac{3}{16}\beta\right\}\frac{1}{m^3}\ldots..\right]$$

Similarly, we determine the contribution of the second series in $h_1(m)$, i.e.

$$\sum_{n=1}^{\infty}\frac{f(n)\beta}{(2m-2n-1)(2m+2n+2)(2m+2n+4)}$$

$$\sim \beta^2\left[-\frac{3}{16}.\frac{1}{m^2} + \frac{1}{144}\times\left\{(-160+9\gamma+24\pi^2)+3(3+6\gamma-\frac{7}{2}\pi^2)\beta - \frac{3}{8}\pi^2\beta^2\ldots\ldots.\right\}\frac{1}{m^3}\ldots\right]$$

Summing up the above contributions correct upto $O\left(\frac{1}{m^3}\right)$, we obtain

$$h_1(m) \sim \frac{m^2(2m+1)(4m+1)\beta P_{2m}(0)t_m}{2(4m+1+\beta)}$$

$$\times\left[\left\{-\frac{(21+3\gamma+8\pi^2)}{24} + \frac{(-9+12\gamma-7\pi^2)}{48}\beta - \frac{\pi^2}{192}\beta^2 + \ldots.\right\}\frac{1}{m^2}\right.$$

$$+\left\{\frac{19}{16}+\frac{(133-9\gamma+24\pi^2)}{144}\beta\right.$$

$$\left.+\frac{(6+12\gamma+7\pi^2)}{96}\beta^2+\frac{\pi^2}{384}\beta^3+....\right\}\frac{1}{m^3}+....\Bigg]$$

(52)

Now, t_m may also be expressed in terms of $P_{2m}(0)$ (23). Also by using (34), the asymptotic expansion of $P_{2m}(0)$ is

$$P_{2m}(0)=\frac{(-1)^m\Gamma(m+\frac{1}{2})}{(\pi)^{\frac{1}{2}}\Gamma(m+1)}\sim\frac{(-1)^m}{(\pi)^{\frac{1}{2}}}(m^{-\frac{1}{2}}),$$

and so asymptotic expansion of t_m is

$$t_m=-\frac{P_{2m}(0)}{(m+1)(2m-1)}\sim\frac{(-1)^m}{(\pi)^{\frac{1}{2}}}(m^{-\frac{5}{2}}).$$

Substituting these values in (52), we arrive the following asymptotic expansion

$$h_1(m)\sim\beta$$

$$\Bigg[\Bigg[\left\{-\frac{(21+3\gamma+8\pi^2)}{24}+\frac{(6+12\gamma-7\pi^2)}{48}\beta\right.$$

$$\left.-\frac{\pi^2}{192}\beta^2+.....\right\}\frac{1}{m^2}$$

$$+\left\{\frac{19}{16}+\frac{(15+6\gamma+16\pi^2)}{96}\beta\right.$$

$$\left.+\frac{(6+12\gamma+7\pi^2)}{96}\beta^2+\frac{\pi^2}{384}\beta^3+...\right\}\frac{1}{m^3}+....\Bigg].$$

$$h_2(m)\sim\beta$$

$$\Bigg[\Bigg[\left\{-\frac{(21+3\gamma+8\pi^2)}{24}+\frac{(6+12\gamma-7\pi^2)}{48}\beta\right.$$

$$\left.-\frac{\pi^2}{192}\beta^2+.....\right\}\frac{1}{m^2}$$

$$+\left\{\frac{1}{4}+\frac{(-27-6\gamma+16\pi^2)}{96}\beta\right.$$

$$\left.+\frac{(6+12\gamma+7\pi^2)}{96}\beta^2+\frac{\pi^2}{384}\beta^3+.......\right\}\frac{1}{m^3}+....\Bigg]$$

$$h_3(m)\sim\frac{\beta}{\beta+2}$$

$$\Bigg[\Bigg[\left\{-\frac{(21+3\gamma+8\pi^2)}{24}+\frac{(6+12\gamma-7\pi^2)}{48}\beta\right.$$

$$\left.-\frac{\pi^2}{192}\beta^2+.....\right\}\frac{1}{m^3}$$

$$+\left\{\frac{1}{4}+\frac{(-27-6\gamma+16\pi^2)}{96}\beta\right.$$

$$\left.+\frac{(6+12\gamma+7\pi^2)}{96}\beta^2+\frac{\pi^2}{384}\beta^3\right\}\frac{1}{m^4}+....\Bigg].$$

Since $h_1(m)$ has the order $1/m^2$, the series $\Sigma h_1(m)$ is convergent and so are the series $\Sigma h_2(m)$ and $\Sigma h_3(m)$. Thus, we conclude from (46) that the contribution of the surfactant to the drag *vis.* $(\lambda+\bar{\lambda})\ X_1$ exists. Of course, we can make numerical estimate of $f(n)$ and use it to determin the value of $\Sigma h_1(m)$, $\Sigma h_2(m)$ and $\Sigma h_3(m)$, and then estimate X_1.

Table 1

β	$k_{\parallel}^{t}$	k_{1}^{t}	$k_{\parallel}^{t}+0.1k_{1}^{t}$	$k_{\parallel}^{t}+0.2k_{1}$
0	8.9916	0	8.9916	8.9916
.1	9.2913	-.0046	9.2908	9.2904
.2	-	-.0055	-	-
.3	-	-.0043	-	-
.4	-	0	-	-
.5	10.498	.0063	10.4986	10.4993
1	11.646	.0659	11.6529	11.6592
5	18.093	1.0902	18.2020	18.3110
10	22.506	2.168	22.7228	22.9396
20	27.531	2.9158	27.8226	28.1142
50	34.624	1.0123	34.7252	34.8265
100	40.151	-3.2348	39.8275	39.5040
∞	∞	$-\infty$	∞	∞

Discussion

The effect of surfactant layer on the drag is determined by the-non dimensional factor X_1 occurring in equation (44). The numerical values of $k_1^t = \pi(\beta + 2)X_1$ which is dependent on the slip coefficient β, are tabulated in Table 1, for $(\lambda+\bar{\lambda})$ = 0.1 and 0.2, along with the values of $k_{\parallel}^{t} = \pi(\beta+2)X_0$, obtained by O'Neill1 *et al*[1]. Since the surfactant layer parameter $(\lambda+\bar{\lambda})$ is positive, it follows from equation (44) that while for positive values of X_1, the drag increases, it decreases for negative values for X_1. It has been numerically show n that $k_{\parallel}^{t}$ and $F = k_{\parallel}^{t} + (\lambda+\bar{\lambda})\, k_1^t$ differ only minutely; hence, the graph of Fin the presence of surfactant layer will be indistingushable from that of k_2^t when it is absent. Therefore, a graph depicting the behavior of k_1^t with β is exhibited in Fig. 2. It is now seen that the drag still increases for $0.2 < \beta < 20$. There is fall in the value of k_1^t when $\beta > 20$; Also, surprisingly for $0 < \beta < 0.4$ and $\beta > 6.07$, k_1^t becomes negative. Extensive numerical calculations ($\beta \sim 10^8$) (not included in Table 1). show that although $k_1^t \to -\infty$ and $F \to \infty$ as $\beta \to \infty$. This may be supported analytically also by making use of the expression (45) for X_0 and the expression (46) for X_1, estimated through $h_1(m)$, $h_2(m)$, $h_3(m)$ as given by (47), (48), (49); X_0 is found to dominate over X_1 for large β.
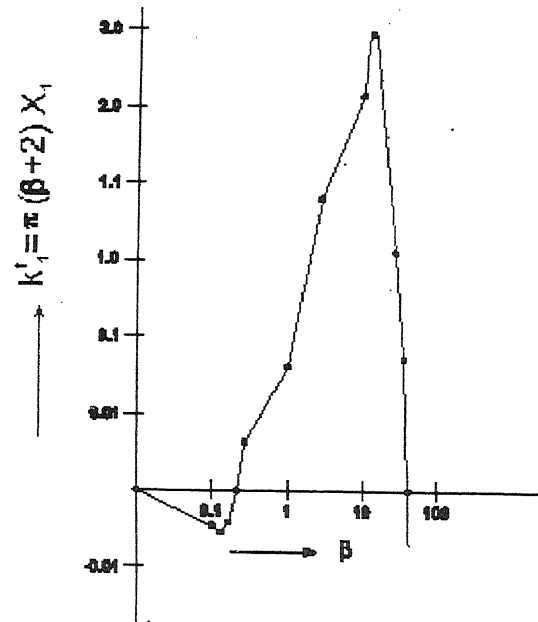
Fig. 2– Variation k of k_1^t with β

The rotational problems investigated by Davis[6], O'Neill and Yano[7] and Davis and O'Nell[8] show that the effect of surfactant layer is to increase the frictional couple corresponding to the drag here. Thus, it may be concluded that our analysis is tenable for $0.2 < \beta > 20$ when the drag continuously increases. When β is very large the fluid tries to stick (no-slip as $\beta \to \infty$) to the hemisphere, so that $v_\theta = -1$ at its corner points ($r = 1$, $\theta = \frac{\pi}{2}$); this contradicts the value $v_\theta = 0$ when the corner point is considered as a point of the bounding plane ($\theta = \frac{\pi}{2}$) where v_θ is now the normal velocity. This manifests in the infinite value of $k_{\parallel}^{t}$ as mentioned in the paper by O'Neill *et al*[1]. This is because the nature of flow changes at the corners, with possible appearance of eddies. On

the other hand for small values of β lying in between 0 and 0.4, only a finer analysis coupled with experimental evidence can explain the decrease in drag.

Acknowledgment

The authors thank the referee for valuable suggesations and corrections incoprorated in the paper.

References

1. O'neill, M.E., Ranger, K.B. & Brenner, H. (1986) *Phys. of Fluid* No. 4, **29** : 913.
2. Basset, A.B. (1988) *A Treatise on Hydrodynamics.* Vol. I and II; Cambridge Delingtion Bell and Co., London.
3. Scriven, L.E. (1960) *Chem. Engrg. Sci.* **12** : 98
4. Happel, J. & Brenner, H. (1983) *Low Reynolds number hydrodymamics,* Pritice Hall englewood Cliffs, NJ.
5. Abramowitz, M. & Stègun, I.A. (1968) *A handbook of mathematical functions,* Dover.
6. Davis, A.M.J. (1980) *Q.J.I. Mech. appl. Math* **43**(3) : 337
7. O'neill, M.E. & Yano, H. (1988) *Q.JI. Mech. appl. Math* **41**(4) : 479.
8. Davis, A.M.J. & O'neill, M.E. (1979) *Int. J. Multiphase Flow* **5** : 413

PROC. NAT. ACAD. SCI. INDIA, 75 (A), I, 2005

Silicified microbolites (stromatolites) of Precambrian age from Jungel Valley (Mahakoshal Group), Sonbhadra district, U.P. - A preliminary geochemical appraisal

J. K. PATI and P. PATI

Department of Earth & Planetary Sciences, Nehru Science Centre, University of Allahabad, Allahabad-211 002, India

E-mail: jkpati@yahoo.co.in

Received October 21, 2003; Revised April 5, 2004; Accepted May 10, 2004

Abstract

Silicified microbolites (stromatolites) of Precambrian affinity having varied morphological forms and structures from Jungel area belonging to Mahakoshal Group were analysed for their major oxide and limited trace element chemistry for the first time. The field observations and mesoscopic structures pertaining to their association with volcanogenic sediments and rocks have been confirmed by their preliminary chemical data. Evidences related to the penecontemporaneous diagenetic activities have also been brought out. The presence of these silicified microbolites is also indicative of the shallow-warm water condition of the proto-basin similar to modern hot spring environments.

(**Keywords** : precambrian/geochemistry/Mahakoshal Group/ Jungel/ silicified stromatolites)

Introduction

The knowledge pertaining to the evolutionary process of early life forms mainly comes from our study of microorganisms associated with modern hot-spring environments or Precambrian silicified microfossils and stromatolites[1]. The fossilization of microbolites due to silicification provides important insight into the microbe-silica interaction during Precambrian times[2-4]. The role of microbes in the silica precipitation is still not well known despite number of experimental studies[1] and the impact of volcanism on biomineralization by these microorganisms at variable pH is not known either. Microbolites are organosedimentary deposits formed due to the sediment-binding and/or carbonate precipitation process of bottom dwelling (benthic) microbes[5]. These microbes are mainly cyanobacteria and eukaryotic algae and the examples include stromatolites, thrombolites, and oncoids. Stromatolites are the most well known of the three forms and are defined as *"accretionary organosedimentary structure[s], commonly thinly layered, megascopic, and calcareous, produced by the activities of mat-building communities of mucilage-secreting microorganisms, mainly filamentous photoautotrophic prokaryotes such as cyanobacteria"*[6]. However, both siliceous and silicified stromatolites are known from Precambrian time despite their rarity in different parts of the world[7-12].

Stromatolites are extensively used for biostratigraphic correlations[7,13,14] and the presence of volcanic deposits within stromatolites help in deciphering the tectono-thermal evolution and palaeogeography of the sedimentary basins[15]. Process of silicification of these early life forms has been a subject of a number of experimental and field studies in modern hot spring environments in recent times[16-20].

The present study reports the geochemistry of Precambrian silicified microbolites from Jungel, Agori Formation, Mahakoshal Group, Central India and also provides unequivocal evidence pertaining to the intimate association of volcanogenic processes and the growth of silicified microbolites rarely observed worldwide.

Geological Setting

The silicified stromatolites observed in Jungel area (Fig. 1) occurs 1.5km SE of Jungel Water Tank, Sonbhadra district, U.P. The outcrop ($24^0 30'$ 28"; $82^0 51'$ 54") is about 220m long and 50m wide with a thickness of ~30m. This was the first reported occurrence of silicified stromatolites associated with volcaniclastics and volcanic rocks from Jungel Valley[10]. The importance of this occurrence lies in its geological setting, well preserved morphology, incorporation of volcanics, and silicified nature. Dwivedi and Yadav[21] have reported "algal mats-stromata" composed of "siliceous cherty material" from Bhitri ($24^0 32'$ 30"; $82^0 48'$ 30"). These microbolites belong to Agori Formation, Mahakoshal Group (earlier called Bijawar Group) of Late Archean-Early Proterozoic affinity[22-24]. The Mahakoshal Group is a typical greenstone sequence comprising of chemogenic sediments, metasediments, metabasics, metatuffs, volcaniclastic, basic-ultrabasic intrusives, vein quartz etc. and is divided into Chitrangi, Agori and Parsoi Formations. Granitoid and gneisses of Bundelkhand craton is considered as the basement[24,25]. The Jungel Valley silicified microbolites are quartz-rich and a few are observed to contain tuffaceous sediments in their matrix. The exposure is closely associated with ash flows and bands, pyroclastics, volcaniclastics and amygdular basalts. Siliciclastic beds have also been found in the vicinity.

Description of Stromatolites

Most of the microbolites (stromatolites) forms acquire columnar shape. In transverse section, they are circular to elliptical. A few forms are elongated in one direction. Some of them are poorly developed similar to algal-mat horizons. One type is slightly convex and linked laterally similar to columnar stromatolite (Fig. 2). Another type is gently convex (Fig. 3) compared to a form which
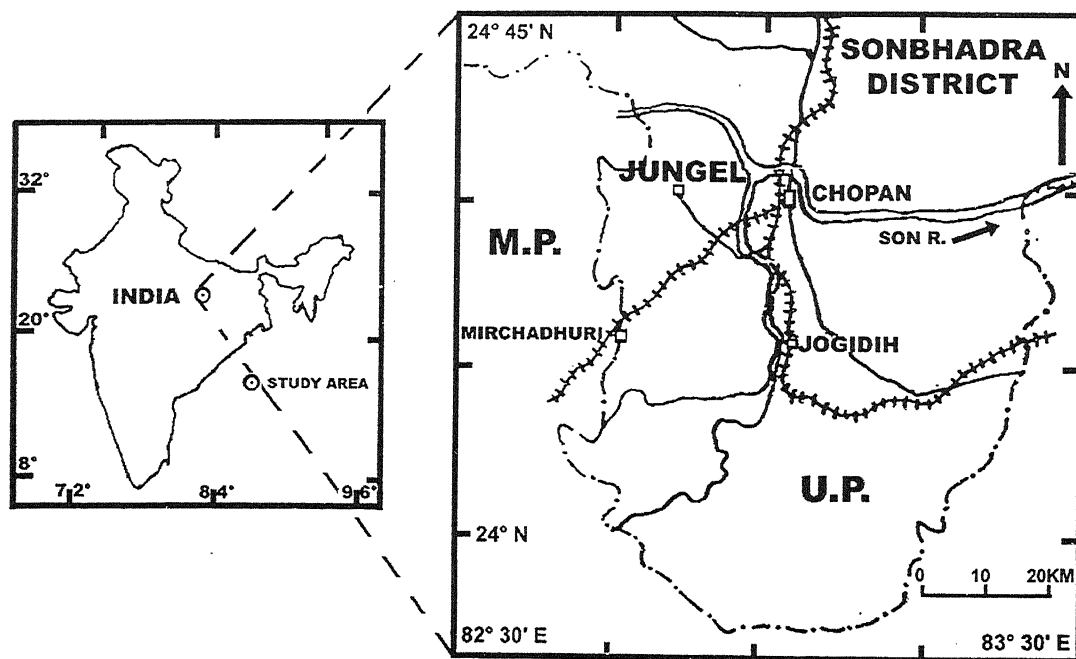
Fig. 1– Location map of Jungel Valley is shown in parts of Sonbhadra district, U.P. and in the Indian subcontinent.
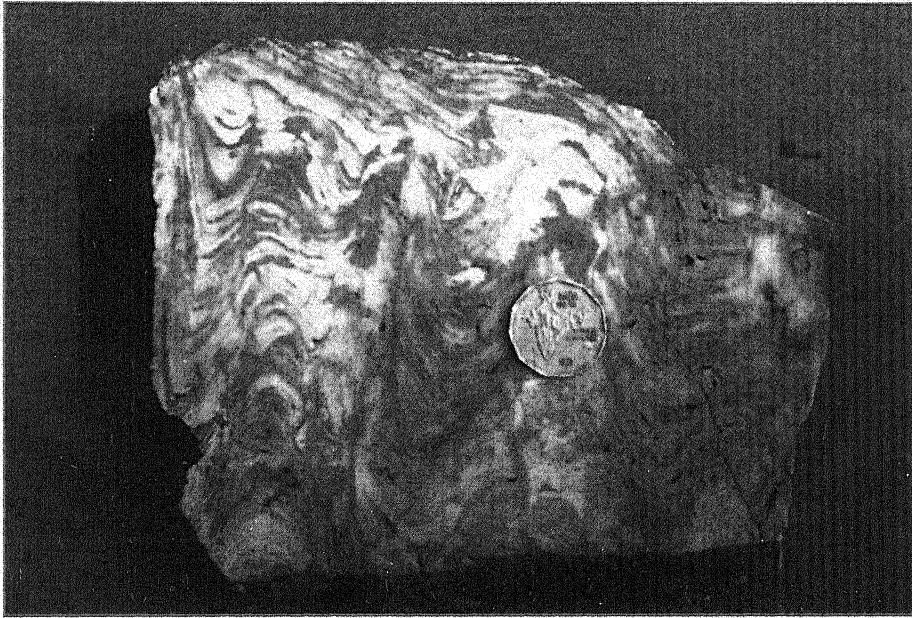
Fig. 2- Transverse sawed section shows slightly convex and linked laterally similar to columnar stomatolite with the base nearly planar.
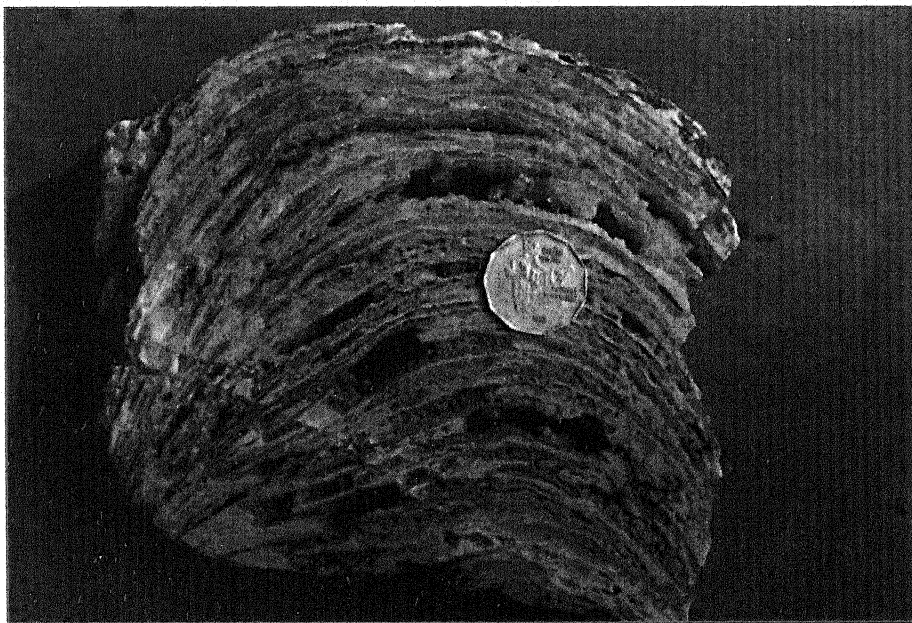
Fig. 3- Sawed section of a gently convex silicified stromatolite with drusy quartz developed in the cavities.
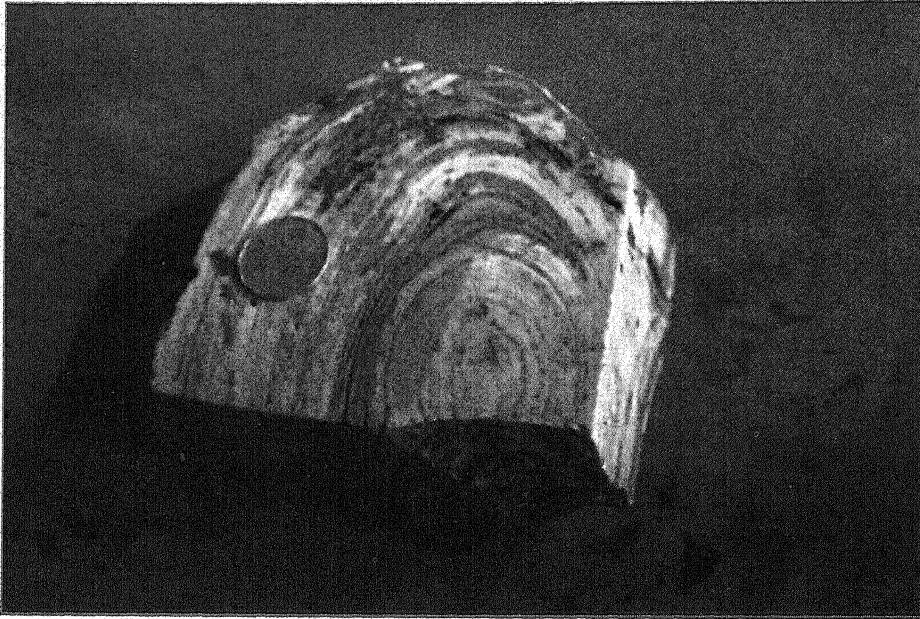
Fig. 4- Sawed section of the silicified stromatolite exhibits in three dimensions the strongly convex nature and near spherical growth of the laminae.

Fig. 5- Dismembered silicified stromatolites are occurring in a volcanogenic matrix. Note the variable orientations of the columns and some are partly fragmented and possibly shows chilling effect.

has strongly domal laminae and the microstructure is banded (Fig. 4). The third type mainly consists of individual columns in variable orientations (Fig. 5) occurring in a volcanics-rich matrix. Some of the columns are fragmented possibly due to the impact of episodic explosive volcanism in the area[24]. Interspaces between laminae are sometimes full of oxidized iron-rich sediments, pyrite crystals and drusy quartz indicating penecontemporaneous and diagenetic activities.

Analytical techniques

Three stromatolite-bearing rock samples were analysed for their major oxides and trace elements using XRF (GSI, Nagpur) and ICP-AES (GSI, Faridabad) techniques, respectively. The broken rock fragments were ground in an electrically driven tungsten carbide mortar to -200 mesh, in steps. The powdered samples were then processed for their chemical analyses. The XRF analyses were carried out using fusion beads and the beads are made by mixing $Li_2B_4O_7$ + Li_2CO_3 with sample in 2:1 flux/sample ratio. The calibration was done using USGS internal standard MRG (1) with a reported accuracy of 1% for major oxides. The trace element analyses were performed by using ICP-AES (JY-JOBIN YVON 70 Model; Chemical Division, GSI (NR), Faridabad). The calibration was carried out using internal standards BRGM-51, 52, and 53 (BRGM, France). The analytical precision is between 2-5%. The major oxide and trace elements analyses are shown in Table (1A and 1B), respectively.

Table 1A– Major oxide analyses (in wt.%) of stromatolite samples (XRF method)

Sample No. Oxides	JMC-22A (Milky white)	JMC-22B (Flesh coloured)	JMC-22C (Brownish grey)
SiO_2	96.67	97.18	87.91
Al_2O_3	0.84	0.75	2.85
Fe_2O_3	0.61	0.83	4.48
TiO_2	0.30	0.31	1.39
CaO	0.30	0.26	0.32
MgO	0.58	0.42	0.37
K_2O	0.19	0.33	0.63
Na_2O	0.10	0.07	0.12
MnO	0.01	0.01	0.03
P_2O_5	0.05	0.01	0.03
LOI	0.41	0.20	1.15
Total	100.06	100.37	99.28

Table 1B– Trace element analyses (in ppm) of stromatolite samples (ICP-AES method)

Sample No.	JMC-22A	JMC-22B	JMC-22C
Li	<10	<10	<10
Be	<2	<2	<2
B	<10	<10	16
V	28	28	77
Cr	46	83	646
Co	<5	<5	7
Ni	27	34	126
Cu	8	7	42
Zn	7	5	47
As	<20	<20	<20
Rb	<5	<5	15
Sr	24	26	43
Y	<20	<20	<20
Nb	25	26	23
Sn	<20	21	22
Ba	163	173	131
La	<20	<20	<20
Ce	<10	<10	17
W	<10	<10	<10
Pb	<10	<10	<10
Bi	<10	<10	<10
Zr	93	161	122

Geochemistry

The stromatolites samples are dominantly composed of quartz with trace amount of chlorite ± magnetite ± pyrite and one sample is found to contain volcaniclastics within the laminae and as matrix within the fragmented stromatolites. The mcro-textural data will be discussed elsewhere. The SiO_2 contents of these silicified microbolites range between 87.91 and 97.18 wt.% similar to chert of Late Archaean age reported from Chitradurga Schist Belt[26]. All major oxides (Al_2O_3, Fe_2O_3, TiO_2, CaO, MgO, Na_2O, K_2O and P_2O_5) show a negative correlation with SiO_2 content similar to rocks of volcanic affinity. The cherts and ferruginous cherts of purely chemical precipitate origin have Al_2O_3 between 0.01 and 0.1 wt.% and TiO_2 between 0.01 and 0.02 wt.%[26]. In the present study, silicified microbolites have comparatively very high Al_2O_3 (0.75-2.85 wt.%) and TiO_2 (0.30-1.39 wt.%) contents. This indicates the role of igneous activity on the composition of silicified microbolites from Jungel area. The low content of alkali components preclude the role of post-depositional changes like diagenesis, metasomatism and/or deformation accompanied by volume gain. The presence of quartz druses between the laminae (Fig. 3) is indicative of possible hydrothermal activity[27] in these silicified microbolites. The concentration of V, Ni, Cr, Sr and Nb in these microbolites is also very high and similar to basaltic rocks. Some of the cherts analyzed from Chitradurga do show high values of V (up to 287ppm), Ni (up to 15.20ppm) and Cr (up to 81.54ppm). However, Chitradurga cherts are of hydrothermal affinity and have higher base metal concentration compared to the silicified microbolites from Jungel Valley. The sample (JMC-22C) containing 646ppm (Cr) and 126ppm (Ni) suggests the possible presence of Ni-bearing chrome spinels. The niobium content is very high for a chert and Nb can be incorporated in structure of Fe-Ti oxide minerals. But the near uniform Nb contents in the microbolites samples with respect to Fe-Ti content does not show a positive correlation. Generally, plume related basalts are Nb enriched[28]. This presents further evidence pertaining to the intimate association of volcanogenic processes and the simultaneous growth and silicification of microbolites. It is well known that the Jungel Valley represents a failed rift system[23] and bound by number of ~E-W trending sub-parallel faults[24]. These brittle structures are partly responsible for tectono-magmatic evolution of the basin[24]. The Zr content of the samples is also high and it is possible that some zircon grains may be present as dispersed phases. It would be interesting to separate the zircons in future and date these microbolites vis-à-vis a significant part of Mahakoshal Group.

Results and Discussions

The present study reveals that the silicified microbolites (stromatolites) are similar to the composition of Precambrian chemogenic precipitates (cherts) found in different parts of the world but contain magmatogenic signatures. These stromatolites are distinct not only in terms of their lithological association but also due to the incorporation of volcanic-derived sediments during and subsequent to their growth as revealed by their mesoscopic textures and geochemistry. The presence of iron oxide and pyrite within these stromatolites also possibly suggest the role of microbes in mineraliztion as nanoparticles similar to well known modern hot spring environments. It also proves that these early life forms did survive and proliferate at very high temperatures during the Precambrian time.

Acknowledgements

Part of the work was carried out at the Geological Survey of India (NR), Lucknow by the first author for which he thanks Mr. Ravi Shankar, Director General (Retd.) and Mr. V.D.Mamgain, Dy. Director General (Retd.) for their encouragement and support. We owe a debt of gratitude to Prof. S. Kumar (Retd.), Department of Geology, Lucknow University, Lucknow, who has been a great source of encouragement and inspiration during the study.

References

1. Benning, L.G., Phoenix, V.R., Yee, N. & Konhauser, K.O. (2004) *Geochemica Cosmochemica Acta* **68** : 729.
2. Konhauser, K.O. (2000) in *Marine Authigenesis: From Global to Microbial.* (Eds. C.R. Glenn, J. Lucas and L. Prévôt) SEPM Special Publication, **66** : 133.
3. Cady, S.L. (2001) *Adv. Appl. Microbiol.* **50** : 3.
4. Toporski, J.K.W., Steele, A., Westall, F., Thomas-Keprta, K.L. & McKay, D.S. (2002) *Astrobiology* **2/1** : 1.
5. Burne, R. V. & Moore, L. S. (1987) *Palaios* **2** : 241.
6. Schopf, J.W. (1999) *Cradle of Life: The Discovery of the Earth's Earliest Fossils.* Princeton University Press.
7. Walter, M.R. (1976) *Stromatolites.* Elsevier Scientific Publishing Co., Amsterdam.
8. Khan, S.U. & Das, B. (1968) *Curr. Sci.* **37** : 171.
9. Awasthi, R.K. (1978) *Workshop on Stromatolites: Characteristics and Utility,* Geol. Surv. India, Udaipur.
10. Pati, J.K. (1997) *Conference on Biosedimentology of Precambrian Basins,* Palaeontological Soc. India, Lucknow, Abstract Vol., p. 11.
11. Cao, R. (1999) *7th International Symposium on Fossil Algae:* Nanjing, China Program and Abstracts Volume.
12. Seong-Joo, L. & Golubic, S. (1999) *Precambrian Research* **96** : 183.
13. Walter, M.R. (1972) *Spec. Pap. Palaeont.* 11 Palaeont. Assoc., London, 190p.
14. Chumakhov, N.M. & Semikhatov, M.A. (1981) *Precambrian Res.* **15** : 229.
15. Chakraborty, P.P., Banerjee, S., Das, N.G., Sarkar, S. & Bose, P.K. (1996) *Mem. Geol. Soc. India* **36** : 59.
16. Hinman, N.W. & Lindstrom, R.F. (1996) *Chemical Geology* **132** : 237.
17. Jones, B., Renault, R. W. & Rosen, M. R. (1997) *J. Sed. Res.* **67** : 88.
18. Carroll, S., Mroczek, E., Alai, M. & Ebert, M. (1998) *Geochim. Cosmochim. Acta* **62** : 1379.
19. Phoenix, V.R., Adams, D.G. & Konhauser, K.O., (2000) *Chem. Geol.* **169** : 329.
20. Konhauser, K.O., Phoenix, V.R., Bottrell, S.H., Adams, D.G. & Head, I.M. (2001) *Sedimentology* **48** : 415.
21. Dwivedi, G.N. & Yadav, M.L. (1992) *GSI (NR) News,* 12 and 13, 5-6.
22. Nair, K.K.K., Jain, S.C. & Yedekar, D.B. (1995) *Mem. Geol. Soc. India* **31** : 403.
23. Bandyopadhyay, B.K., Roy, A. & Huin, A.K. (1995) *Mem. Geol. Soc. India* **31** : 433.
24. Pati, J.K. (1998) *F.S. (1990-1994) Final Report,* Geol. Surv. India (NR), Lucknow, p. 205.
25. Raza, M. & Casshyap, S.M. (1996) *Mem. Geol. Soc. India* **36** : 287.
26. Gnaneshwar Rao, T. & Naqvi, S. M. (1995) *Chemical Geology* **121** : 217.
27. Dong, G., Morrison, G. & Jaireth, S. (1995) *Econ. Geol.* **90** : 1841.
28. Kerrich, R., Polat, A., Wyman, D. & Hollings, P. (1999) *Lithos* **46** : 163.

Kind Attention : Fellows and Members of the National Academy of Sciences, India
(Please fill items and return to the Managing Editor – Proceedings of the National Academy of Sciences, India
(Sec A – Physical Sciences; Sec B – Biological Sciences)

The Editorial Boards and Board of Editors of the Journals of the Academy viz. **Proceedings of the National Academy of Sciences, India (Sec A – Physical Sciences), Proceedings of the National Academy of Sciences, India (Sec B– Biological Sciences)** and **National Academy Science Letters,** request its esteemed Fellows and Members to inform their willingness for acting as learned referees for the research papers received for publication in the above Journals. They are also requested to suggest other names of subject experts who may be requested for refereeing as per following proforma.

UPDATED DATA OF REFEREES' PANEL FOR THE JOURNALS OF THE NATIONAL ACADEMY OF SCIENCES, INDIA

(I) 1. Name, Designation, Affiliation and ....

Postal Address of the Fellow/Member ....

....

....

(a) Telephone No. (with area code) ....

(b) Fax No. (with area code)..

(c) E-mail Address..

2. State whether a Fellow or Member..

3. Subject/Sub-disciplines of your expertise in which you are willing to act as Referee.

Sl. No.	Major Disciplines (Such as Physics etc.)	Sub-discipline alonwith super-speciality	Experimental/Theoretical or both
1.		(i) (a) (b)	
2.		(ii) (a) (b)	
3.		(iii) (a) (b)	

(II) Suggestions regarding additional referees

Sl. No.	Name(s) & Address of those whom you suggest for refereeing	His/Her Major Disciplines (such as Physics etc.)	His/Her Sub-disciplines alongwith any Super-specialities	Experimental/Theoretical or Both
1.			(i) (a) (b)	
2.			(i) (a) (b)	
3.			(i) (a) (b)	

Signature of the Fellow/Member

THE NATIONAL ACADEMY OF SCIENCES, INDIA

5, Lajpatrai Road, New Katra, Allahabad - 211002

Guidelines for the Authors/Contributors for submitting papers

Proceedings of the National Academy of Sciences, India
(Section A – Physical Sciences)

[A) WHAT TO SUBMIT

The following categories of papers are published in the Proceedings of the National Academy of Sciences, India (Section A - Physical Sciences) :

(1) **Review Articles:** This should be a critical review highlighting the present status and an overview of the past work on any relevant subject of current topical interest. It has to be written in a manner to help either in initiating the work in that particular area or in increasing the comprehension of the current challenges. If such an article is accepted by the Academy for publication, then **Rupees Two Thousand** would be given to the "corresponding author" after the publication of the paper in the Proceedings to meet the contingency expenses. Ordinarily, the Review Article should not exceed 25 printed pages.

(2) **Original Articles:** This should give new results obtained by the authors and be prepared in the format of the journal. Ordinarily such papers should not be more than 12 printed pages.

(3) **Special Issues for Conference Proceedings:** Proceedings of National and International Conferences, as a special issue of the journal, can also be brought out with organizers as Guest Editors. At least, one of the Guest Editors should be Fellow of the Academy. Guest Editors shall be responsible for proper refereeing of the papers and for ensuring their high quality.

It is presumed that the articles submitted for publication have not been submitted to any other journal by the authors. Authors shall be liable themselves for such an act.

[B) WHO CAN SUBMIT

(1) All scientists (Indian or Foreign) can directly send their article for publication. **If there are more than one author, each author should certify that he/she agrees to the submission of the review/research paper.**

(2) In addition to above, all the Fellows of the National Academy of Sciences, India are also authorized to forward quality papers in their research field for publication in the journals of the Academy. The name of the communicating Fellow would be printed in the paper as "Communicated by ....................F.N.A.Sc".

The communicating Fellow should certify that:

(i) The forwarded paper is in his/her field of specialization,

(ii) He/she has read the paper and reviewed it carefully.

However, if the Editorial Board finds it necessary, it may get the paper reviewed again.

[C] WHOM TO SUBMIT

The papers should be sent to the Managing Editor, Proceedings of the National Academy of Sciences, India (Section A – Physical Sciences); 5 Lajjpat Rai Road, New Katra, Allahabad - 211 002

[D] HOW TO SUBMIT

The authors may submit the papers directly or forwarded through a Fellow of the Academy as prescribed above. It is mandatory to submit "An Electronic Version" as well as "three hard-copies". The text of the manuscript as per format of the journal outlined below, and preferably with scanned figures, should be supplied as a plain ASCII file (Wordstar 5.5 or 7.0 and Microsoft Word for Window 6.0 are also acceptable, but ASCII is preferred). The language of the journal is English.

[E] FORMAT OF THE MANUSCRIPT

(i) Title of the paper should be in **bold** and running (14-font size) through the full page width.

(ii) **Author's name/Affiliations** may also run through the full page width. Names should be in 12 point font-size and **bold** while affiliations should be 8 point font size in *italics*. Please note that if any of the author is a Fellow of the Academy, then he should write F.N.A.Sc. after his name.

(iii) **Abstract** should be typed in 8 point font sizes "**bold**".

(iv) **Keywords** (maximum 5 words/phrases, each separated by slash [/]) should follow the Abstract.

(v) **Contents of the text**

(a) This is to be typed on A4 page in double space in10 point font size.

(b) The text of the paper should be arranged into suitable headings like Introduction, Materials and Method, Theory or Model, Results, Discussion, Conclusions/Summary, Acknowledgements, References, etc.

(c) Please note that the Proceedings are published in "two column format". Therefore, the authors are required to draw the figures tables/equations in such a way that they can be easily reduced to one column width (~ 7.5 cm) at the time of publication. Figures must be original drawings or exceptionally sharp glossy prints drawn with stencil and UNO pen.

(d) All references should be indicated in the text by superscript Arabic numerals, e.g. 'Mirri[1] while working on...'. The list of references should be arranged in order of their occurrence in the text. References should be given in the following style:

1. Mirri, M.A. (1982), J. Chem. Phys. 58: 282 (for articles in journals)

White, M. J. D. (1973) Animal Cytology and Evolution, 3rd Ed., Cambridge University Press, London, p. 320 (for books)

Osgood, C.F. (1977) in Number Theory and Algebra: ed., Zasserhause, H., Academic Press, New York, p. 10 (for edited books)

Abbreviations of the names of periodicals should conform to those given in the World list of Scientific Periodicals.

[F] MISCELLANEOUS

(i) All papers will be screened by a strict refereeing procedure. However, the responsibility for the authenticity of the contents lies with the authors.

(ii) If a paper is recommended for revision, a maximum of 2 months would be given to authors for revising the manuscript after which it would be treated as a fresh communication.

(iii) Authors will receive galley proof of their paper from the Academy's Editorial Office. They should return the corrected proof within a week of its receipt. If return of the proof is delayed, the proof will be corrected by the Academy, but the responsibility will be entirely that of the author(s).

(iv) No change in the text of the paper will be made after the matter has been composed by the Press. If it is absolutely essential, a postscript may be added.

(v) Reprints: 25 free reprints will be given to the corresponding author for each paper.

[G] SUBSCRIPTION RATE OF THE JOURNALS

Annual Subscription for both Sections : Rs. 500.00; **for each Section** Rs. 250.00; **Single Copy :** Rs. 100.00, **Foreign Subscription :** (a) for one Section: US $100, (b) for both Sections US $200. **(Air Mail charges included in foreign subscription)**